# CHARACTERIZATION OF PEPTIDE AMPHIPHILE NANOFIBERS THEIR INTERACTIONS WITH CHONDROPROGENITOR CELLS AND MORPHOLOGICAL ANALYSIS OF TISSUES FROM TRANSGENIC ANIMALS

A THESIS

SUBMITTED TO THE MATERIALS SCIENCE AND NANOTECHNOLOGY PROGRAM OF THE GRADUATE SCHOOL OF ENGINEERING AND SCIENCE OF BILKENT UNIVERSITY

IN PARTIAL FULFILLMENT OF THE REQUIREMENTS

FOR THE DEGREE OF

MASTER OF SCIENCE

By

AYŞEGÜL TOMBULOĞLU

July, 2012

I certify that I have read this thesis and that in my opinion it is fully adequate, in scope and in quality, as a thesis of the degree of Master of Science.

……

Assist. Prof. Dr. Ayşe Begüm Tekinay (Advisor)

I certify that I have read this thesis and that in my opinion it is fully adequate, in scope and in quality, as a thesis of the degree of Master of Science.

…….

Assoc. Prof. Dr. Mustafa Özgür Güler (Co-Advisor)

I certify that I have read this thesis and that in my opinion it is fully adequate, in scope and in quality, as a thesis of the degree of Master of Science.

…….

Assoc. Prof. Dr. Aykutlu Dâna

I certify that I have read this thesis and that in my opinion it is fully adequate, in scope and in quality, as a thesis of the degree of Master of Science.

…….

Assist. Prof. Dr. Fatih Büyükserin

Approved for the Graduate School of Engineering and Science:

…….

Prof. Dr. Levent Onural

Director of the Graduate School of Engineering and Science

# ABSTRACT

## CHARACTERIZATION OF PEPTIDE AMPHIPHILE NANOFIBERS THEIR INTERACTIONS WITH CHONDROPROGENITOR CELLS AND MORPHOLOGICAL ANALYSIS OF TISSUES FROM TRANSGENIC ANIMALS

Ayşegül Tombuloğlu

M.Sc. in Materials Science and Nanotechnology

July, 2012

Peptide amphiphiles, molecules able to self assemble into three dimensional networks resembling to extracellular matrix which is excessive in cartilage tissue, are suitable candidates for overcoming cartilage tissue defects and diseases which constitute central health problems throughout ages. Understanding developmental processes that underlie cartilage formation is also key for regenerating cartilage. In this study, peptide amphiphiles were synthesized, their potential for cartilage regeneration was investigated and a model for cellular aggregation, which is a central process in embryonic cartilage development, was established with chondroprogenitor cells and peptide amphiphile scaffolds. On scaffolds, chondroprogenitor cells aggregated without requiring any additional bioactive factors as opposed to cells grown without

scaffolds. Addition of insulin to the medium enhanced the size of the aggregates suggesting scaffolds may be interacting with insulin. Similar to native cartilage tissue, collagen II was massively produced in aggregates. GAG-PA which is designed to mimic glycosaminoglycans and Glu-PA which only presents glutamic acid were used to construct scaffolds with oppositely charged Lys-PA presenting lysine. Formation of aggregates was observed regardless of the PAs used. Use of both GAG-PA and Glu-PA induced larger number of aggregates than only Glu-PA. Differential effect of GAG-PA couldn't be inferred completely and might be investigated in more detail.

In a second part of the study, tissue morphologies of lynx3 null mutant mice were studied. Lynx3 is a recently discovered protein belonging to Ly6-superfamily. It is expressed mainly within epithelial lining of respiratory, digestive and genital tracts and is involved in nicotinic acetylcholine receptor desensitization. In this study, morphologies of lynx3 null mice with that of wild type mice were compared to see whether lynx3 has a gross effect on the tissues in which it is expressed. Any significant difference in the morphologies of lung, trachea and thymus cannot be observed. Little variations in esophagus, stomach and female reproductive organ were seen, however, it was not clear whether these variations are related to individual differences or not and the relevance of the variations with lynx3 expression could not be seen clearly. More detailed analysis of tissues may provide additional insight to understand function of lynx3 and the cholinergic mechanisms within various tissues.

Short peptides able to pass cell membrane and deliver genes into cells are outstanding alternatives to virus based transfection systems. In the third part of the study, peptide

amphiphiles designed to mimic the natural polycationic proteins through forming nanofibers which exhibit positively charged residues at high density, were synthesized. Peptide amphiphiles could form stable complexes with DNA, through neutralization of charges and formation of hydrogen bonds. However, efficient transfection of the gene couldn't be provided by any complexes *in vitro.* The study presents primary results upon which more detailed investigation can be built.

**Keywords:** Cartilage, peptide amphiphiles, aggregation, chondroprogenitor cells, chondrogenic differentiation, lynx3, cell penetrating peptides.

# ÖZET

## PEPTİT AMFİFİL NANOFİBERLERİNİN KARAKTERİZASYONU, KONDROSİT ÖNCÜLÜ HÜCRELERLE ETKİLEŞİMLERİ VE TRANSGENİK HAYVANLARA AİT DOKULARIN MORFOLOJİK ANALİZİ

Ayşegül Tombuloğlu

Malzeme Bilimi ve Nanoteknoloji Programı, Yüksek Lisans

Tez Yöneticisi: Yard. Doç. Dr. Ayşe Begüm Tekinay

Temmuz, 2012

Kıkırdak dokusunda çok yoğun bulunan hücrelerarası matrise benzer üç boyutlu ağlar kurabilen peptit amfifiller, çağlar boyu çözümsüz kalmış temel sağlık sorunları teşkil eden kıkırdak dokusu hasarları ve hastalıklarının üstesinden gelmeye uygun adaylardır. Kıkırdak dokusu oluşumunun altında yatan temel süreçleri anlamak da kıkırdak rejenerasyonu için kilit öneme sahiptir. Bu çalışmada, biyoaktif peptit amfifil nanofiberlerin kıkırdak rejenerasyonuna yönelik potansiyelleri incelenmiştir ve kondrosit öncülü hücreler ve peptit amfifillerle embryonik kıkırdak gelişiminde merkezi bir süreç olan hücresel toplanma için bir model, oluşturulmuştur. Peptit amfifillerin oluşturduğu iskeleler üzerinde hücreler, iskele olmadan kültürlenen

hücrelerin tersine, fazladan etken maddelere ihtiyaç duymadan toplanmışlardır. Besiyerine insülin eklenmesi, oluşan hücre yığınlarının boyutunu arttırmıştır ki bu sonuç insülin ve iskelelerin etkileşiyor olabileceğini akla getirmektedir. Hücre yığınlarında, hücreler arası matris ve kollajen II, doğal kıkırdak yapısına benzer şekilde büyük miktarlarda üretilmektedir. Glikozaminoglikanlara benzemek üzere tasarlanmış GAG-PA, ve yalnızca glutamik asit sergileyen Glu-PA, lizin sergileyen zıt yüklü Lys-PA ile iskeleler inşa etmede kullanılmıştır. Hücre yığınlarının oluşumu, kullanılan peptit amfifillere bağlı olmaksızın gözlemlenmiştir. İskelelerde GAG-PA ve Glu-PA'nın birlikte kullanımı yalnızca Glu-PA'nın kullanıldığı iskelelere göre daha fazla hücre yığını oluşumu tetiklemiştir. GAG-PA'nın farka neden olan etkisi yeterince iyi çözümlenememiş olup daha ayrıntılı araştırılabilir.

Çalışmanın ikinci kısmında, Lynx3 ifade etmeyen transgenik farelerin doku morfolojileri çalışılmıştır. Ly6 üst-ailesine ait olan Lynx3, yakın zamanda keşfedilen, bir proteindir. Solunum, sindirim ve üreme kanallarının epitel hattı boyunca ifade edilmektedir ve nikotinik asetilkolin reseptörlerinin duyarsızlaştırılmasında görev almaktadır. Bu çalışmada, Lynx'3ün ifade edildiği dokularda önemli bir etkisi olup olmadığını görmek amacıyla Lynx3'süz (transgenik) farelerin morfolojileri yabani tür farelerle karşılaştırılmıştır. Akciğer, trake ve timus dokularında kayda değer herhangi bir farka rastlanmamıştır. Özofagus, mide ve dişi üreme organında ufak farklılıklar görülse de bunların bireysel farklılıklardan kaynaklanıp kaynaklanmadığı, ve de farklılıkların lynx3 proteininin ifadesiyle alakası açıkça görülememektedir. Dokuların daha ayrıntılı analizi, lynx3'ün dokulardaki görevinin ve çeşitli kolinerjik mekanizmaların anlaşılmasında ışık tutacaktır.

Hücre zarını geçebilen ve genleri hücrelere taşıyabilen küçük peptitler, virüs tabanlı transfeksiyon sistemlerine karşı belli başlı seçenekler arasında yer almaktadır. Çalışmanın üçüncü kısmında, yüksek yoğunlukta artı yüklü aminoasit zincirleri sergileyen nanofiberler oluşturma yoluyla doğal polikatyonik proteinlere benzeyecek peptit amfifil molekülleri tasarlanmıştır. Peptit amfifiller yüksüzleşme ve hidrojen bağları oluşturma yoluyla DNA ile sağlam-kararlı kompleksler meydana getirmişlerdir. Fakat *in vitro*'da, oluşturulan komplekslerden herhangi biri içerdiği genin etkin transfeksiyonunu sağlayamamıştır.

**Anahtar kelimeler:** Kıkırdak, peptit amfifiller, toplanma-yığın oluşturma, kondrosit öncülü hücreler, kondrojenik farklılaşma, lynx3, hücre-delen peptitler

## Acknowledgements

First of all, I'd like to express my gratitude to my principal advisor Assist. Prof. Dr. Ayşe Begüm Tekinay for her patience, her support and guidance which I appreciate very much. For sure, I couldn't have come this far without support that she provided.

I also thank to my advisor Assoc. Prof. Dr. Mustafa Özgür Güler for his valuable ideas and helps throughout the study. I thank for the many things that I learned from both my supervisors.

I'd like to thank Assoc. Prof. Dr. Aykutlu Dâna, also Dr. Emine Deniz Tekin for interesting views and discussions.

Special thanks to project partner, Seher Üstün, who was always cooparative and worked with me till late hours.

It was nice to meet, Büşra and Rashad Mammadov, Yavuz Dagdaş, Selim Sülek, Handan Acar, Sıla Toksöz, Ruslan Garifullin, Hakan Ceylan, Hilal Ünal, Samet Kocabey, Selman Erkal, Zeliha Soran, Elif Duman, Selma Bulut, Göksu Çinar, Melis Şardan, Oya Ustahüseyin, Aref Khalily, Dr. Rükan Genç, Dr. Fatih Genişel, Gözde Uzunallı, Murat Kılınç, Gülcihan Gülseren, all the members of Sustainable Technologies Laboratory especially Ahmet Emin Topal, Alper Devrim Özkan, Burcu Gümüşçü, "Pınar-Özgün-Diren", Ayşe Özdemir, Ebuzer Kalyoncu, Berna Şentürk, Pelin Tören and very sweet junior students Rabia Suluyayla and Aydan Torun, members of Nanotextile Laboratory and all UNAM members that I've met but cannot list here. I thank for all kinds of moral and technical support that I've got from all of them.

I’d like to thank Zeynep Ergül Ülger for numerous helps and moral support which are very valuable and also for funny organizations. I also thank Zeynep Erdoğan and Hüseyin Avni Vural for the helps and the knowledge provided during experiments.

I would like to thank to UNAM (National Nanotechnology Research Center) ,TÜBİTAK (The Scientific and Technological Research Council of Turkey) Grants 111M710 and 109T990, TWAS Grant, IRG249219 and Loreal Young Women Investigator Award for financial support.

Finally, I’d like to thank to my family and relatives for their efforts during my education which are vey important.

## LIST OF ABBREVIATIONS

| | |
|---|---|
| PA: | Peptide Amphiphile |
| ECM: | Extracellular Matrix |
| GAG: | Glycosaminoglycan |
| MSC: | Mesenchymal stem cell |
| FGF: | Fibroblast growth factor |
| TGF-β: | Transforming growth factor- β |
| BMP: | Bone morphogenetic protein |
| F-moc: | 9-Fluorenylmethoxycarbonyl |
| HBTU: | 2-(1H-Benzotriazol-1-yl)-1,1,3,3-tetramethyluronium hexafluorophosphate |
| DIEA: | N, N-Diisopropylethylamine |
| DMF: | Dimethylformamide |
| TFA: | Trifluoroacetic Acid |
| LC-MS: | Liquid Chromatography-Mass Spectrometry |
| HPLC: | High performance liquid chromatography |
| DMEM: | Dulbecco's modified Eagle's medium |
| FBS: | Fetal Bovine serum |

| | |
|---|---|
| MTT: | (3-(4,5-Dimethylthiazol-2-yl)-2,5-diphenyltetrazolium bromide |
| PBS: | Phosphate buffered saline |
| PFA: | Paraformaldehyde |
| LM: | Light microscopy |
| SEM: | Scanning Electron Microscopy |
| CD: | Circular Dichroism |
| ACh: | Acetylcholine |
| Ly6SF: | Ly6 Superfamily |
| KO: | Knockout |
| WT: | Wild type |
| ChAT: | Choline acetyltransferase |
| GPI: | Glycosyl phosphotidylinositol |
| nAChR: | Nicotinic acetylcholine receptors |
| mAChR: | Muscarinic acetylcholine receptors |
| GFP: | Green Fluorescent Protein |

**TABLE OF CONTENTS**

**CHAPTER 1FUNCTIONAL PEPTIDE AMPHIPHILES FOR CARTILAGE TISSUE REGENERATION ..... 1**

**1.1 Introduction ..... 1**

1.1.1 Biochemical composition of cartilage tissue ..... 2

1.1.2 Cartilage Tissue Engineering ..... 3

1.1.2.1 Artificial scaffolds for cartilage tissue engineering ..... 4

1.1.2.1.1 Basic properties of scaffold forming materials: biocompatibility, bioresorption and biodegradability ..... 5

1.1.2.1.2 Biochemical properties of scaffold materials for enhancing bioactivity ..... 8

1.1.2.1.3 Natural polymers ..... 9

1.1.2.1.4 Synthetic polymers ..... 14

1.1.2.1.5 Synthetic peptides ..... 16

1.1.2.1.6 Structural and mechanical properties of the scaffolds ..... 20

1.1.2.1.7 Injectable formulations ..... 24

1.1.2.2 Cell sources for cartilage tissue engineering ..... 26

1.1.3 Cartilage and Chondrocyte Biology for Tissue engineering ..... 27

1.1.3.1 A general perspective for development of skeletal elements ..... 27

1.1.3.2 Chondrogenic differentiation at monolayer cell culture ..... 29

**1.2 Experimental Section ..... 31**

1.2.1 Materials ....31

1.2.2 Design, synthesis and purification of functional peptide amphiphiles for chondrogenic differentiation ....31

1.2.2.1 Synthesis of peptide amphiphiles....35

1.2.2.2 Purification of peptide amphiphiles ....36

1.2.3 Chemical and physical characterization of peptide amphiphiles and peptide amphiphile combinations....36

1.2.3.1 LC-MS ....36

1.2.3.2 Oscillatory rheology....37

1.2.3.3 Circular Dichroism....37

1.2.4 Monolayer (2D) culture of ATDC5 cells on peptide amphiphile scaffolds....38

1.2.4.1 Peptide amphiphile coating on polystyrene multiwell plates ....38

1.2.4.2 Monolayer culture conditions ....39

1.2.4.3 MTT assay ....39

1.2.4.4 Quantitative analysis of aggregates ....39

1.2.4.5 Safranin-O staining ....40

1.2.4.6 Scanning electron microscopy ....40

1.2.4.7 Immunocytochemistry ....40

**1.3 Results and Discussion....41**

1.3.1 Characterization of peptide amphiphiles and peptide amphiphile scaffolds ..... ....41

1.3.2 Monolayer culture of ATDC5 cells on scaffolds ..... 56

1.3.2.1 MTT assay ..... 56

1.3.2.2 Formation of ATDC5 aggregates ..... 59

1.3.2.3 Morphology of aggregates and ATDC5 cells on different scaffolds ..... 59

1.3.2.4 Quantitative analysis of aggregates on different peptide amphiphile scaffolds .... 63

1.3.2.5 Safranin-O Staining ..... 69

1.3.2.6 Scanning Electron Microscopy ..... 72

1.3.2.7 Immunocytochemistry ..... 74

**1.4 Conclusion ..... 75**

**CHAPTER 2MORPHOLOGICAL ANALYSIS OF VARIOUS ORGANS FROM LYNX-3 BAC TRANSGENIC MICE IN COMPARISON WITH WILD TYPE MICE ..... 77**

**2.1 Introduction ..... 77**

2.1.1 LY6 superfamily of genes/proteins ..... 78

2.1.2 Lynx homologous genes ..... 79

2.1.3 Acetylcholine receptors ..... 81

**2.2 Experimental Section ..... 86**

**2.3 Results and Discussion ..... 87**

2.3.1 Trachea ..... 87

2.3.2 Lungs ..... 90

2.3.3 Esophagus ..... 92

2.3.4 Stomach ..... 94

2.3.5 Thymus ..... 96

2.3.6 Female reproductive organ ..... 98

**2.4 Conclusion ..... 100**

**CHAPTER 3 CHARACTERIZATION OF PEPTIDE AMPHIPHILES AS GENE DELIVERY AGENTS ..... 129**

**3.1 Introduction ..... 101**

3.1.1 Cell Penetrating Peptides ..... 101

3.1.2 Peptide amphiphiles in gene delivery ..... 105

**3.2 Materials and Methods ..... 107**

3.2.1 Materials ..... 107

3.2.2 Design and Synthesis of Peptide Amphiphiles ..... 107

3.2.3 LC-MS ..... 110

3.2.4 Biuret test ..... 110

3.2.5 Gel retardation assay ..... 110

3.2.6 Circular Dichroism ..... 111

3.2.7 In vitro transfection ..... 111

**3.3 Results and Discussion ..... 112**

3.3.1 Characterization of peptide amphiphile-DNA complexes ..... 112

3.3.2 In vitro transfection....121

**3.3.3 Conclusion ....122**

**TABLE OF FIGURES**

**Figure 1.** Scaffold as a template for cell adhesion and proliferation. .....5

**Figure 2.** Synthetic peptides in articular cartilage regeneration. .....20

**Figure 3.** Basic structure of articular cartilage and strategies for recapitulating architectural features .....23

**Figure 4.** Postulated condensation steps during cartilage formation .....30

**Figure 5.** Chemical structures of peptide amphiphiles (a) Glu-PA, (b) Lys-PA, (c) GAG-PA .....33

**Figure 6.** Schematics of Fmoc Solid Phase Peptide Synthesis .....34

**Figure 7.** Electrospray ionization mass spectra of the Glu-PA.....43

**Figure 8.** Reverse Phase-HPLC chromatogram of Glu-PA. Retention time 12-13 minutes .....44

**Figure 9.** Electrospray ionization mass spectra of the Lys-PA.....45

**Figure 10.** Reverse phase-HPLC chromatogram of Lys-PA. .....46

**Figure 11.** Electrospray ionization mass spectra of the GAG-PA. .....47

**Figure 12.** Reverse phase-HPLC chromatogram of GAG-PA. Retention time 10-11 minutes .....48

**Figure 13.** Circular Dichroism spectra for various PA combinations .....51

**Figure 14.** Strain sweep oscillatory rheology measurements of gels with GAG-PA, .....53

**Figure 15.** Strain sweep oscillatory rheology measurements of gels without GAG-PA, ..54

**Figure 16.** Strain and loss moduli of gels at 0.5% strain and 10 rad/s, .....55

**Figure 17.** MTT assay cell quantities normalized with respect to cells grown on tissue culture plate .....58

**Figure 18** ATDC5 cells grown on GAG-PA/Lys-PA (- charge) .....61

**Figure 19** ATDC5 cells grown on Glu-PA/Lys-PA .....62

**Figure 20.** Average aggregate areas for ATDC5 cells grown on GAG-PA/Lys-PA (neutral), GAG-PA/Lys-PA (- charge), Lys-PA/Glu-PA (neutral) and Lys-PA/Glu-PA (- charge) for 18 days in media without insulin (at top), or with insulin (at bottom). .....65

**Figure 21.** Total areas for ATDC5 cells grown on GAG-PA/Lys-PA (neutral), GAG-PA/Lys-PA (- charge), Lys-PA/Glu-PA (neutral) and Lys-PA/Glu-PA (- charge) for 18 days in media without insulin (at top), or with insulin (at bottom). .....66

**Figure 22.** Number of aggregates for ATDC5 cells grown on GAG-PA/Lys-PA (neutral), GAG-PA/Lys-PA (- charge), Lys-PA/Glu-PA (neutral) and Lys-PA/Glu-PA (- charge) for 18 days in media without insulin (at top), or with insulin (at bottom). .....67

**Figure 23.**Average perimeters for ATDC5 cells grown on GAG-PA/Lys-PA (neutral), GAG-PA/Lys-PA (- charge), Lys-PA/Glu-PA (neutral) and Lys-PA/Glu-PA (- charge) for 18 days in media without insulin (at top), or with insulin (at bottom). .....68

**Figure 24.** Safranin-O staining of ATDC5 cells and primary rabbit chondrocytes. .....70

**Figure 25.** Safranin-O staining of ATDC5 cells and primary rabbit chondrocytes. .....71

**Figure 26.** Aggregates observed with SEM at various scales .....73

**Figure 27.** Collagen II expression within an aggregate grown on Glu PA/Lys PA (- charge) .....74

**Figure 28.** Chemical structure of acetylcholine, acetylcholine is an ester of acetic acid and N,N,N-trimethylethanolammonium cation .....81

**Figure 29.** Hematoxyline & Eosin stained sections of cartilaginous airways of various phenotypes. .....89

**Figure 30.** Hematoxyline & Eosin stained sections of lungs for lynx3 expressing and lynx3 deficient mice. ....91

**Figure 31.** Hematoxyline & Eosin stained sections of esophagus for lynx3 expressing and lynx3 deficient mice. ....93

**Figure 32.** Hematoxyline & Eosin stained sections of esophagus for lynx3 expressing and lynx3 deficient mice. ....95

**Figure 33.** Hematoxyline & Eosin stained sections of thymus for lynx3 expressing and lynx3 deficient mice. ....97

**Figure 34.** Hematoxyline & Eosin stained sections of female reproductive organμ for lynx3 expressing and lynx3 deficient mice. ....99

**Figure 35.** Chemical structures of peptide amphiphiles ....108

**Figure 36.** Agarose gel electrophoresis of peptide amphiphile-DNA complexes at various charge ratios and naked DNA....113

**Figure 37.** Agarose gel electrophoresis of several peptide amphiphile-DNA complexes at 2:1 positive to negative charge ratio....114

**Figure 38.** Circular Dichroism spectra of peptide amphiphiles at changing molar concentrations....116

**Figure 39.** Circular Dichroism of peptide amphiphile-DNA complexes at 2:1 positive to negative charge ratio (Z+/Z-) ....117

**Figure 40.** Circular Dichroism of peptide amphiphile-DNA complexes at 4:1 positive to negative charge ratio (Z+/Z-) ....118

**Figure 41.** Circular Dichroism of peptide amphiphile-DNA complexes at 10:1 positive to negative charge ratio (Z+/Z-) ....119

**Figure 42.** Circular Dichroism of peptide amphiphile-DNA complexes at 20:1 positive to negative charge ratio (Z+/Z-) ....120

**Figure 43.** Transfected MCF7 cells with plasmid DNA-peptide amphiphile complexes and naked DNA on day 2. .....121

# CHAPTER 1

# BIOACTIVE PEPTIDE AMPHIPHILE NANOFIBERS FOR CARTILAGE TISSUE REGENERATION

This work is partially described in the following publication:

Tombuloglu, A.T.; Guler, M.O.; Tekinay, A.B.; Materials for Articular Cartilage Regeneration. *Recent Patents on Biomedical Engineering*. 2012, X, X-X.

## 1.1 Introduction

Many health problems remaining to be untreatable throughout the human history can be overcome by utilizing new biomedical materials. Healing cartilage defects is one of the problems causing significant health issue due to low regeneration capacity of the cartilage tissue. Scaffolds as three-dimensional functional networks provide promising tools for complete regeneration of the cartilage tissue. Diversity of materials and fabrication methods give rise to many forms of scaffolds including injectable and mechanically stable ones. Various approaches can be considered depending on the condition of cartilage defect. A scaffold should maintain tissue function within a short time, and should be easily applied in order to minimally harm the body.

Peptide amphiphiles seem to be promising materials for supporting cartilage regeneration. In this study, the aim was to investigate the potential of peptide amphiphiles as materials for cartilage tissue regeneration.

### 1.1.1 Biochemical composition of cartilage tissue

Cartilage tissue has a characteristic environment with high water content. Water content of the articular cartilage constitutes about the 70% of the cartilage weight [1]. Proteoglycan molecules; the proteins bearing attached carbohydrate chains with high negative charge density are the main elements responsible with the high water contribution to the tissue. The long carbohydrate chains in the extracellular matrix called glycosaminoglycans are crucial for tissue functionality and integrity. Most of the GAGs carry negative charges which attract positively charged molecules and this results in osmotic pressure driven capture of the water molecules. High amount of water causes the tissue to be stiffer and it is very significant for distribution of stresses uniformly throughout the tissue. Moreover, GAG molecules act as reservoirs for growth factors and they can be essential for proper functioning of growth factor molecules. Aggrecan is the most prominent proteoglycan and it contains chondroitin sulfate chains on its protein core. Perlecan is another proteoglycan, having attached chondroitin sulfate and heparane sulfate on its backbone. Its presence was shown to be required for cartilage tissue formation. Decorin, biglycan and fibromodulin are other proteoglycans that are smaller and these are important for tissue function and arrangement as they interact with other ECM components [2, 3].

Collagens, especially collagen II, are the most populated proteins in cartilage tissue. They are of vital importance for the tissue [4]. Aggrecan, and collagen II, a member of the collagen family, are thought to be characteristic markers of cartilage tissue. A cartilaginous tissue is usually described as having high collagen II/collagen I ratio and high aggrecan content. If the collagen II/ collagen I ratio increases in a mesenchymal stem

cell population or if the amount of aggrecan increases, these are considered to be indications for differentiation into cartilage tissue [3, 5]. Besides collagen II, other members of the collagen family such as collagen VI, IX, X, and XI are also present in the cartilage in considerable amounts. Close microenvironment of the chondrocytes is rich in collagen VI. Collagen X is generally found in calcified areas [6].

### 1.1.2 Cartilage Tissue Engineering

Unlike many other tissues, articular cartilage does not have sufficient regenerative capacity in case of an injury due to i) absence of vasculature, which limits access to blood and lymphatic elements and ii) absence of neurons, which isolates the tissue from regulatory mechanisms of nervous system. Regenerative response may be possible if blood finds a way to reach the defect area from underlying bone to form fibrin matrices where cells can proliferate. Chondrocytes are densely covered with extracellular matrix and have limited capacity for proliferation and migration to heal the defect in adult tissues. Only bone marrow cells can attempt to restore the defect through a fracture in the cartilage tissue. Complete regeneration of the cartilage tissue is rarely observed [7]. Osteoarthritis is a prevalent joint disorder and is a major cause of cartilage injuries affecting mostly individuals over age of 65 [8]. Severe pain, loss of motility and stiffness are among its symptoms. Several pharmacological and surgical therapeutic strategies have previously been developed for the treatment of osteoarthritis [9]. Utilization of biomedical materials, which is a relatively novel approach, is recently being used in surgical practices.

#### 1.1.2.1 Artificial scaffolds for cartilage tissue engineering

Scaffold materials can be produced for various purposes depending on the nature of the cartilage defect and the surgical procedure that will be utilized. Novel material compositions or techniques for scaffold construction can be developed for objectives including culturing and differentiation of cells in vitro [10], administration of cells to defect site [11], administration and controlled release of biologically active agents such as growth factors [12], genes [13] or drugs [12] to the defect site, providing mechanical support for cells at the defect site [14], or attracting cells and active factors [15] within the defect. A common rationale behind using three-dimensional scaffolds is to enhance cellular adhesion and proliferation to form a functional tissue and to allow for transport of nutrients and waste (Figure 1). In general, healing a target tissue requires use of an appropriate cell source along with a scaffold. For cartilage tissue regeneration, chondrocytes or other cells capable of becoming chondrocytes are used as the cell source. Chondrocytes, typically exhibit round morphology and express high levels of aggrecan and collagen II. In a monolayer culture, chondrocytes lose their phenotype and become fibroblast-like cells, whereas three-dimensional scaffolds generally don't lead to dedifferentiation. Fibroblast-like cells are not qualified as chondrocytes to form completely functional cartilage tissue [16]. Therefore, a scaffold for cartilage tissue regeneration should support the chondrocyte phenotype and synthesis of cartilage extracellular matrix.

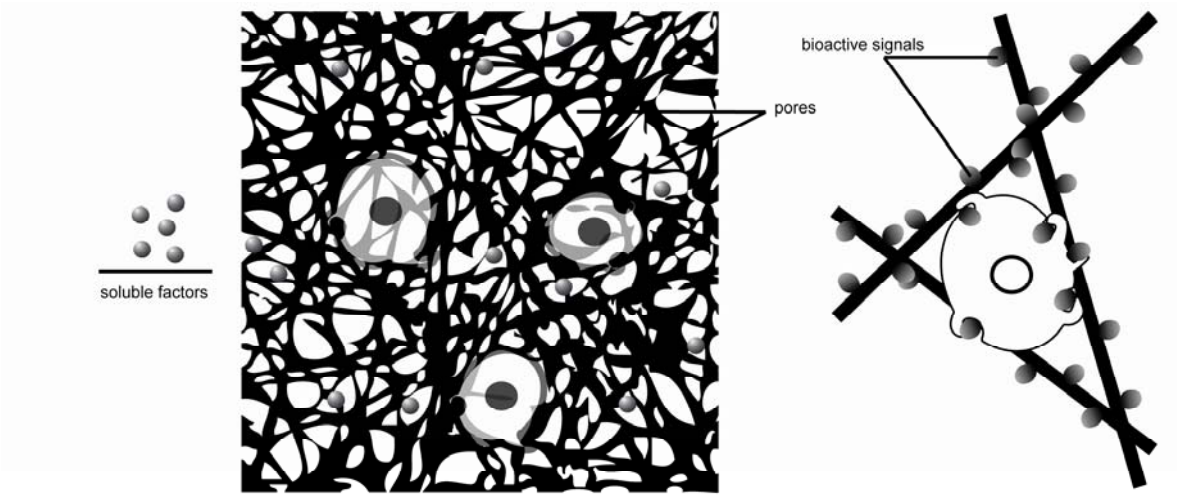


**Figure 1.** Scaffold as a template for cell adhesion and proliferation. Scaffold provides an extracellular matrix like environment for cells at the defect site. Ideally, a scaffold for cartilage regeneration should have interconnected pores allowing movement of cells and free diffusion of soluble factors. Cells can sense and react to bioactive signals incorporated within the scaffold which results in overall improvement in functional tissue formation.

### 1.1.2.1.1 Basic properties of scaffold forming materials: biocompatibility, bioresorption and biodegradability

As knowledge for interaction of materials with biological elements has expanded, various requirements have emerged and they lead to development of enhanced new therapeutic approaches. In earlier biomedical materials, major emphasis was on compatibility of materials within the body, more prominently on minimal immunogenicity and toxicity. Later, well integration of materials to its close biological environment became an important issue. Biocompatibility involves both the ability of the scaffold to be well integrated to its biological environment and its constituent cells, in addition to not causing any undesirable immunogenic responses or toxic outcomes [17]. Biocompatibility is generally considered on basis of individual materials rather than devices composed of processed materials. However, it would be better to assess the biocompatibility of devices

in their complete forms since surface characteristics and architecture of devices may lead to undesired effects [18].

Hydrophilicity of a biomaterial is a key parameter affecting cell adhesion and proliferation properties, which are important for integration of the material within the surrounding tissue. In some studies, altering hydrophilicity was used for improving biocompatibility of materials. For example, by combining hydrophilic blocks within polymers, better cell adherence, and improved biocompatibility were obtained [19]. In another patent, a method for increasing the hydrophilicity of tissue constructs was described. Gas-clustered ion beam irradiation was used for rendering tissue constructs prone to cell adhesion and growth [20]. Blending natural biopolymers is another way to improve hydrophilicity for better cell adhesion and proliferation [21].

Scaffolds that are composed of natural materials are generally biocompatible with similar hydrophilic content and chemical cues with cartilage microenvironment. On the other hand, chemical production processes, additives or immunogenicity of these materials can be problematic. Cross-linking agents and chemical modifications can decrease biocompatibility due to cytotoxic effects [10]. To avoid possible harmful effects, less toxic or non-toxic cross-linking agents might be preferred. An example of such cross-linking agents is tripolyphoshate, which was offered for producing biocompatible chitosan nanoparticles [22]. Succinimydylated polyethylene glycol synthesized as a cross-linking agent is able to carry out cross-linking at physiological conditions and has low cytotoxicity [23]. A series of alternative techniques involving mixing basic components of cartilage extracellular matrix under controlled conditions comprise a way to achieve cartilage like matrices. These techniques, collectively called as self organization methods, do not require the use of any organic solvents or cross-linking reagents [24].

Immunogenicity risk is especially high for tissue materials obtained from other species. Materials of interspecies origin should be totally purified from immunoreactive components, particularly alpha-gal epitope on cells of non-primate organisms, which are known to lead to severe immune reactions. A way of eliminating immunogenicity of non-human extracellular matrix is to treat the matrices with galactosidases after destructing cells through lysing and/or gamma irradiation [25]. Decellularization of extracellular matrix obtained from alpha 1,3 galactosyltransferase deficient organisms also results in loss of immunogenic response to a great extent [26]. Natural polymers as a scaffold material are generally regarded as less immunogenic than synthetic polymers. However, enzymatic treatment may be required to remove immunogenic fragments within proteins [27] and filtering may be essential to remove endotoxins, which may induce inflammation [28]. Culturing constructed scaffolds within an inner cavity of the body is a way of immune conditioning to prevent rejection of the scaffold [29].

Development of bioresorbable materials has been desired in applications for replacement of material with newly forming tissue. Bioresorbability and biodegradability are similar terms; biodegradability is breakdown of macromolecules to smaller subunits; and bioresorbability is elimination of the subunits from the body [30]. Bioresorbability is important, since degradation products may accumulate in the site leading to undesired outcomes such as incomplete regeneration of defects. During restoration of cartilage defects, implanted matrix should be gradually replaced by healthy cartilage tissue, thus materials with very slow degradation rates are not usually preferred. Degradation rate should match the rate of new tissue formation, since rapid degradation may lead to loss of mechanical support and elimination of cellular extracellular matrix deposition. For cartilage regeneration, materials that can stay largely intact for four to ten weeks are

preferred [31]. For these reasons, developing methods allowing controlled degradation rate of materials is important. For controlled biodegradation, cross-linking density [5, 11, 26[11, 32], monomer composition [33], or hydrophilicity [34] can be altered. It is also possible to control degradation properties of scaffolds by incorporating peptide sequences that are susceptible to metalloproteinases. Incorporating peptides particularly specific to cleavage by MMP-7 enzymes within scaffolds is a way to make them more degradable as the cells differentiate into chondrocyte lineage due to increased activity of MMP-7 enzymes in the course of chondrogenic differentiation [35]. With suitable modifications, optimal degradation rate can be obtained.

#### 1.1.2.1.2 Biochemical properties of scaffold materials for enhancing bioactivity

Bioactivity is one of the most important aspects protected by various patents. Altering the behavior of cells in a way that cells change their gene expression profile, adhere specifically, proliferate or differentiate are different means of bioactivity. In the case of natural polymers, bioactivity results from the cues already present within the backbone in many cases. However, synthetic polymers generally lack the necessary bioactivity. Therefore, many patents on synthetic polymers include additional signals enhancing bioactivity. Bioactivity enhancing signals can be various epitopes incorporated within the polymer backbone or growth factors specific for the tissue. Peptides can be conjugated to polymers by using nucleophilic addition chemistry. Strong nucleophiles such as thiol groups in cysteine residues and conjugated unsaturated groups such as acrylates provide attachment sites between peptides and the polymer backbone [36]. Using growth factors with the scaffolds is a common approach for stimulating cells to repair the tissue. Growth

factors within TGF-beta superfamily, particularly BMP subtypes, are frequently preferred for articular cartilage regeneration [12, 37-39]. Proteins binding to BMPs [40]or genes encoding growth factors [13] can also be supplemented for additional bioactivity. For a better understanding of bioactivity, natural polymers, synthetic polymers and peptides for cartilage regeneration will be described below.

#### 1.1.2.1.3 Natural polymers

Natural biomaterials extensively studied as artificial scaffolds involve native cartilage extracellular matrix biopolymers including collagen, hyaluronic acid, chondroitin sulfate, and other naturally derived polymers (e.g. fibrin, alginate, chitosan and silk). In many inventions, hyaluronic acid, chondroitin sulfate and collagen are included within scaffolds for promoting cartilage tissue formation within the defect [25, 41].

Constituting 15% of the wet cartilage tissue, collagen is a major element of mechanical, structural and also biochemical importance. Among a plethora of proteins, collagen II is the most abundant protein within articular cartilage tissue. Increased activity of collagenases and denaturation of collagen II within cartilage is considered as an indication of osteoarthritis [42, 43]. As the most abundant protein in extracellular matrix, collagen is a widely used biomaterial for tissue engineering. Patented collagen based scaffolds are composed of primarily collagen II or a mixture of collagen I and collagen II [41, 44, 45]. Matrices with high collagen I content were reported to be better at attracting cells from subchondral tissue within the defect and matrices high collagen II content to be better for preventing dedifferentiation of chondrocytes [41].

Collagen is insoluble in cold water due to its secondary structure. When heated, hydrogen bonds contributing to secondary structure are broken and collagen gradually becomes soluble as denaturation takes place [45]. Collagen can be solubilized with the help of pepsin or acetic acid [46, 47]. Treating acidified collagen with enzymes (i.e. pepsin) is beneficial for elimination of immunogenic parts of collagen found at protein terminals. Atellopeptide is a collagen, which lacks immunogenicity due to enzymatic treatment [27].

Use of glycosaminoglycans, particularly, hyaluronic acid and chondroitin sulfate within scaffolds is common due to their bioactivity. In order to increase bioactivity, polysaccharides including glycosaminoglycans can be cross-linked covalently through aldehyde groups obtained by oxidizing terminal hydroxides of saccharide units on the backbone [48]. Injecting a blend of hyaluronan and chondroitin sulfate salts within a cartilage defect provided as much as 94.5% regeneration [49]. Hyaluronic acid is a prominent polysaccharide with its chondroprotective, anti-inflammatory, analgesic properties and bioactivity [50]. Hyaluronic acid formulations without any modification provide insufficient mechanical properties and short retention times within the joint. Cross-linking and hydrophobic modification techniques are used for eliminating mechanical weakness of hyaluronic acid based scaffolds [51]. A common strategy for strengthening the hyaluronic acid scaffolds is esterification of free carboxyl groups of glucuronic acid with a variety of alcohols (HYAFF®) [52]. These polymers can vary in solubility and mechanical strength depending on the extent of esterification and the type of alcohols used. HYAFF® polymers can be processed in order obtain fibers, sponges and microspheres [53]. Culturing chondrocytes from various sources within HYAFF11, a benzyl ester of hyaluronic acid, was successful in maintaining chondrocyte phenotypes

and providing uniform proliferation of cells. In a recent patent, benzyl esters of hyaluronic acid and auto-cross-linked hyaluronic acid for three dimensional matrices to encapsulate chondrocytes or mesenchymal cells were disclosed. Auto-cross-linked hyaluronic acid is obtained by internal esterification in which free carboxyl groups react with hydroxide groups to provide intra or inter molecular cross-linkages [54].

Methods for esterification of hyaluronic acid with hydrophobic organic molecules can be used for attachment of insoluble drugs such as rhein on hyaluronic acid backbone facilitating intra-articular administration of these drugs. Micrometer sized particles of hyaluronic acid were utilized for this purpose. These particles were produced at very low temperature and by conjugation to hydrophobic molecules with suitable solvents and dialyzing [55]. Esterifying rhein with hyaluronic acid can also be carried out by reacting hyaluronic acid with acid chloride of rhein in non-polar aprotic solvents. Esterified product which involves rhein, exhibited improved chondroprotective effect compared to unmodified hyaluronic acid [56]. Cross-linking hyaluronic acid is possible by incorporating diverse functional groups on the hyaluronic acid [57]. Photo-cross-linking is another option for enhancing mechanical properties and durability of hyaluronic acid. For this purpose, photoreactive reagents like divinylsulfone [58], or propiophenone [59], can be inserted on the backbone. Hyaluronic acid has protective role in cartilage degeneration and due to this function, it is substantially used in formulations for treating degenerative diseases such as osteoarthritis. Molecular weight of hyaluronic acid affects the efficiency of protection in a way that protective function of hyaluronic acid gets better with increased molecular weight of the polysaccharide [60].

Fibrinogen is a soluble plasma glycoprotein that takes part in blood coagulation cascades. Fibrin, the polymeric form of fibrinogen, is a naturally occurring scaffold formed in the case of injury to support the local cells [61]. A fibrin scaffold is subject to fibrinolysis, and the degradation rate increases with time, which may be beneficial for offering flexibility in tissue formation. On the other hand, fast degradation may result in production of insufficient amount of extracellular matrix and lack of mechanical stiffness [62, 63]. Anti-fibrinolytic agents may be included to provide the scaffold longer-term durability [10, 64]. However, anti-fibrinolytic agents decrease the biocompability of the scaffolds [65]. Stable fibrin scaffold without any anti-fibrinolytic agents is prepared by pouring plasma protein solution, which doesn't include thrombin, onto molded thrombin solution and freeze drying the clotted blend. Implantation of obtained sponge doesn't require completely open surgery and two independent surgical interventions [66].

Chitosan, is a linear polysaccharide composed of 1,4 linked β-D-glucosamine residues, which exhibit N-acetyl glucosamine groups. Chitosan has a polycationic backbone and it can form hydrogels with the negatively charged glycosaminoglycans. Remarkable similarity of chitosan with glycosaminoglycans is also an important feature, which may facilitate interaction with signaling proteins and provide material for extracellular matrix synthesis [67]. The glucosamine residues found in chitosan are reported to be beneficial for osteoarthritis treatment [68]. Substantial increase in the amount of chondrocytes upon injection of chitosan into the knee articular cavity of rats was demonstrated [69]. Chondrocytes cultured on chitosan substrates remained viable and maintained chondrocyte phenotype [70]. Behind the biocompatibility and biodegradability; antimicrobial properties [71], bioactivity [72] and high abundance of the chitin in nature

[73] make chitosan a potential biomaterial for a scaffold to be used in cartilage tissue regeneration. Chitosan is obtained by deacetylation of chitin; a structural polysaccharide that exist in exoskeletons of invertebrates and fungal cell walls. In such organisms, chitin resorption is balanced for both permitting the growth or morphogenesis and supporting the organism. Thus, it is both enzymatically degradable and has enough strength for providing reinforcement [74]. On the other hand, highly crystalline nature of chitin prevents dissolving the material in various solvents. Therefore, chitin is modified to obtain easily processable forms. Chitosan is generally produced by a process in which chitin is treated with alkaline solutions for the discharge of the acetyl groups. Chitin derivative obtained in this way is soluble in aqueous solution of organic acids [75]. Lysozyme is the major enzyme responsible for degradation of chitosan in human body. It acts primarily on acetylated residues of chitosan. Thus, the degradation rate of chitosan scaffolds within the body can be altered with the extent of the deacetylation. Some chemical modifications via reactive primary amines throughout the backbone for altering degradation rate and mechanical strength are also possible [76, 77]. Use of chitosan as a thermo-gelling scaffold material with suitable additives like glucosamine salts [62], or glycerolphosphate is also remarkable [78, 79].

Alginates are linear polysaccharides similar to chitosan and are synthesized by brown algae such as Laminaria hyperborea and lessonia living in shore waters [80]. They are linear and unbranched block copolymers of 1,4-linked-D-mannuronic acid (M) and L-gluronic acid (G) residues. The building blocks may be sequenced in an alternating (i.e. GMGMGM) or recurring manner (i.e. MMMMM or GGGGGG) according to the source of alginate. Association between carboxylate groups of G blocks and multivalent cations

induces gel formation [81]. Alginates are produced at molecular weights between 50-100,000 kDa. Viscosity and mechanical properties are related to molecular weight distribution, concentration and the stochiometric proportion with the cations [82-84]. Native cartilage-like tissues were reported to be obtained within alginate hydrogel scaffolds [85]. Human mesenchymal stem cells were differentiated to mature chondrocytes in three-dimensional alginate gels in the presence of chondrogenic medium containing TGF-β3 [86].

Silk proteins possess frequently occurring sequences resulting in abundant β-sheet structure providing great mechanical strength to the silk fibers. In their natural form, silk proteins enclose two protein components called fibroin and sericine. Fibroin is a fibrous protein with intense β-sheets constituting the backbone, whereas sericine is an adhesive protein that joins together fibroin fibers. Fibroin isolated from silk can be processed to obtain porous or fibrous matrices. For obtaining fibroin from natural silk, sericine is separated by a process known as degumming. Degumming involves boiling the silk within sodium carbonate solution and extensive washing with water. Among patents based on silk, salt leaching, freeze drying and gas foaming methods were used for making porous scaffolds, and electrospinning with polyethyleneoxide was used for making fibrillar scaffolds [87, 88]. Supplementation of silk fibroins with 30% glycerol stabilized α-helix structures and more malleable films were obtained [89].

#### 1.1.2.1.4 Synthetic polymers

Unlike naturally derived polymers, scaffolds based on synthetic polymers are flexible in design and they don't cause disease transmission. Synthetic polyesters composed of

lactide and glycolide monomers such as PLGA (poly [lactic-lactic-co-glycolic acid]) [90], and PLA (poly lactic acid) [91] constitute a commonly studied group of synthetic materials for cartilage tissue engineering. These materials have been used in medical applications for a long time [92, 93]. Degradation kinetics of these polymers can vary extensively in a scale of days to years depending on molecular weight, polymer morphology, crystallinity and composition [19, 94, 95]. Polymers of ε-caprolactone have good mechanical properties and slower degradability rate. Monomer ε-caprolactone can be copolymerized with glycolic acid and lactic acid. Insolubility of these polymers results in lower cell adhesion. Furthermore, acidic degradation products trigger an autocatalytic mechanism, which effects the fabricated scaffolds negatively [19, 96].

Another synthetic polymer is polyethyleneoxide (PEO), which can be obtained in the form of gel by cross-linking. Semi-interpenetrating network hydrogels supporting function and viability of chondrocytes were obtained by encapsulating chondrocytes in dimethacrylated PEG matrix and subsequently irradiating the PEO-PEODM mixture containing cells for photo-cross-linking [97].

Among other synthetic polymer alternatives for cartilage regeneration are polyurethanes [98, 99], poly (N-isopropyl acrylamide) [100], poly vinyl alcohol [101] and carbon fibers [102].

Naturally derived polymers offer biocompatibility and bioactive signals, while synthetic polymers offer flexibility in design and eliminated risk of contamination. Thus, efforts are directed towards hybrid materials combining the advantages of synthetic and natural materials. In this regard, more research is being carried on to develop various

combinations (involving synthetic polymers poly (α-hydroxy esters) and PEGs, manufactured with collagen [103], hyaluronic acid [104], chondroitin sulfate [105], alginate [106], fibrin [90]).

#### 1.1.2.1.5 Synthetic peptides

Synthetic peptide technology enabled a wide range of opportunities in design and development of regenerative scaffold materials. Disadvantages of synthetic and natural polymers can be partially or completely eliminated with various peptides designed for functionalization or scaffold formation (Figure 2). Synthetic polymers can be made bioactive by modification with peptides [107-109].

Adhesive peptide sequences are important signals, which can be inserted on the backbones of inert synthetic polymers. Biological cell adhesion to extracellular matrix is the result of interaction between integrins, a family of cell surface receptors, and extracellular matrix elements like fibronectin, displaying the specific epitope (i.e. RGDS peptide). Integrins mediate between the extracellular matrix and cytoskeleton, and trigger the intracellular signaling pathways. Peptide nanofiber matrices exhibiting RGDS epitoe at van der Waals density were used for studying cell adhesion [110, 111].

Construction of phage libraries allowed scientists to discover diverse functional peptide sequences. For example, WYRGRL is a peptide sequence revealed by phage display, which can specifically bind to collagens on cartilage tissue [112]. Microparticles functionalized with this peptide can deliver cargo selectively to cartilage tissue, increasing efficiency and mitigating side effects of the delivery system [112]. Another interesting feature of synthetic peptides is that they can form larger assemblies via physical

interactions if they are properly designed. Amphiphilic peptides with alternating hydrophilic and hydrophobic amino acids like poly (Val-Lys) [113], poly (Glu-Ala) [114], poly (Tyr-Lys) [115], poly (Lys-Phe) [116], poly (Lys-Leu), or [(Val-Glu-Val-Orn)1-3]-Val [117] are inclined to assemble into β-sheet structures and form aggregates depending on pH or ionic strength of the medium. These β-sheet forming peptides with alternating polarity can form hydrogels, which are composed of micro-scale long fibers of 10-20 nm in diameter. These hydrogels resemble native cartilage with high water content and dense fibrillar structure and cells can be uniformly dispensed within their fibrillar network. When these hydrogels were used for three-dimensional culture of chondrocytes, they provided appropriate medium for chondrocytes to produce and deposit cartilage-like extracellular matrix for a period of as long as 4 weeks. Mechanical properties of the gels were enhanced, while cells accumulate new extracellular matrix [118]. Peptides, which show random coil to beta hairpin transition in response to various stimuli such as light, change in ionic concentration or pH, also form biocompatible hydrogels suitable for cell culture or cell delivery [119].

A remarkable class of peptidic biomaterials in tissue engineering is composed of β-sheet forming small peptides conjugated to alkyl chains. Commonly known as peptide amphiphiles, these molecules primarily assemble via non-covalent interactions including hydrophobic interactions provided by alkyl chains and hydrogen bonds between amino acid residues to form nanofibrillar networks. Diverse design possibilities exist for these molecules including altering length of the alkyl tail, altering C-terminal amino acids which drive β-sheet formation and branched backbones. For example, modification of C-terminal peptide part of peptide amphiphiles with bioactive molecules can provide these

molecules capability to support differentiation, maintenance, or proliferation of the cells [111, 120]. RGD presenting peptide amphiphiles have been used for a number of tissue engineering applications such as osteogenic differentiation of MSCs [120], or dental tissue regeneration [121]. Peptide amphiphiles with branched backbones were shown to be more effective for supporting cell adhesion and spreading [110, 111]. For culturing and implantation purposes, hydrogels of peptide amphiphiles had promising results for healing cartilage defects and degenerative joint diseases. A novel TGF-beta binding peptide revealed by phage display (i.e. HSNGLPL peptide) was integrated with peptide amphiphile structure to support regeneration of chondral defects and cartilaginous differentiation of mesenchymal stem cells. In vitro culture of mesenchymal stem cells in the presence of TGF-β, on hydrogels of peptide amphiphiles with TGF-β binding epitopes had remarkable results with increased expression of chondrocyte markers. The molecule was also applied with microfracture technique to defects on rabbit knees. When used with TGF-beta, peptide amphiphiles provided restoration of the functional tissue. Moreover, peptide amphiphiles were also capable of forming hyaline-like tissue formation in the absence of growth factor supplement [15, 122].

Peptides can be also designed by modeling functional domains of biologically active proteins. B2A is a synthetic peptide consisting of heparin binding fragment, hydrophobic fragment and BMP receptor binding fragment. With its receptor binding fragment (i.e. AISMLYLDENEKVVL), B2A binds to and modulates BMP2 receptors and promotes chondrogenic differentiation of mesenchymal stem cells [123].

Synthetic peptides resembling natural collagens, called collagen mimetic peptides have been made subject of various inventions [124-126]. In their most basic form, collagen

mimetic peptides have the amino acid sequence –(Pro–Hyp–Gly)x– which is inspired from frequently repeated tripeptide in the amino acid sequence of collagen. Collagen mimetic peptides (CMPs) can form triple helices in aqueous environment, similar to native collagen proteins. Heat denaturation of triple helices formed by collagen mimetic peptides is reversible in contrast to collagen which turns into gelatin when heated. CMP has the ability to bind native or denaturated collagen I fibers. Three-dimensional culture of chondrocytes within PEG hydrogel modified with CMPs, improved synthesis of glycosaminoglycan and collagen compared to control PEG hydrogel. This result indicates improvement in cartilage tissue forming capacity of chondrocytes due to presence of CMPs, which possibly lead to greater interaction of cells with the extracellular matrix [126].

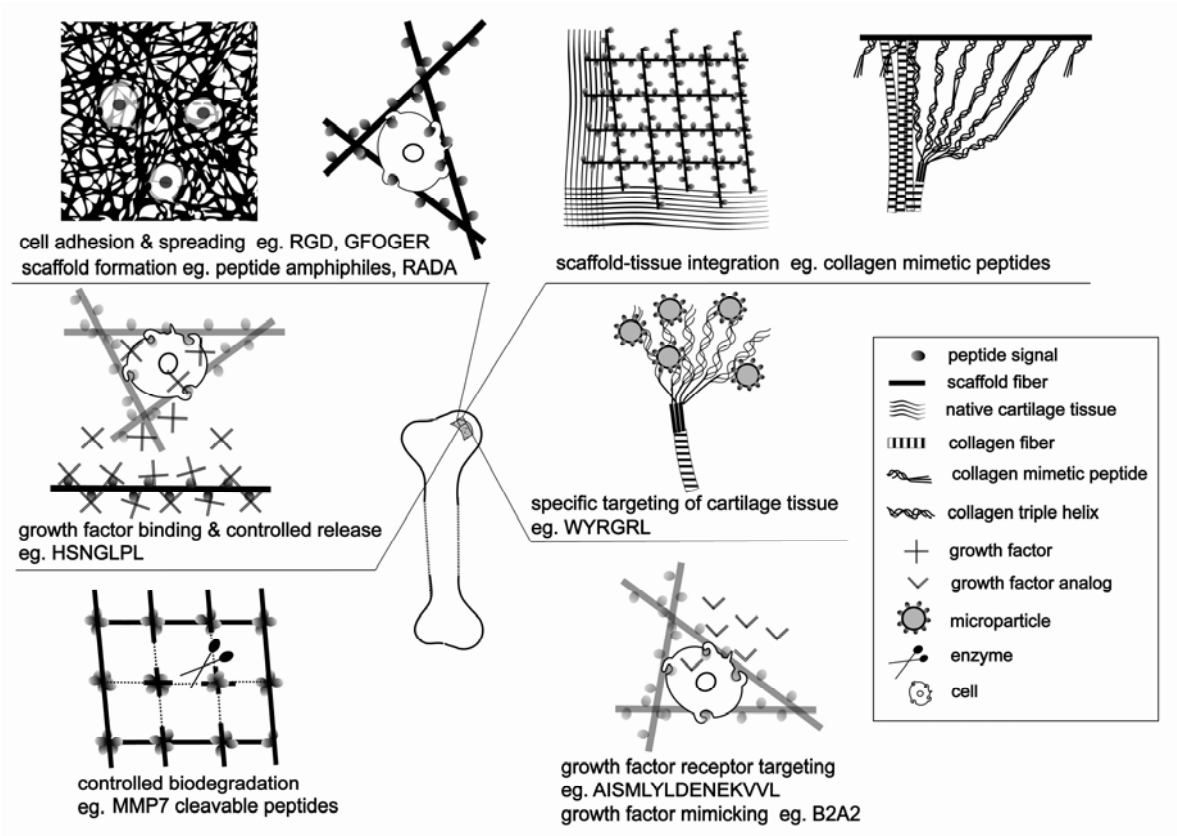


**Figure 2.** Synthetic peptides in articular cartilage regeneration. Peptidic materials can be used for forming scaffolds and for numerous functionalization purposes. Properly designed peptides like peptide amphiphiles might act as building blocks for three dimensional networks on which cells can adhere and proliferate [110,117]. Peptide signals activating integrin mediated pathways such as RGD [110] and GFOGER [126] can be incorporated within scaffold for enhancing cell adhesion and spreading. Peptides may facilitate integration of scaffold with the tissue. Collagen mimetic peptides which are able to anneal with collagen chains of the native tissue constitute an example for specific peptides capable of enhancing integrity between scaffold and tissue [124-127]. Peptides affine to growth factors may be used for decorating scaffold fibers for binding and release of growth factors in a controlled manner [15,122]. Peptides than can specifically bind cartilage components can be used to functionalize microparticles for targeting cartilage tissue and minimize side effects associated with non-specific delivery of agents [112]. Peptides that are susceptible to specific extracellular enzymes may be inserted in the structure of the scaffold. In this way, degradation will be in response to cellular secretion of enzymes which may differ quantitatively during progress of differentiation [35]. Peptides targeting growth factor receptors can be developed for making synthetic growth factor analogs functioning to enhance chondrogenic differentiation [123].

## 1.1.2.1.6 Structural and mechanical properties of the scaffolds

Articular cartilage can withstand very high mechanical loads conducted by bones. Preferably, mechanical properties of scaffolds to be implanted should be similar with the

mechanical properties of native cartilage tissue. Materials should possess sufficient strength and stiffness for providing a temporary support which will act like functional cartilage tissue until complete tissue remodeling is achieved. In several studies, strength and stiffness of matrix was shown to be important in stimulation of various differentiation routes. Cells sense and react to scaffold mechanics by altering gene expression profile [127]. Mechanical properties of materials (i.e. compressive strength) are also important for their handling before and during implantation [128].

Articular cartilage owes its mechanical properties to the orientation of collagen and proteoglycan fibers and high density of negative charges provided by glycosaminoglycans, which draw high amounts of water. Composition and orientation of extracellular fibers vary throughout different zones of cartilage implementing specific mechanical properties at each zone (Figure 3A). An approach for mimicking specific structure of cartilage tissue is to construct hydrogels with multiple layers [129, 130]. In a recent study, three-layered hydrogel including cells was developed to achieve similar architecture to articular cartilage. All layers include polymerizable materials, while hyaluronic acid, chondroitin sulfate and MMP7 cleavable peptides with chondroitin sulfate were included respectively in different layers. Specific components of each layer were shown to stimulate cells to synthesize extracellular matrix proteins differentially enabling mimicking of natural layers within articular cartilage. According to the study, the layers were combined together by cross-linking gelling solution placed on top of the previously formed gel with UV irradiation. This was performed twice to obtain a three-layered gel [130].

Implants with oriented fibers aim to provide improved mechanical properties with better resemblance to architecture of native cartilage, which contains oriented collagen fibers. Electrospinning method has been also used to obtain scaffolds composed of randomly oriented fibers with very high mechanical strength and uniform distribution of fibers [131]. Electrospinning can also be used to obtain uniform scaffolds with fibers oriented in a parallel manner. Constructs with parallel aligned fibers, which could be used both for culturing cells and as implants for osteochondral defects were obtained by collecting electrospun fibers on winding shaft [132]. To make an implant with a similar architecture to fibrillar cartilage, triphasic implant construct with vertically aligned polymer hollow bodies were previously produced [133].

On several patents, hybridizing porous or fibrillar scaffolds with a secondary scaffold was performed for enhancing overall mechanical properties of the scaffold. Porous scaffold combined with a rapid prototyped backbone has advantages of uniformity, interconnectivity and mechanical stability [128]. Highly porous materials encapsulated within outer rims designed to distribute the compressive load were proposed as a possible solution for large articular defects [134]. Another example is three-dimensionally weaved structures filled with gelatinous material. This construct also enables high density seeding of cells with uniform distribution and high overall mechanical strength resembling the natural tissue [14]. Similarly, biphasic sponge-gel composites combine mechanical properties of sponge and cell seeding properties of gel to obtain a greater body [135].

The scaffolds may be constructed in a variety of architectures such as sponges and fibrillar matrices. In all cases, porosity and interconnectivity of the scaffold are important parameters. Cells should be able to infiltrate between pores and migrate to form clusters.

Transport of nutrients and waste should be optimal. Freeze drying is a common process for obtaining porous matrices. An example is highly porous scaffolds obtained by lyophilizing chitosan-acetic acid solutions. The process mechanism depends on the separation of ice crystals from chitosan acetate salts during lyophilization. The pore sizes and pore orientations which are the main parameters influencing mechanical properties of the scaffolds can be controlled with rate of freezing and the geometry of thermal gradients [41, 77, 136]. Enlarging the pores in one side of the scaffold is also possible by leaching method [137].

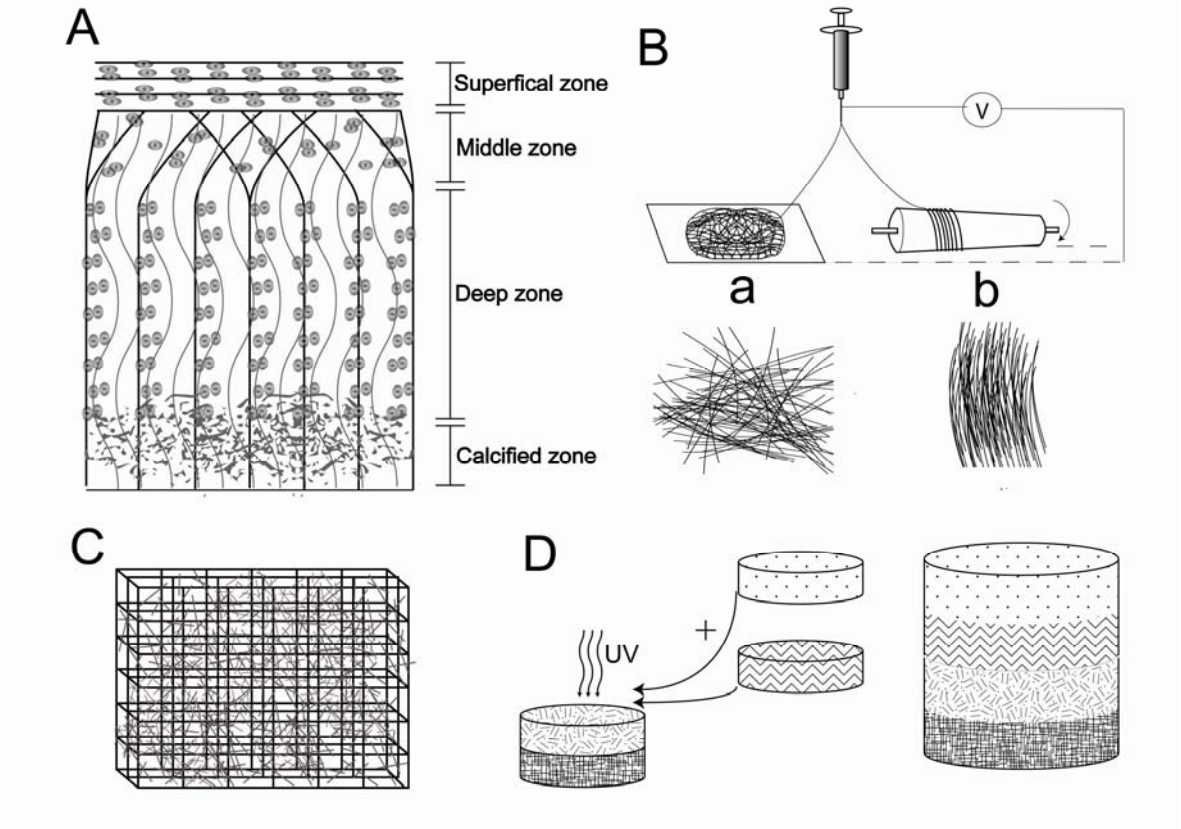


**Figure 3.** Basic structure of articular cartilage and strategies for recapitulating architectural features, (A) Articular cartilage is composed of four distinct zones, superficial zone, middle zone, deep zone and calcified zone. Collagen fibers represented as black lines are arranged in a special way which is crucial for shock absorbing properties and resistance to high compressive loads. In superficial zone, collagen fibers are aligned parallel to each other; in the middle zone, fibers are partially aligned; in deep zone, fibers are mostly perpendicular to the plane of joint surface. Proteoglycans, represented by wavy lines, contribute to

mechanical properties by attracting water. Image was partially adapted from [132]. (B) Electrospinning method can be used for producing fibers aligned (a) randomly [131], or (b) in a parallel fashion [132]. Aligned fibers can be used to reinforce scaffolds like collagen fibers. (C) A scaffold with high mechanical strength can be combined with soft matrices for attachment and uniform distribution of cells. Solid free form techniques offer ways to design convenient architectures which can be shaped to exactly fit into the defect and to achieve mechanical properties similar to cartilage [128]. (D) Separate hydrogels may be used to mimic biochemical composition of different zones. Hydrogels with photosensitive chemical groups can be joined together through UV exposure. Image was partially adapted from [129, 130].

#### 1.1.2.1.7 Injectable formulations

One of the difficulties in the clinical application of engineered scaffolds for cartilage repair is requirement of surgical operation for inserting the scaffold into the defect area. Cross-linked materials in the form of hydrogel can be administered into the joint via injection, but high viscosity may cause difficulty during injection [138]. Thus, in situ forming hydrogels, which can be applied easily with injection, became a center of focus [139]. In general, hydrogels are composed of cross-linked polymer chains and supramolecular constructs that are able to absorb or encapsulate water to an excessive degree. The hydrogels may be formed in situ by injecting water soluble blends that are modified to show their gel forming behaviors under physiological conditions or by an external stimulus. In situ forming hydrogels can be formed by chemical or physical cross-linking of components. Chemical cross-linking is established by joining functional groups on the backbone of polymer chains. Photo-cross-linking is a common example for chemical cross-linking. Physical cross-linking involves van der Waals interactions, hydrophobic interactions, hydrogen interactions and ionic interactions between the constituent atoms or groups of polymer chains [139]. Photo-cross-linkable materials were published in several patents as in situ gelling compositions, which can be applied within cartilage defects. A patented composition involves oligo (poly ethylene glycol) fumarate,

pyrrolidinone monomer and photo-initiator, which can be injected within cartilage defect and polymerized with UV exposure [11]. In another patent, a dual component system was defined in which similar components do not polymerize by themselves. Upon UV exposure interpenetrating or semi-interpenetrating networks are formed [140]. Collagen can also be combined with acrylated polyethylene glycol through artificially inserted thiol groups, which can be photo-polymerized by illuminating with UV to obtain hydrogels [141].

Hydrogels based on thermosensitive polymers, self assembling into micelles above a critical temperature and concentration can be utilized as injectable biomaterials for cartilage regeneration. Glycerol phosphate added chitosan solution is a well known thermo-gelling system, which shows transition to gel between 30-60 °C. Gelation occurs possibly through weakening of chitosan and water interactions due to glycerol phosphate mediated reorientation of water molecules and clustering of chitosan molecules into a larger assembly [78]. Chitosan and glycerol phosphate tend to gel or precipitate at room temperature when stored as a mixture. Holding these separately and mixing prior to implantation brought the advantage of longer term storage without formation of unstable structures [79]. Chitosan glucosamine salt compositions, which are injectable solutions with pH 6.5-7.6 at room temperature, can form gels when temperature exceeds a critical point which is about 25 °C[67].

Various block polymers such as PEO-PLGA-PEO tend to gel in response to increase in temperature and these constitute alternative biocompatible in situ gelling systems [138]. Repair of cartilage defects with poly (DL-lactic acid-co-glycolic acid) / (poly (ethylene glycol) graft copolymer showing sol-gel transition above 37 °C has been reported [142].

Hyaluronic acid can be attached to thermo-gelling block copolymers for prolonging the retention time of hyaluronic acid in the joint cavity. Modified hyaluronic acid product is also easily injectable and gels in the body [138].

Some of the patented injectable formulations include solutions, which can gel inside the body by interacting with abundant cations found within extracellular medium. Additional salts may be supplemented for better gelation. Alginate is a material which can gel by injection with divalent cations [86]. Acid solubilized collagen can be dialyzed against EDTA for removing trace amount of salts. Collagen solution obtained this way rapidly forms gel through fibrillogenesis when exposed to salts or fluids at 37 °C [46, 143].

Peptide amphiphile molecules can also function as in situ forming injectable gels triggered by concentration, divalent cations or pH. Assemblies reaching from scales of microns to centimeters can be obtained [110, 111, 144]. Soluble peptidic materials can form three-dimensional matrices depending on the physical and chemical properties of their sequences. Amphiphilic peptides with alternating hydrophilicity can be delivered into the cavity with cells and bioactive agents. These peptides can form hydrogels that can encapsulate water in the range of 99-99.9% [118].

#### 1.1.2.2 Cell sources for cartilage tissue engineering

Chondrocytes from hyaline cartilage and nasal cartilage can be used as cell sources [145]. The cells are however unstable in monolayer (2D) culture; synthesis of proteoglycans and collagen II reduces while collagen I expression is upregulated. As a result, cells become fibroblast-like, losing phenotype as cartilage cells. Redifferentiation to original phenotype may be stimulated by culturing fibroblast-like cells in three dimensional environment.

Using serum free culture and FGF-2 supplementation lessen the effect of dedifferentiation and enables easier transition to chondrocyte phenotype [146]. Donor tissues may not be found frequently, another obstacle for utilization of chondrocytes as cell sources [145, 147].

Mesenchymal stromal cells isolated from adipose and bone marrow may also be utilized for cartilage tissue engineering [148]. MSCs are known as immunoregulatory cells as they are able to be ignored by immune recognition and block the host defense mechanisms [149].

Another potential cell source for producing cartilage may be the chondrocyte precursors which can easily differentiate into chondrocytes when suitable conditions are supplied. Inner layer of periosteum consists of osteoblastic cells, responsible for local appositional bone growth. Osteoprogenitor cells produced in this layer mostly become osteoblasts but they also posses the chondrogenic potential [150].

### 1.1.3 Cartilage and Chondrocyte Biology for Tissue engineering

#### 1.1.3.1 A general perspective for development of skeletal elements

The origin of long skeletal elements for a tetrapod can be traced back to the formation of limb bud during embryogenesis. Cells from lateral plate mesoderm at specific locations in the flank become determined to form the limb primordium at specific limb fields. Exact mechanism for limb field positioning has not yet been elucidated. However, Hox genes such as Hoxc6, Hoxc8, and Hoxb5 are known to be major regulators for specification of forelimb and hindlimb locations [151]. After determination of the limb field positions,

specified cells within lateral plate mesoderm proliferate with a significantly higher cell division rate than non-determined cells [152]. As a result of differential proliferation, limb bud consisting of mesenchyme cells covered with an ectodermal jacket develops.

At the most distal part of limb buds, ectodermal cells grow thicker to form a specialized structure called Apical Ectodermal Ridge (AER). Interaction of AER with mesodermal cells is particularly important for limb bud development. Its removal was reported to be resulting in cessation of limb bud growth [153, 154]. Adjacent to AER is the progress zone, where cells proliferate in the opposite direction to ectodermal ridge. Zone of polarizing activity, another important feature for limb bud development, is thought to act in symmetry [155].

To date, two different views exist for how joints between skeletal elements become specified. According to first view, formation of long bones starts with mesenchymal condensations which exist as uninterrupted bodies. The proximal part of a mesenchymal body gives rise to humerus or femur, distal part soon becomes radius/ulna or tibia/fibula and digits. During developmental progress, firstly, cells within mesenchymal bodies differentiate to chondrogenic cells as a response to secreted growth factors. For some cells at the putative joint region, ongoing chondrogenic differentiation is suppressed with antagonistic chemokines; choggin and nordin. These nonchondrocytic cells form the interzone separating the skeletal elements consisting of chondrocytic cells. In this way, three layers occur within the condensation, interzone and two outer layers. Joint ligaments, synovial lining originate from the cells of the interzone, the outer layers become the bones and the cartilage tissue covering the ends of bones [156].

According to the other view, after mesenchymal condensation, skeletal elements which would later become bones, are initiated as independent chondrogenic entities and continue developing independently. Bones, humerus, radius and ulna, for example start as three discrete cartilaginous regions in a Y shaped mesenchymal condensation. Articular cartilage forms later as the cells from interzonal region differentiate to chondrocytes [157].

Mesenchymal condensations, has been a subject of major interest, in order to enlighten skeletal development. Many mutations related to developmental abnormalities show their effect at the condensation stage [158].

### 1.1.3.2 Chondrogenic differentiation at monolayer cell culture

At monolayer culture, chondrogenic differentiation is many times accompanied by aggregate formation similar to mesenchymal condensation at development. Monolayer culture studies with chondroprogenitor cells and mesenchymal cells have also been performed.

ATDC5 is a feeder independent teratoma stem cell line. In the presence of insulin, ATDC5 cells migrate to form clusters which then become aggregates of approximately 100 μm diameter. Chondrocyte markers like Collagen II, Aggrecan, Sox 9 are expressed at a higher level after cells form aggregates. Aggregation of ATDC5 cells resembles cellular condensation and subsequent chondrogenic differentiation during development [159, 160].

Recently, directed chondrogenic differentiation of embryonic stem cells was succeeded with feeder independent two-dimensional (2D) cultures. Interestingly, stages of

chondrogenic differentiation of embryonic stem cells are very similar to the stages observed for ATDC5 cells [161].

Primary chondrocytes, also form aggregates when seeded on indented surfaces with micro-scale grooves. These chondrocytes maintained type II collagen expression and round morphology. On the other hand, when cultured on flat tissue culture plate, chondrocytes gained fibroblast like morphology, indicating dedifferentiation of cells [162].

Chondrogenic condensation process has many complications and unknowns to be revealed. A late study was into skeletal morphogenesis and put forward a hypothetical scheme for condensation and cartilage formation. According to this scheme condensation starts by cell sorting where proximally or distally determined cells are accumulated within distinct aggregates which are partly homogenous in cell determination which then forms proximo-distally specified clusters. Clusters then compact into tighter, less spread cellular bodies. In compaction step, BMP signaling is considered to be the main driver. Activation of the transcription factor Sox9 provides cells to gain and maintain chondrogenic phenotypes [163].

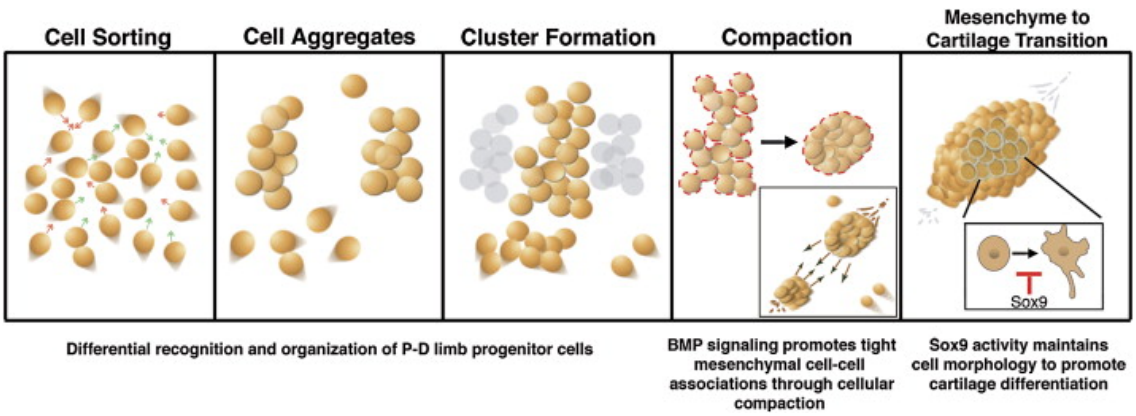


**Figure 4.** Postulated condensation steps during cartilage formation [163]

## 1.2 Experimental Section

### 1.2.1 Materials

Fmoc protected aminoacids (NovaBiochem, Sigma Aldrich), Rink amide MBHA resin (NovaBiochem), Lauric acid (Merck), 2-(1H-Benzotriazole-1-yl)-1,1,3,3-tetramethyluronium tetrafluoroborate (HBTU) (ABCR), triisopropylsilane (AlfaAesar), 4-sulfobenzoic acid, 95% (AlfaAesar), were some of the chemicals used for synthesis of peptide amphiphiles. Fmoc-Glu(OtBu)-Wang resin was synthesized by Ruslan Garifullin. Other chemicals and solvents like dichloromethane, N,N-dimethylformamide, N-ethyldiisopropylamine, trifluoroacetic acid, diethylether, acetonitrile, and ammonium hydroxide were purchased from Sigma-Aldrich, Alfa Aesar and Merck.

### 1.2.2 Design, synthesis and purification of functional peptide amphiphiles for chondrogenic differentiation

Peptide amphiphiles constitute a class of molecules containing soluble peptide groups linked to hydrophobic alkyl tail. The role of alkyl tail is to drive molecular assembly through hydrophobic interactions. Peptide sequence mostly determines the type and geometry of self assembly. Design of the molecules used in this study has been used in a variety of studies [164-166].

Three peptide amphiphiles were synthesized in this study, GAG-PA, Glu-PA, Lys-PA. On the N-terminal, each PA molecule has a hydrophobic tail constituted of 12 carbons. Length of 12 C provides the sufficient hydrophobicity for micelle formation yet dynamicity of the network formation is preserved. The first four amino acids attached to

$C_{12}$ tail, with the sequence "VVAG" interact with each other via intermolecular hydrogen bonds which collectively form beta sheets in aqueous solution. A charged spacer amino acid and the bioactive sequence follow the beta sheet forming sequence.

In this study, GAG-PA (Figure 5c) was designed to present a glycosaminoglycan mimetic sequence at its C-terminal. Lys-PA (Figure 5b) and Glu-PA (Figure 5a) do not carry any specific bioactive signal. Lys-PA is positively charged at neutral pH with the sequence, $C_{12}$-VVAGK-Am. Glu-PA is negatively charged at neutral pH with the sequence $C_{12}$-VVAGE-OH. Lys-PA and Glu-PA were used for adjusting the net charge of the scaffolds, and for constituting scaffolds without bioactive signals.

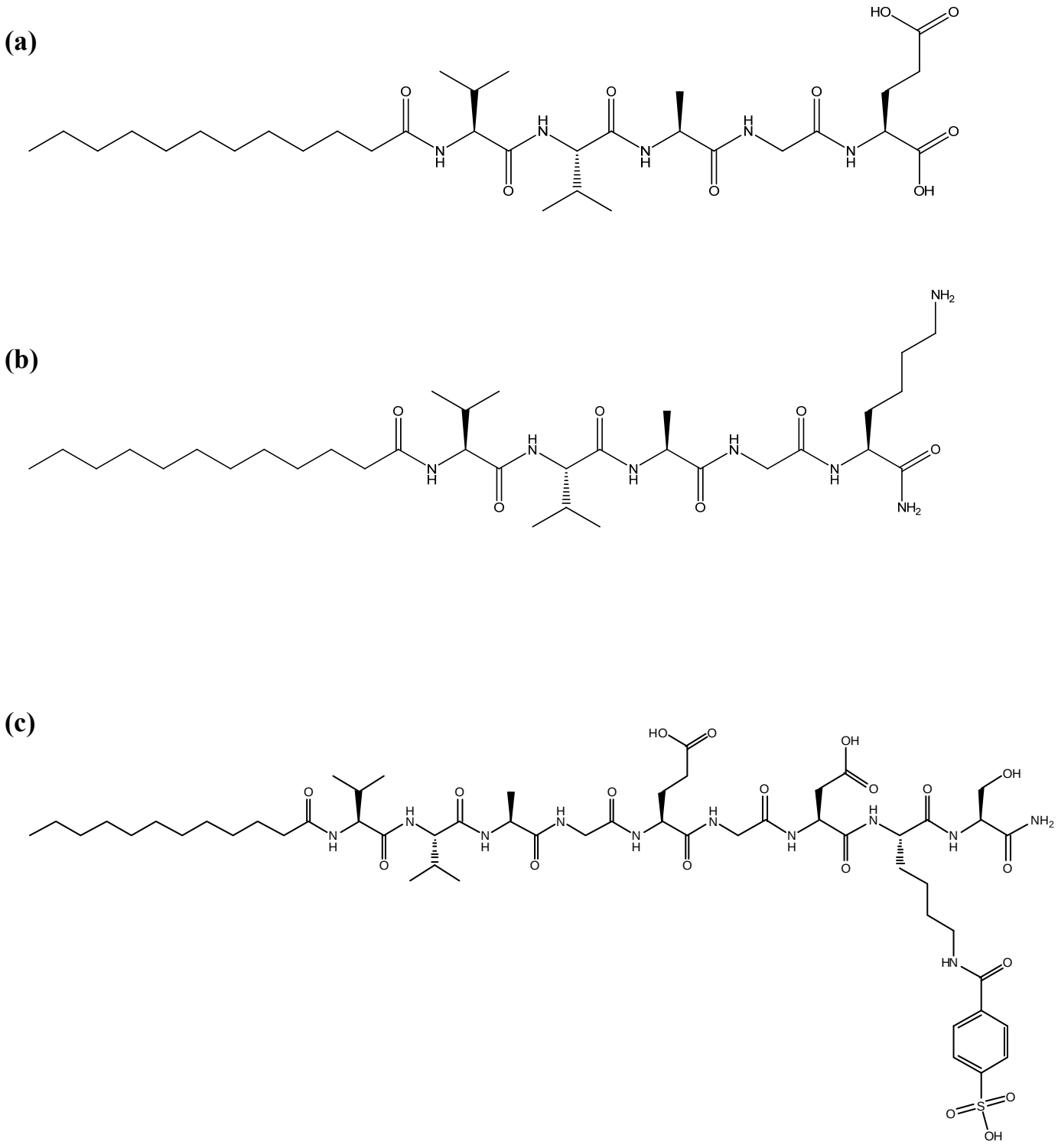


**Figure 5.** Chemical structures of peptide amphiphiles (a) Glu-PA, (b) Lys-PA, (c) GAG-PA

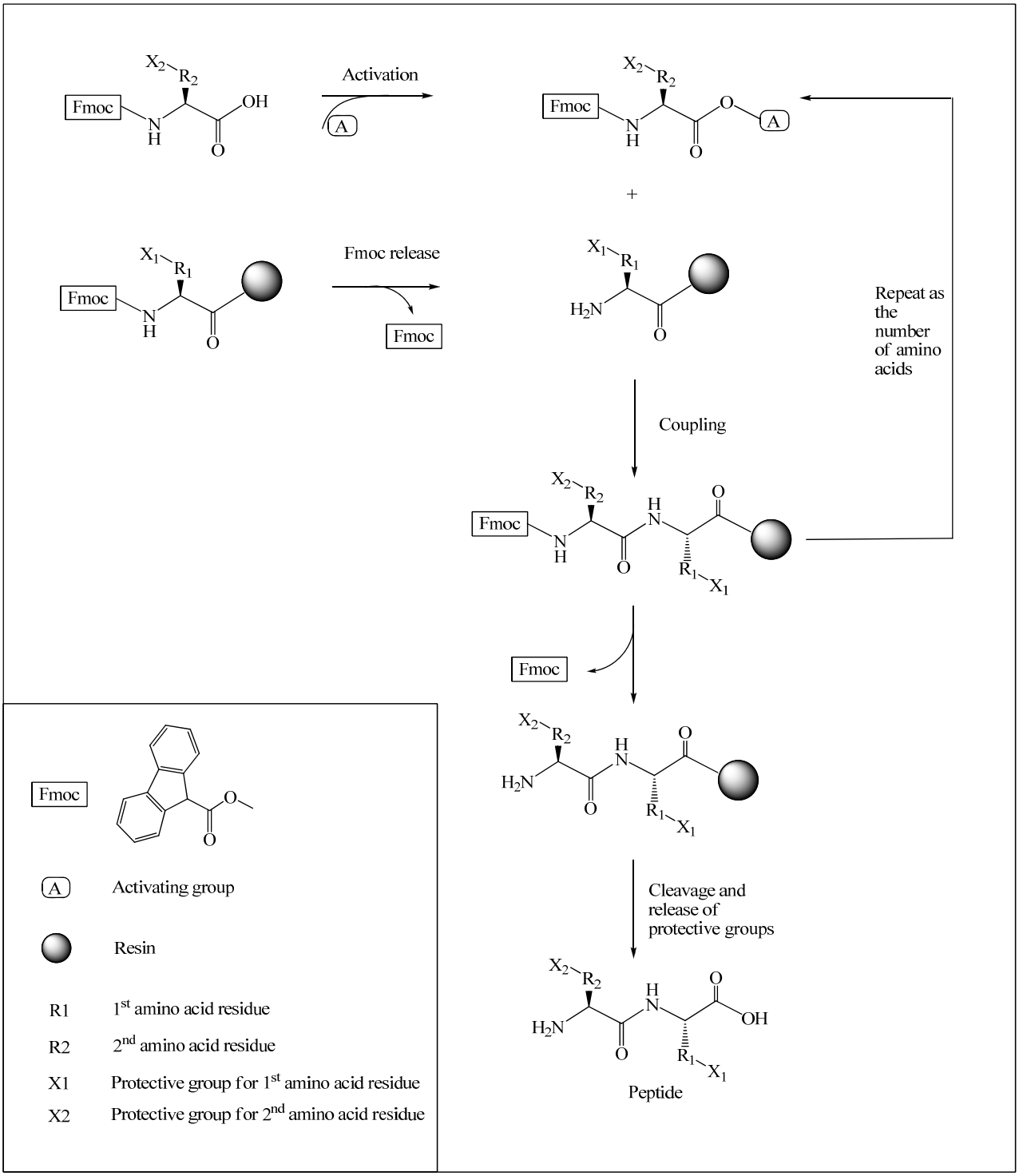


**Figure 6.** Schematics of Fmoc Solid Phase Peptide Synthesis

### 1.2.2.1 Synthesis of peptide amphiphiles

Peptide amphiphiles used in this study were synthesized with standard solid phase Fmoc chemistry. Synthesis protocol is represented at Figure 6. Rink Amide MBHA resin (for GAG-PA and Lys-PA), Fmoc-Glu-(OtBu)-Wang (for Glu-PA) were used as solid supports. Starting amounts of resins which were determinative for the theoretical yield were either 0.25 mmol or 0.50 mmol. Fmoc groups were cleaved by treating the solid phase with 20% piperidine in DMF for a period of 20 minutes. Fmoc protected amino acids were dissolved in 10 ml DMF and activated with O-Benzotriazole-N,N,N',N'-tetramethyl-uronium-hexafluoro-phosphate (HBTU), and *N*-ethyl-diisopropylamine (DIEA) in an equivalency ratio of 2:1.95:3, respectively showing the relative amounts of Fmoc protected amino acid, HBTU and DIEA with respect to the theoretical yield. Coupling of Fmoc protected amino acid and growing peptide chains was carried out for 2 hours in the reaction vessel. Kaiser test was performed at the end of each coupling, for a rough evaluation of reaction's completeness. Coupling was repeated if it was incomplete according to the test. For the purpose of blocking unreacted ends, resin was treated with 10% acetic anhydride for 30 minutes after each coupling. After coupling all Fmoc protected amino acids by applying the steps mentioned above, alkyl tail was attached following the same protocol, but using lauric acid instead of Fmoc protected amino acid. Fully grown peptide amphiphiles were cleaved from resin, and side chain protective groups of functional groups were removed in a cleavage step of 2 hours with trifluoroacetic acid (TFA): triisopropylsilane (TIS): water at the ratio of 95:2.5:2.5. Solution containing the cleavage products was collected at a round bottom flask and resin

was washed several times with DCM. DCM was removed, and TFA was removed to a large extent with rotary-evaporation. Peptide amphiphile was triturated by adding ice-cold diethylether into the solution which was left overnight at -20 ˚C. Diethylether was decanted after centrifugation at 8000 rpm for 15 minutes. Product was dissolved in dd$H_2O$, frozen at -80 ˚C and freeze-dried at -50 ˚C for two days.

#### 1.2.2.2 Purification of peptide amphiphiles

Peptide amphiphiles were purified with reverse phase HPLC system equipped with Zorbax Extend-C18 21.2 x 150 mm column for Glu-PA and GAG-PA. Before performing HPLC, the column was cleaned with a gradient up to 100% of solvent B to eliminate any peptidic material that remained absorbed on the column. Pure peptide amphiphile was eluted applying a linear gradient of 2% to 70% of solvent B for a period of 30 minutes. (A: 0.1% ammonium hydroxide in water B: 0.1% ammonium hydroxide in acetonitrile.)

Since impurities within Lys-PA were minimal, Lys-PA was not purified.

### 1.2.3 Chemical and physical characterization of peptide amphiphiles and peptide amphiphile combinations

#### 1.2.3.1 LC-MS

Molecular mass and purity of peptide amphiphiles were confirmed with Agilent 6530-1200 Q-TOF LC-MS equipped with ESI-MS.. Purity by peptide content was monitored at 220 nm. For Lys-PA Zorbax Extend-C18 21.2 x 150 mm column, and for GAG-PA and Glu-PA Zorbax Extend C18 column were used. A: 0.1% trifluoroacetic acid in water and B: 0.1% trifluoroacetic acid in acetonitrile gradient was used.

### 1.2.3.2 Oscillatory rheology

Oscillatory rheology measurements were performed with Anton Paar Physica MCR301. For all measurements 25 mm parallel plate was used at 0.5 mm interval. Total gel volume was adjusted to fill the whole cylindrical space between the stage and the plate. PA solutions of 10 mM were freshly prepared, sonicated for 30 minutes. After loading one PA solution at the center of the stage, counter charged PA solution was added dropwise on it. Just after, plate was brought to measurement position. For maturation gel was incubated in this position for 15 minutes before initiating the measurement. For strain sweep measurements, angular frequency was kept constant at 10 rad/s, strain was increased between 0.1%-100%, storage and loss moduli were recorded at each strain.

### 1.2.3.3 Circular Dichroism

Circular Dichroism study was performed with J-815 Jasco spectrophotometer. All spectra were obtained at a wavelength interval of 190-300 nm. Spectra were obtained at a digital integration time of 4 s, bandwidth of 1 nm, and data pitch of 0.1 nm. Three subsequent spectra were averaged for each sample. Quartz cuvettes with 2 mm pathlengths were used for measurements. According to the following formula, ellipticity was converted to molar ellipticity with the unit degree $cm^2$ $mol^{-1}$.

$$[\theta] = \frac{100x\theta}{(CxI)}$$

[θ]: Molar ellipticity, θ: Ellipticity in degrees, C: Concentration in M, l: length in cm

### 1.2.4 Monolayer (2D) culture of ATDC5 cells on peptide amphiphile scaffolds

#### 1.2.4.1 Peptide amphiphile coating on polystyrene multiwell plates

Pure peptide amphiphiles, GAG-PA, Lys-PA and Glu-PA were dissolved in $ddH_2O$. pH of peptide amphiphile solutions were approximately adjusted to 7. PA solutions were sonicated for 30 minutes. Concentration of PAs was measured with Nanodrop. Four different combinations were determined for coating surface of tissue culture plate wells. Peptide amphiphiles were combined, each PA at 1 mM concentration at the ratio given in Table 1.

For two of the combinations, PA content were adjusted in a way to satisfy full neutralization, while excess one negative charge in total was considered for the other two combinations. In order to provide homogenous coating, PAs of same charge were firstly added to wells, and then counter-charged PAs together were added dropwise to nearly all areas of the wells slowly. Coatings were left for about two days in laminar flow hood for drying. After drying, coatings were UV sterilized.

**Table 1.** Formulations used in the study for obtaining scaffolds

| Combinations | PA content % (PA volume/total volume x 100) | | |
|---|---|---|---|
| Scaffold, Net charge | GAG-PA | Glu-PA | Lys-PA |
| GAG-PA/ Lys-PA, neutral | 25 | - | 75 |
| Lys-PA/ Glu-PA, neutral | - | 33.3 | 66.6 |
| GAG-PA+Glu-PA/ Lys-PA, negatively charged | 25 | 33.3 | 41.7 |
| Lys-PA/ Glu-PA, negatively charged | - | 50 | 50 |

### 1.2.4.2 Monolayer culture conditions

ATDC5 cells were cultured on PA coated 96-multiwell plates, 48-multiwell plates and 24-multiwell plates according to the aim of the experiment. As control, cells were also seeded on non-coated polystyrene wells. For 96-multiwell plates 10000 cells/well, for 48-multiwell plates 20000 cells/well, and for 24-multiwell plates 50000 cells/well were determined as initial cell seeding density. Cells were cultured with either maintenance medium containing 1:1 mixture of Dulbecco's modified Eagle's medium (DMEM) and Ham's F12 supplied with 10 µg/ml human transferring (Sigma-Aldrich), and 5% FBS or with differentiation medium containing maintenance medium plus 10 µg/ml bovine insulin. Cell culture studies were carried out by Seher Üstün.

### 1.2.4.3 MTT assay

ATDC5 cells were cultured on 96-multiwell plates at a density of 15000 cells per well using maintenance medium without phenol red. At specific time points grown cells were treated with MTT reagent and absorbance values were recorded with plate reader. Data obtained for each scaffold combination (n=3) were normalized with respect to cells grown on tissue culture plate to obtain relative cell quantity.

### 1.2.4.4 Quantitative analysis of aggregates

Cell aggregates were grown on scaffolds for 18 days (three wells for each scaffold combination). During follow-up, 10 non-overlapping 5x photo frames were taken from each of three wells periodically. Size values of aggregates (area, perimeter, major, minor) and number of aggregates were quantified with ImageJ for each frame. For each well, 10

frames were pooled to determine the number of aggregates per well and the average area of aggregates. Average area was calculated according to:

$$\text{Average area of aggregates} = \frac{\text{Total area of aggregates (within 10 frames)}}{\text{Number of aggregates (within ten frames)}}$$

Mean values and standard deviations were obtained from 3 wells.

### 1.2.4.5 Safranin-O staining

Cells were fixed with 4% PFA in PBS for 15 minutes. Fixed cells were washed with PBS then treated with 2% BSA for 30 minutes for blocking to prevent nonspecific staining of the scaffold. Fixed cells were stained with 0.1% Safranin-O in 0.1% acetic acid for 5 minutes at room temperature, and then washed with PBS.

### 1.2.4.6 Scanning electron microscopy

Cell aggregates grown for 5 days on Glu-PA/Lys-PA coated slides were washed three times with PBS and fixed with gluteraldehyde for 1.5 hours, then treated with Osmium tetroxide for 30 minutes. The samples were dehydrated with a series of ethanol of increasing concentrations. Samples were, critical point dried and Au-Pd coated. Sample preparation was done by Seher Üstün. Critical point drying and SEM was performed in cooperation with Yavuz Selim Dağdaş.

### 1.2.4.7 Immunocytochemistry

Collagen II production of aggregates were evaluated with immunocytochemistry with collagen-II antibody. Cell aggregates grown for 14 days on GAG-PA+Glu-PA/Lys-PA

scaffold were washed three times with PBS and fixed with 4% PFA in PBS for 15 minutes and then blocked with 10% BSA treatment for 30 minutes. For immunofluorescence staining incubation with primary antibody was carried overnight. Next day, after washing three times with with PBS, aggregates were incubated with secondary antibody for one hour.

For nuclei staining, samples were treated for PBS-TX 0.1% for 10 minutes and then incubated with nuclei staining dye TO-PRO.

All staining protocols were carried in dark. The stainings were performed together with Seher Üstün.

## 1.3 Results and Discussion

### 1.3.1 Characterization of peptide amphiphiles and peptide amphiphile scaffolds

Three peptide amphiphiles were synthesized in order to construct scaffolds for culture of ATDC5 cells. Crude products were purified if the amount of impurities exceeded 80% by peptide content. GAG-PA, Glu-PA and Lys-PA had expected molecular weights (Figure 7, 9, 10); with high purities (Figure 8, 10, 12).

GAG-PA contains sulfobenzoyl, carboxyl and hydroxide groups in its structure mimicking glycosaminoglycans. Main rationale in the design of this peptide amphiphile was that the composition of cartilage tissue mainly involves proteoglycans with negatively charged glycosaminoglycans and scaffolds carrying GAG signals would help chondrogenic differentiation.

Counter charged peptide amphiphiles of 1% (w/v) concentration together formed self-supporting gels which could be seen with naked eye. This is an expected result indicating the formation of nanofiber networks.

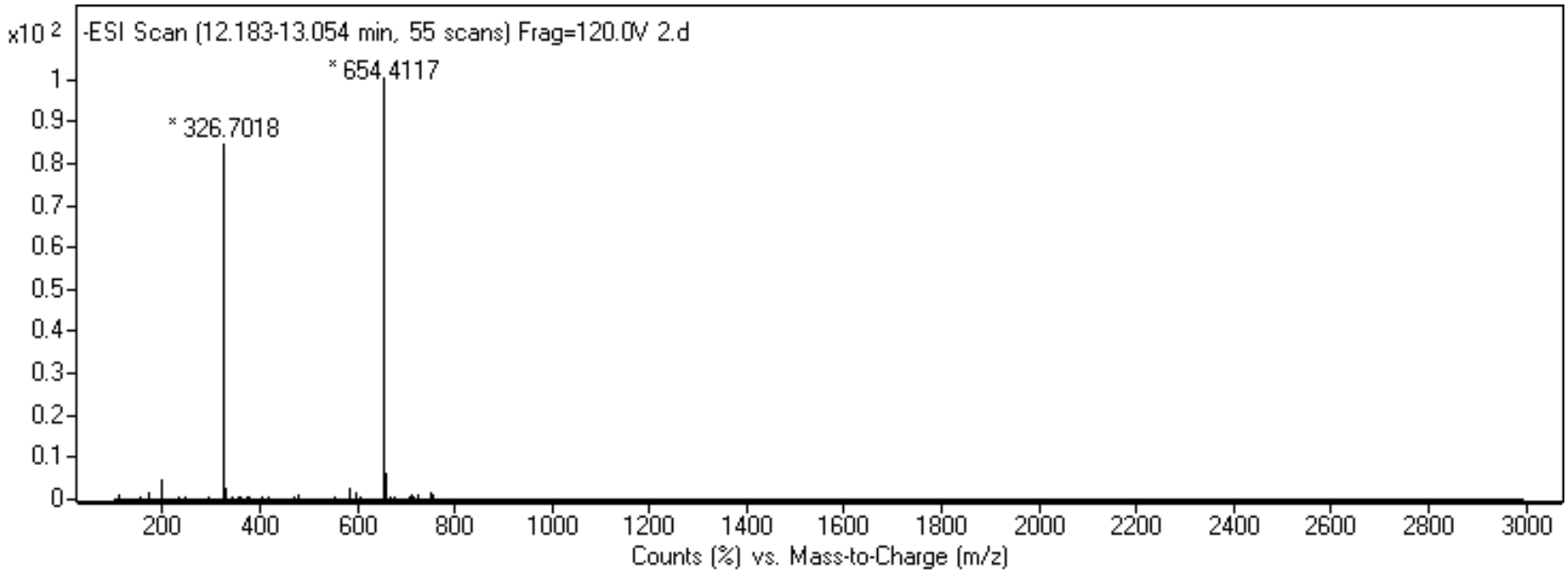


**Figure 7.** Electrospray ionization mass spectra of the Glu-PA. $[M\text{-}H^{+}]^{-1}_{observed}$=654.42, $[M\text{-}H^{+}]^{-1}_{calculated}$=654.82, $[M–2H^{+}]^{-2}/2_{\ observed}$ =326.7, $[M–2H^{+}]^{-2}/2_{\ calculated}$ = 326.91

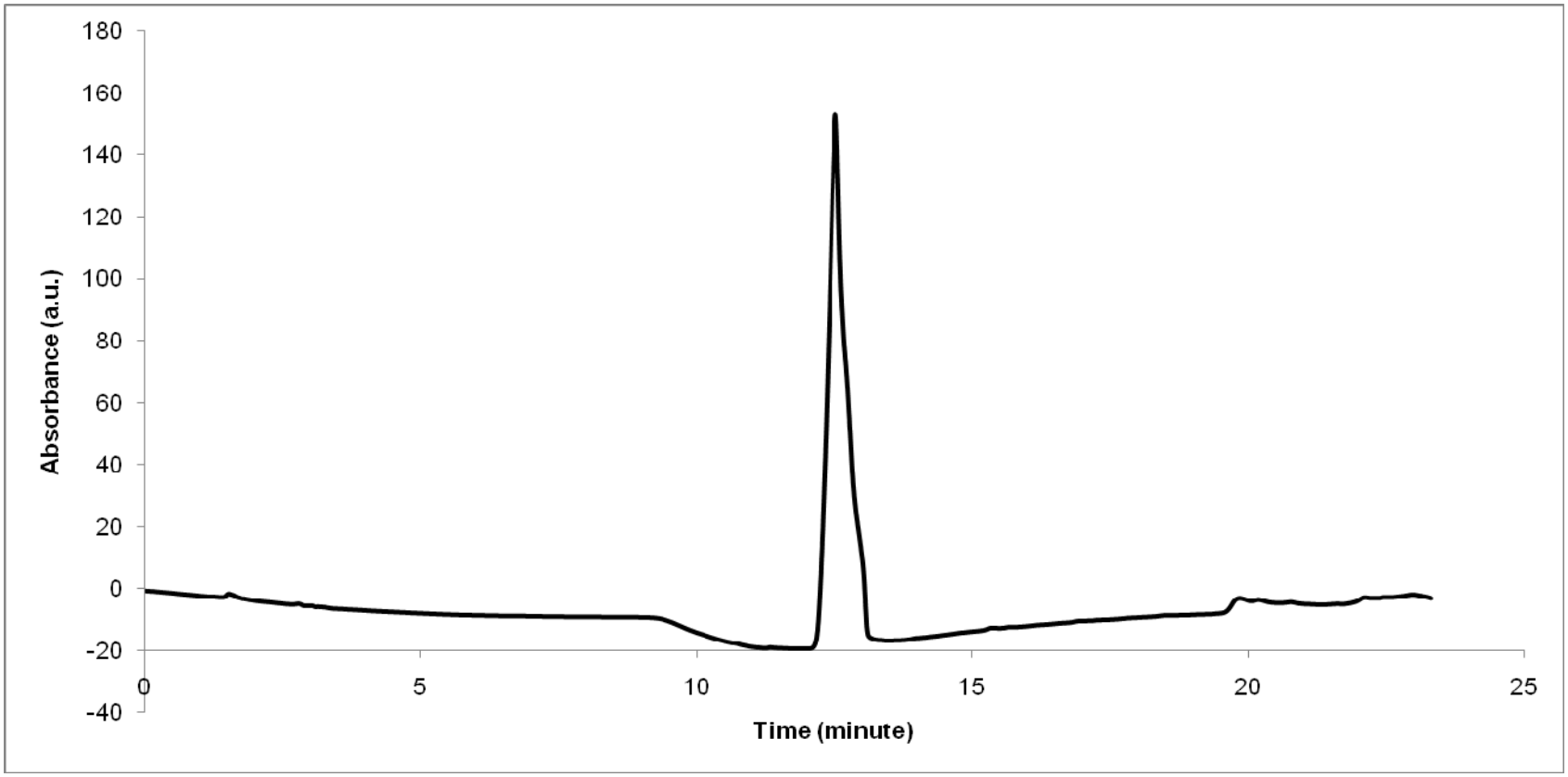


**Figure 8.** Reverse Phase-HPLC chromatogram of Glu-PA. Retention time 12-13 minutes

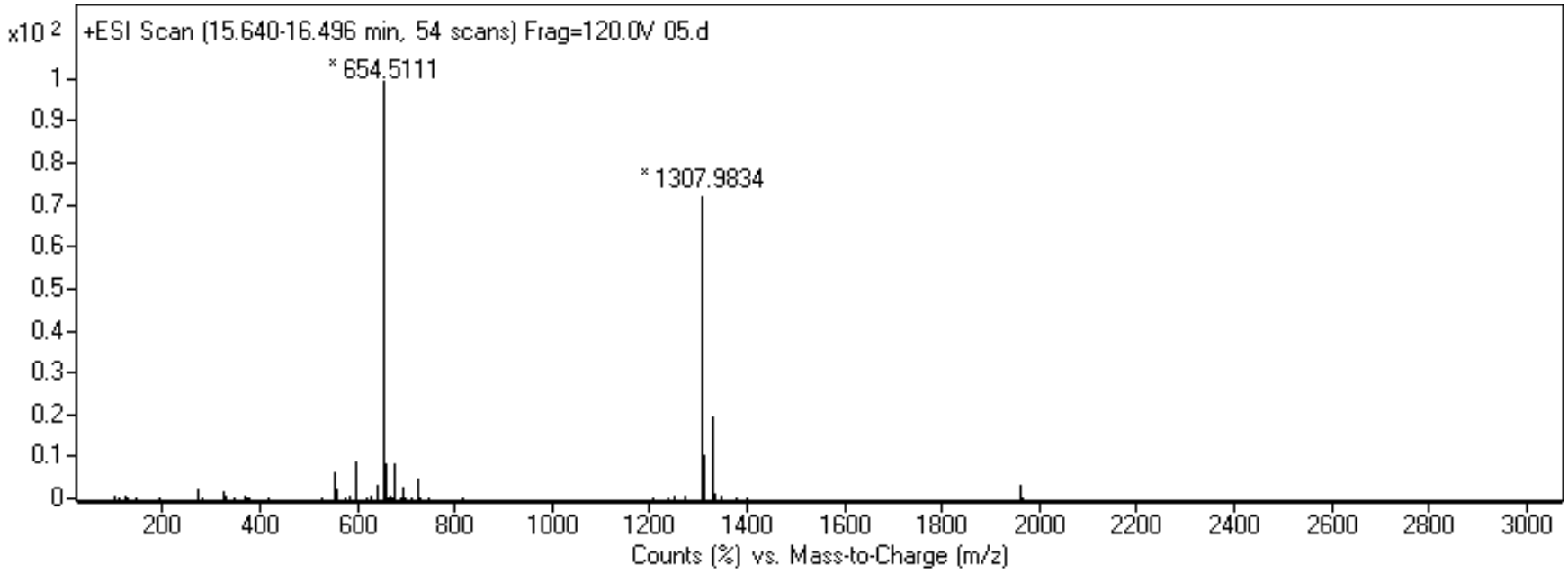


**Figure 9.** Electrospray ionization mass spectra of the Lys-PA. $[M+H^+]^{+1}_{observed}$=654.51, $[M+H^+]^{+1}_{calculated}$=654.9, $[2M+H^+]^{+1}_{observed}$ =1307.9, $[2M+H^+]^{+2}_{calculated}$ = 1308.8

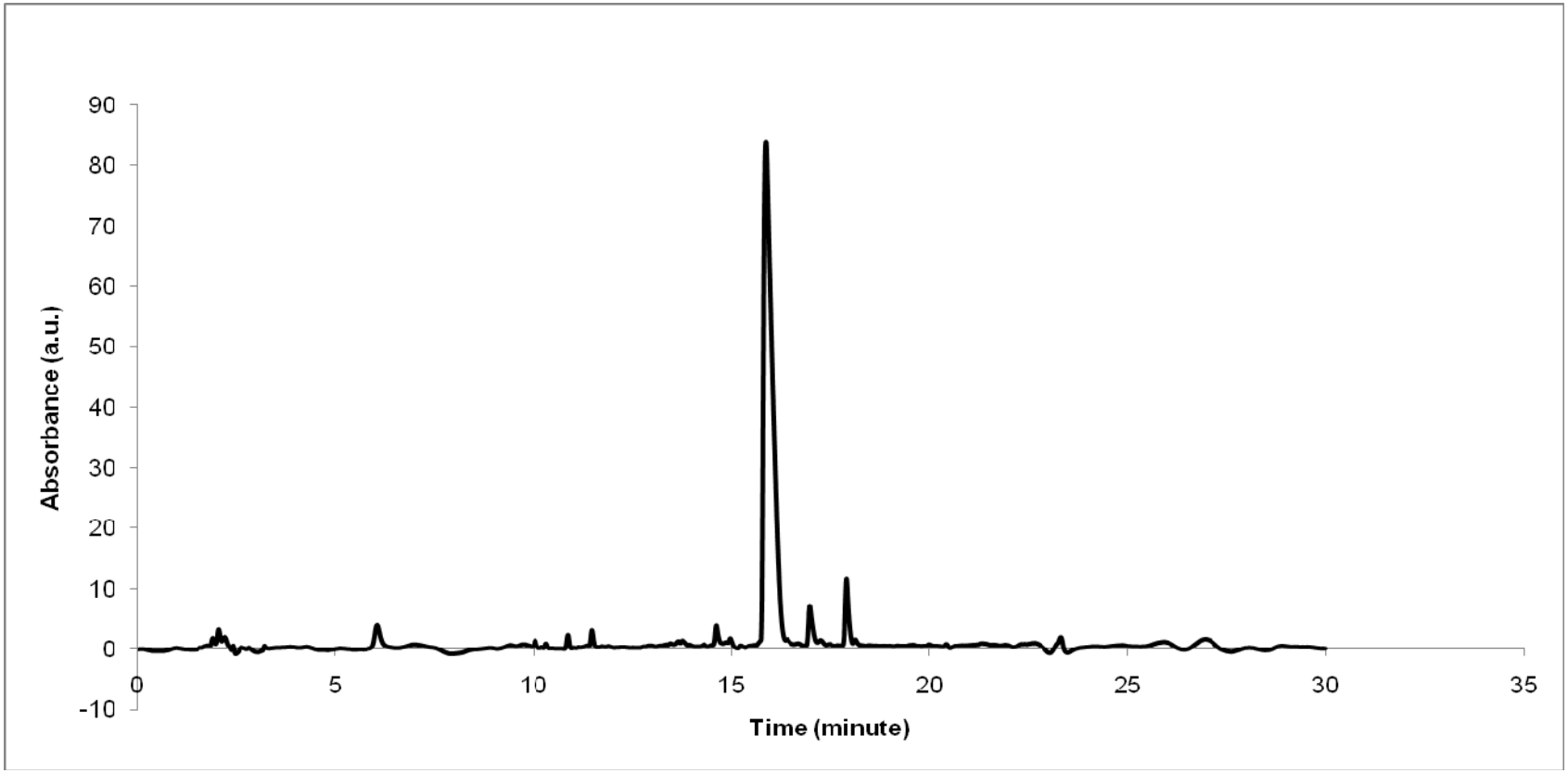


**Figure 10.** Reverse phase-HPLC chromatogram of Lys-PA. Retention time 15-16 minutes

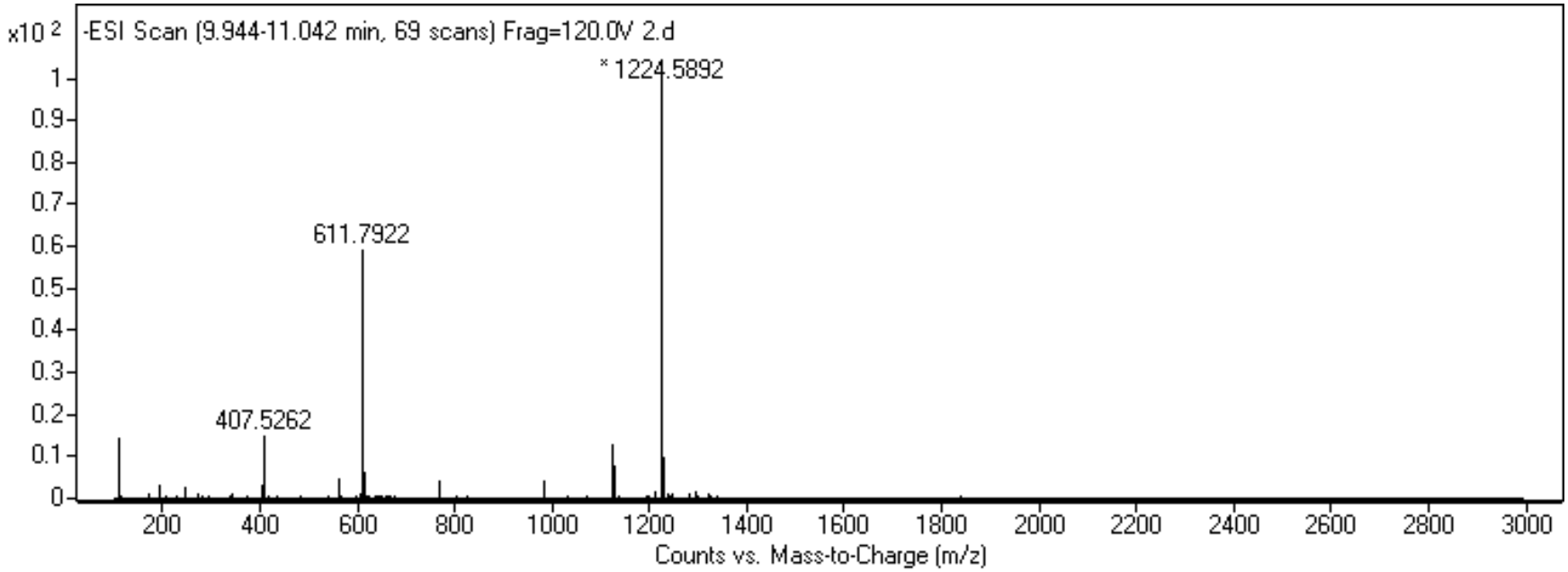


**Figure 11.** Electrospray ionization mass spectra of the GAG-PA. $[M\text{-}H^{+}]^{-1}_{observed}$= 1224.59, $[M\text{-}H^{+}]^{-1}_{calculated}$= 1224.59, $[M\text{–}2H^{+}]^{-2}/2_{\ observed}$ = 611.792, $[M\text{-}2H^{+}]^{-2}/2_{\ calculated}$ = 611.795

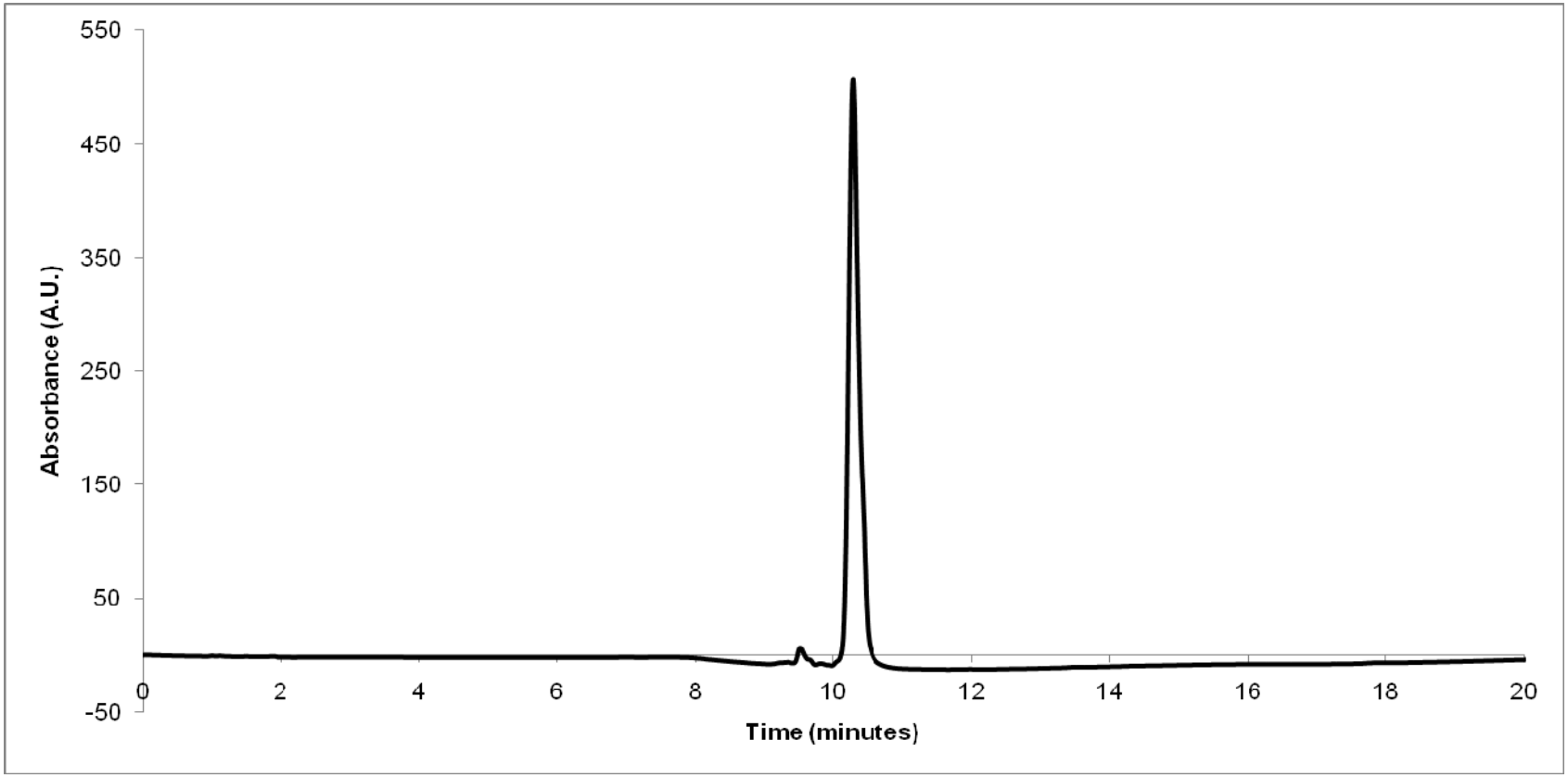


**Figure 12.** Reverse phase-HPLC chromatogram of GAG-PA. Retention time 10-11 minutes

Formation of nanofibers from peptide amphiphiles is driven by hydrophobic interactions and beta sheet forming ability of the peptide sequence, Val-Val-Ala-Gly-. Since, formation of beta-sheets was essential for self assembly, and for scaffold formation, secondary structure of individual peptide amphiphiles and four different combinations were investigated with Circular Dichroism (Figure 13).

Circular Dichroism spectra of polypeptides are based on the interaction of chromophores that are arranged in a specific way within a chiral environment. Secondary structure of polypeptides is associated with the patterns observed within spectra.

At neutral pH, Glu-PA and GAG-PA exhibit the characteristic random coil spectra with the minima around 198 nm. Lys-PA has a spectrum similar to the negatively charged peptide amphiphiles, however with a broader signal around 200 nm and a minimum around 220. This is most possibly a compound spectra involving both random coil and beta sheet signals. Lys-PA may be forming some primary forms of self-assembly. Theoretically, GAG-PA and Glu-PA carry 3 and 2 negative charges respectively at pH 7, whereas Lys-PA has one positive charge. Electrostatic repulsion of the identical charges, counteracts the hydrophobic interactions and hydrogen bonds which work together to initiate self assembly. Two net charges may be capable to drive individual molecules apart and one net charge might have been insufficient to completely block the assembly in the case of Lys-PA.

Peptide amphiphiles were combined in ways to have full neutralization or one net negative charge. When Lys-PA was added to neutralize negative charges of Glu-PA and GAG-PA, random coil bands immediately disappeared and beta-sheet was observed instead with maxima at around 200 nm and minima at around 220 nm.

Glu-PA and Lys-PA were mixed in one to one ratio or one to two ratio, theoretically resulting in negatively charged or neutralized systems. However, these two different ways of mixing resulted in nearly the same spectra.

GAG-PA and Lys-PA were mixed in one to three ratio to have a neutralized system. In this case the spectrum was similar with the spectra of Glu-PA/Lys-PA systems, but with different $\theta_{200}$:$\theta_{220}$ ellipticity proportion. Without changing the molar percentage of GAG-PA to the total peptide content, Glu-PA was inserted to the system to obtain net one negative charge. $\theta_{200}$:$\theta_{220}$ proportion changed to resemble more to the Glu/Lys spectrum. There isn't vast information in literature on whether such differences in the Circular Dichroism spectra are reflections to minor changes in secondary structure. However, a proportion $\theta_{200}$:$\theta_{220}$ with enhanced $\theta_{200}$ and a minute red shift in $\pi$-$\pi^*$ transition region in the case of Glu-PA/Lys-PA, may be an indication of twisted beta sheet structure [167].

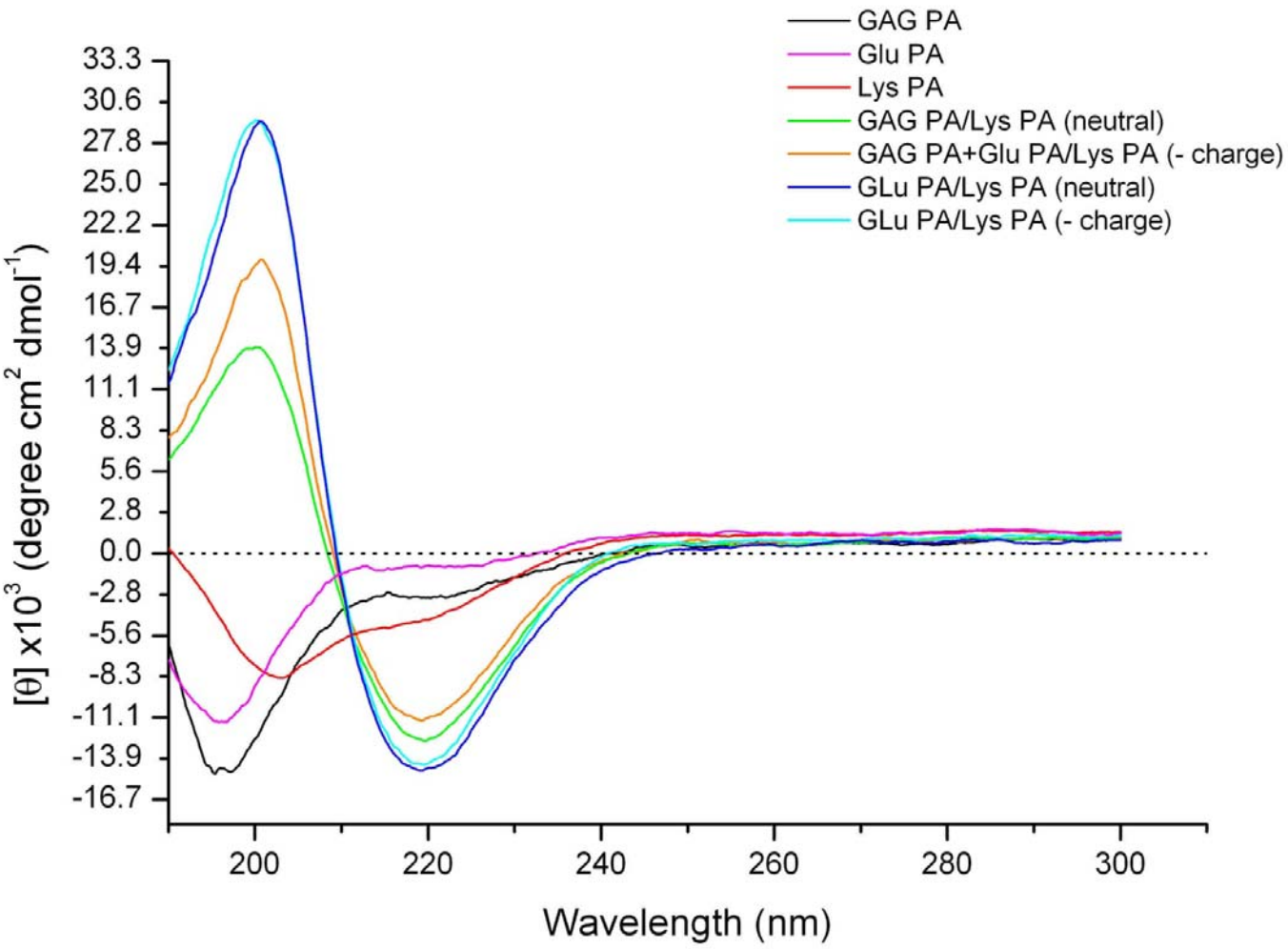


**Figure 13.** Circular Dichroism spectra for various PA combinations

Gel formation properties of the same combinations used in Circular Dichroism were investigated with oscillatory rheology.

Storage and loss moduli were measured at varying strains and constant angular frequency. Storage modulus corresponds to the energy stored within the material and resist when forces act to deform the gel. Loss modulus corresponds to energy that is dissipated when the material is deformed. Material is considered as gel when storage modulus exceed loss modulus [168] .

Strain sweep tests show that counter-charged PA molecules form gels which stay in linear viscoelastic region up to 1% strain. Beyond 1% strain, gels gradually lose mechanical strength, and stability. At 0.5% strain, storage moduli of gels changed between 1-3kPa, loss moduli between 200-500 Pa. At this particular strain, neutralized GAG-PA/Lys-PA gel is significantly stronger. Other three combinations are closer in stiffness, without displaying any significant difference in storage and loss moduli. It is noteworthy that neutralized GAG-PA/Lys-PA has a different Circular Dichroic profile.

Both interfiber and intrafiber bonds contribute to macro-mechanical properties of the fibrillar network system. Ten fold larger storage moduli of $Ca^{2+}$ gels with respect to storage moduli of HCl gels was apparently attributable to interfiber bonds rather than intrafiber bonds [164].

In this work, extra negative charge present in two combinations may have lead to reduction in gel stiffness due to interfibrillar repulsions. On the other hand, there may be slight changes in the secondary structure of combinations, depending on the presence of GAG-PA or Glu-PA. Besides interfiber interactions, intrafiber bonds may have played an important role in overall mechanical strength.

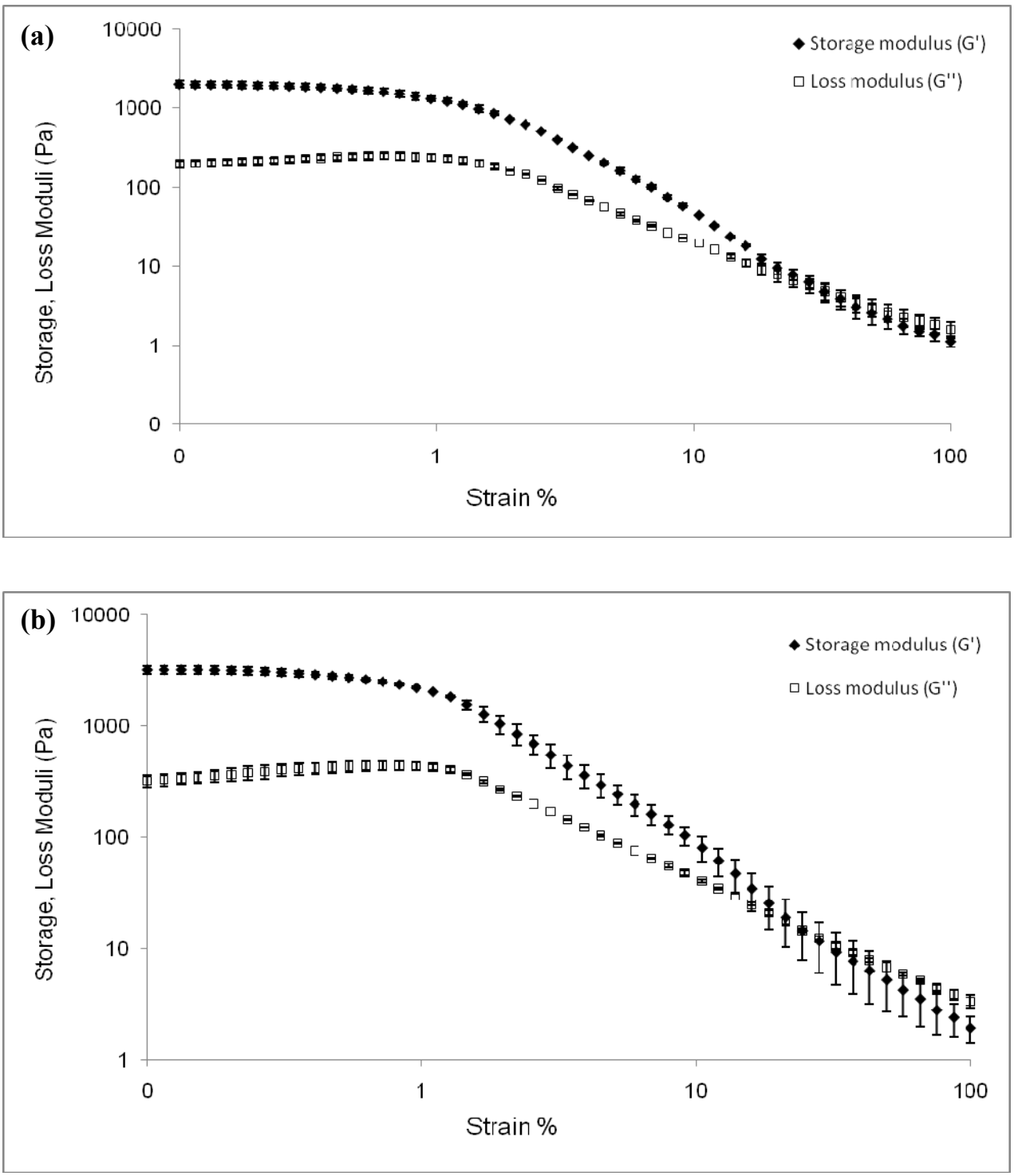


**Figure 14.** Strain sweep oscillatory rheology measurements of gels with GAG-PA, (a) GAG-PA + Glu-PA/Lys-PA (- charge), (b) GAG-PA/Lys-PA (neutral)

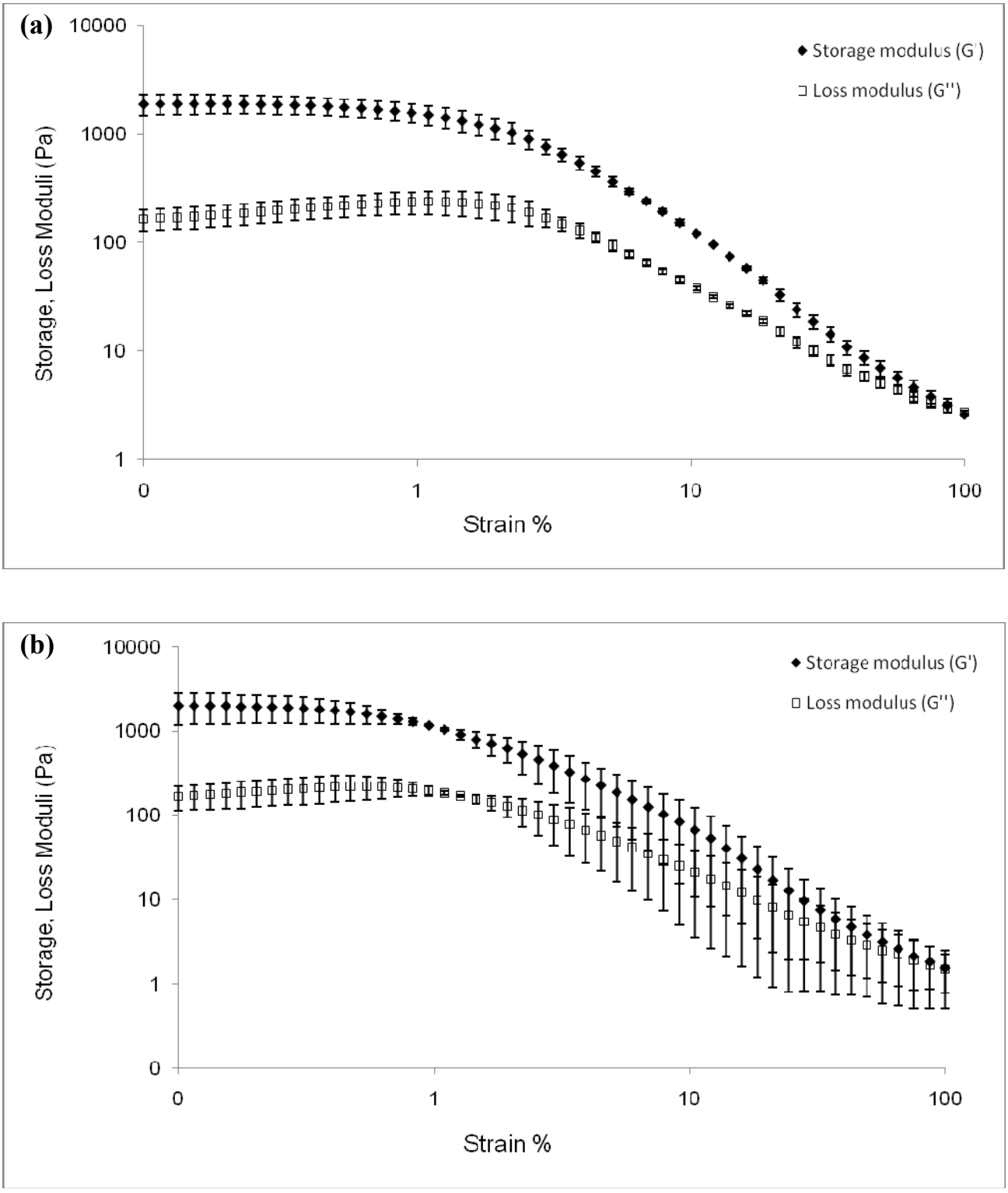


**Figure 15.** Strain sweep oscillatory rheology measurements of gels without GAG-PA, (a) Glu-PA/Lys-PA (- charge), (b) Glu-PA/Lys-PA (neutral**)**

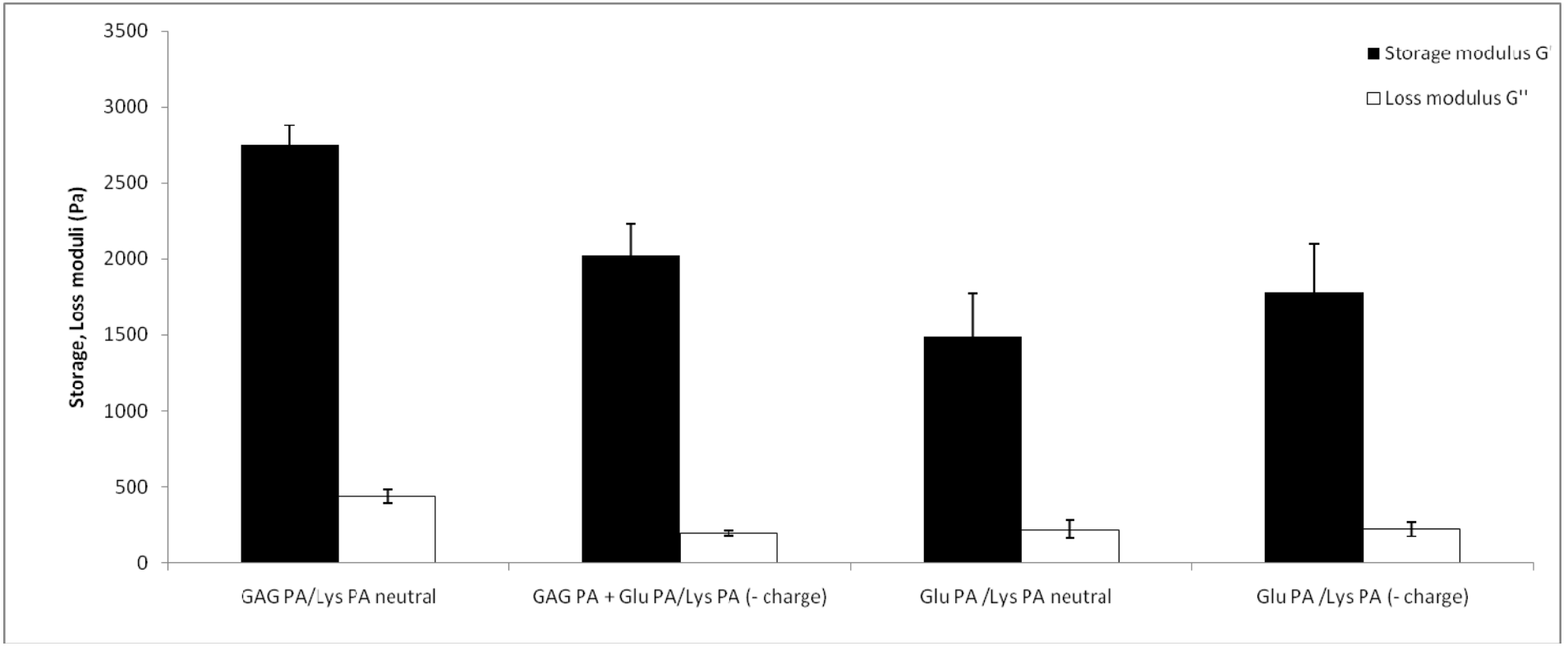


**Figure 16.** Strain and loss moduli of gels at 0.5% strain and 10 rad/s, values represent mean ±SD, n=2

Formation of gels when mixed with oppositely charged molecules is desired for a biomaterial to be used in cartilage regeneration, since such material can be applied with easy injection procedure and does not require complex operations. Peptide amphiphiles used in this study are soluble around physiological pH due to charged amino acids in their structure. When, these charges are neutralized, weak interactions become prominent and three-dimensional network is rapidly assembled. From this perspective, when rheological properties of synthesized PAs are taken into consideration, these PAs hold promise as injectable biological scaffolds.

### 1.3.2 Monolayer culture of ATDC5 cells on scaffolds

ATDC5, a chondroprogenitor cell line was used to constitute a model for chondrogenesis on coated PA layers. Differentiation of ATDC5 towards chondrocyte like phenotypes has been subject of many studies. In the presence of insulin or insulin-like growth factor (IGF), ATDC5 cells form aggregates and while expression of Col-II, and Sox9 increases.

ATDC5 cells were seeded on polystyrene plates with or without peptide amphiphile coating. Interestingly, ATDC5 cells formed aggregates when seeded on PA coated wells, even though insulin was not present in the medium. Aggregation process was followed for a 21 day period and evaluated for different aspects.

#### 1.3.2.1 MTT assay

MTT assay was done in order to assess viability of the scaffolds. However within 48 hours, ATDC5 cells aggregated unexpectedly, even though insulin which is considered as the required factor for differentiation of ATDC5 cells was not present within the medium.

On the other hand, no morphological change was observed for ATDC5 cells seeded on uncoated tissue culture plate wells.

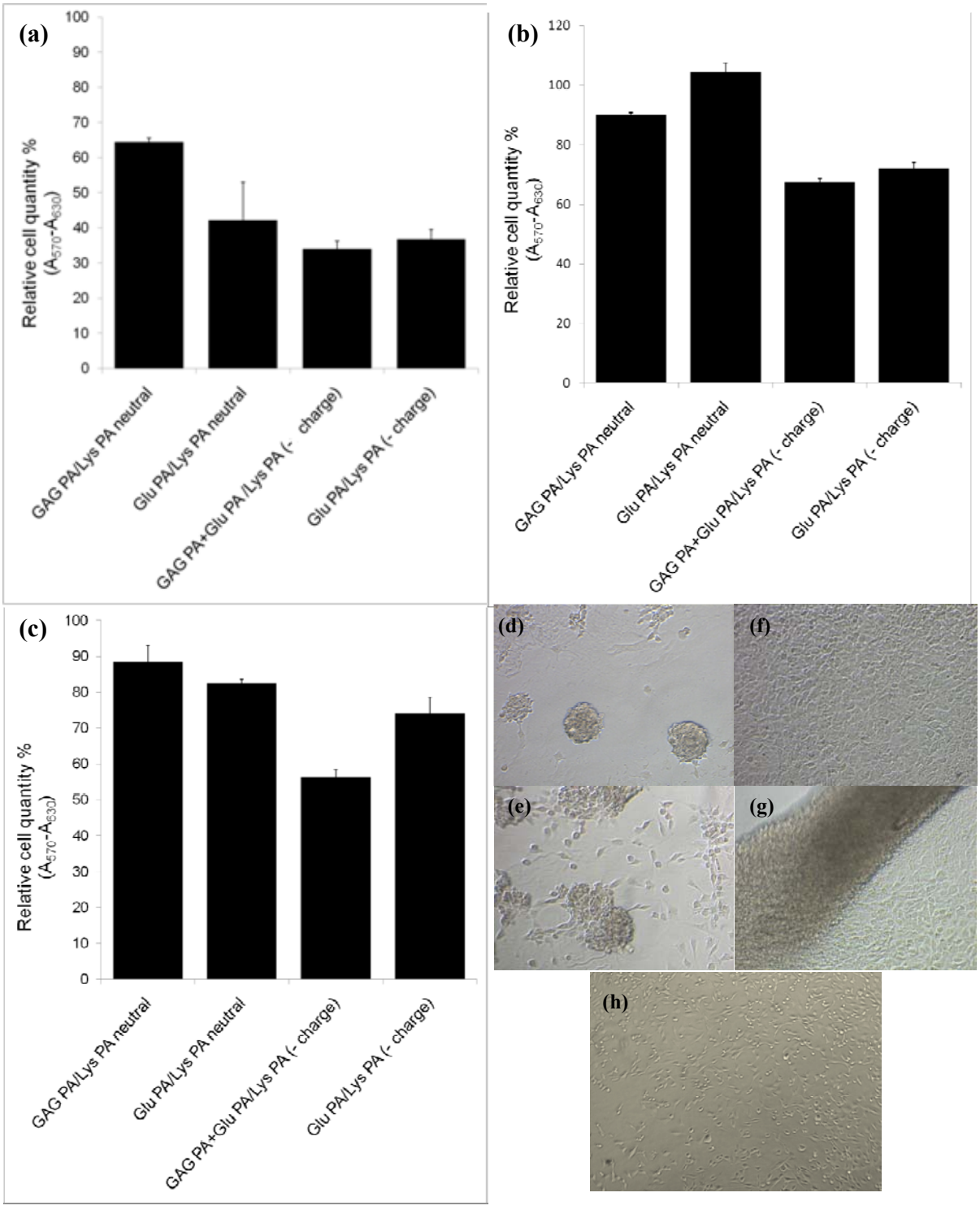


**Figure 17.** MTT assay cell quantities normalized with respect to cells grown on tissue culture plate (a) 48h (b) 72 h (c) 96 h (d-g) ATDC5 cells on coated wells (d) Glu-PA/Lys-PA (- charge) (e) GAG-PA + Glu-PA/Lys-PA (- charge) (f) Glu-PA/Lys-PA (neutral) (g) GAG-PA + Glu-PA/Lys-PA (neutral) (h) ATDC5 cells on uncoated well

Aggregation of ATDC5 cells is a process that is observed during chondrogenic differentiation. Aggregation in the absence of any bioactive signals might be explained with possible absorbtion and stabilization of autocrine factors released by ATDC5 cells on nanofibers. Bioactive factors with increased density possibly stimulated cells for differentiation.

Since growth of cells might be ceased by chondrogenic differentiation, MTT results obtained and normalized with respect to uncoated plate, do not truly reflect viability profiles of cells grown on PA scaffolds. This can also be validated from 10x LM images; cells forming larger aggregates generally had lower cell quantity.

#### 1.3.2.2 Formation of ATDC5 aggregates

#### 1.3.2.3 Morphology of aggregates and ATDC5 cells on different scaffolds

After observing aggregate formation of ATDC5 cells on scaffolds without supplementing any bioactive signals after 48 hours, ATDC5 cells were seeded on each PA combination and observed for a 20 day period.

Aggregation starts 1 day after seeding ATDC5 cells on scaffolds. On day 3, cell clusters seem to be dispersed with more spread cells. The clusters on day 3, do not have distinctive borders and strict circular shape. Through day 7, cell clusters become compacter, round aggregates with more distinctive borders. From 7 days to 18 days, aggregates increase in size, reaching an assumptive diameter of 100-300 μm on day 18. Cellular bridges between aggregates were notable features. Another interesting point was that, aggregates unified to

form larger aggregates with the shape of intersecting Venn diagrams or unified spheres. On day 18, aggregates became so compact that individual cells within aggregates could hardly be identified. This might also be due to the growth of cells at the third dimension, production and coverage of dense extracellular matrix. Even hydroxiapatite crystals might have formed on aggregates.

Progress of ATDC5 aggregation on peptide amphiphile scaffolds, fits to an aggregation scheme proposed for cartilage formation [163]. According to this scheme cells starts to form dispersed clusters which get larger. A next step is the compaction of the clusters. In this step, associations between cells get stricter. Compaction of clusters is told to be mediated by BMP signaling. Compact aggregates increase in size. Sox 9 expression induces cells to chondrocyte like phenotypes.

In a separate study, primary chondrocytes were seeded on surfaces with stripes of nano-size on which chondrocytes formed aggregates. Time-lapse imaging of cells revealed, collision of cells to form aggregates and collision of smaller aggregates to form larger aggregates [162]. This mechanism might also be valid for our study, since unification of aggregates was observed.

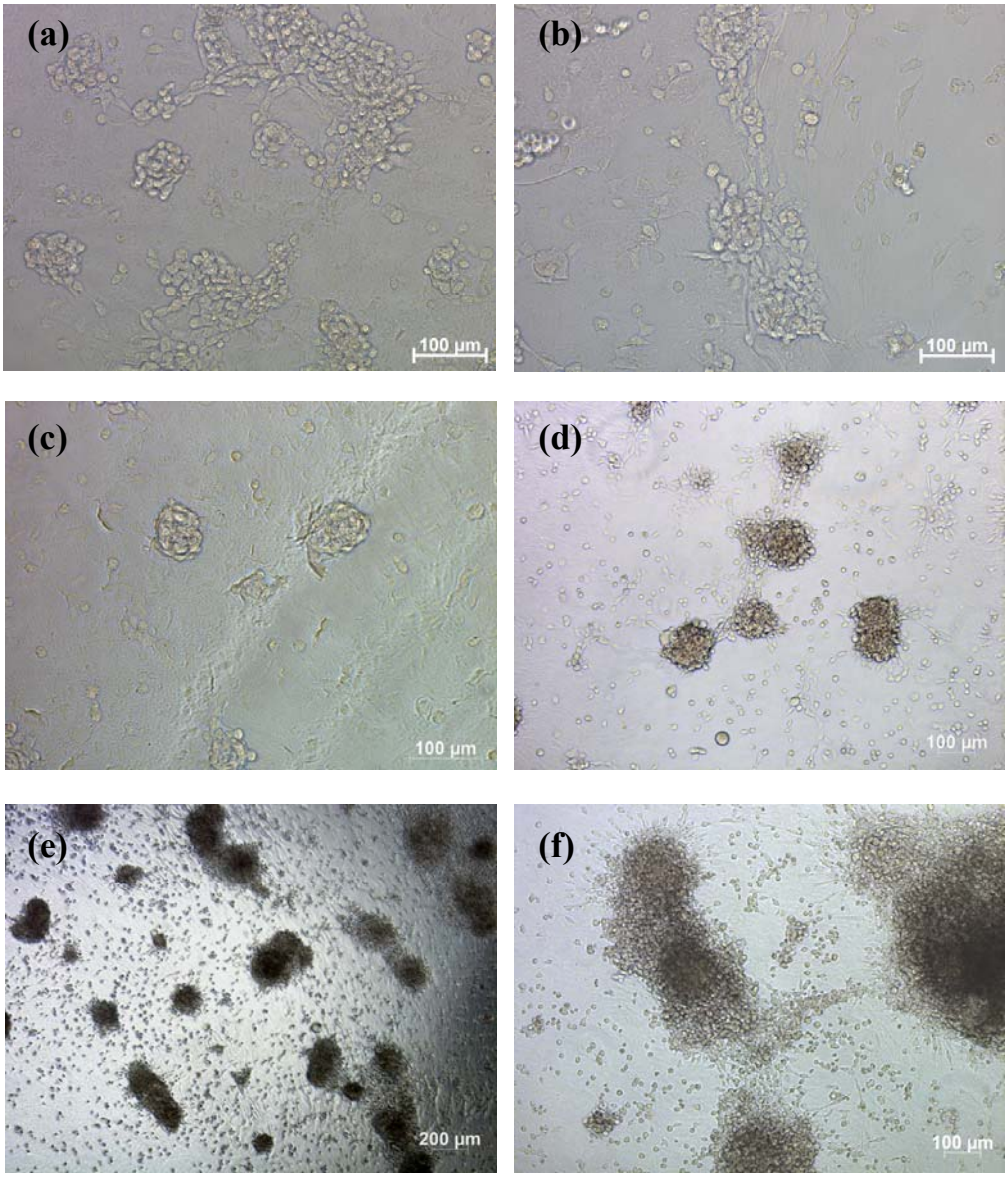


**Figure 18.** ATDC5 cells grown on GAG-PA/Lys-PA (- charge) (a) 1 day (b) 3 days (c) 7 days , (d) 17days (e), (f) 18 days

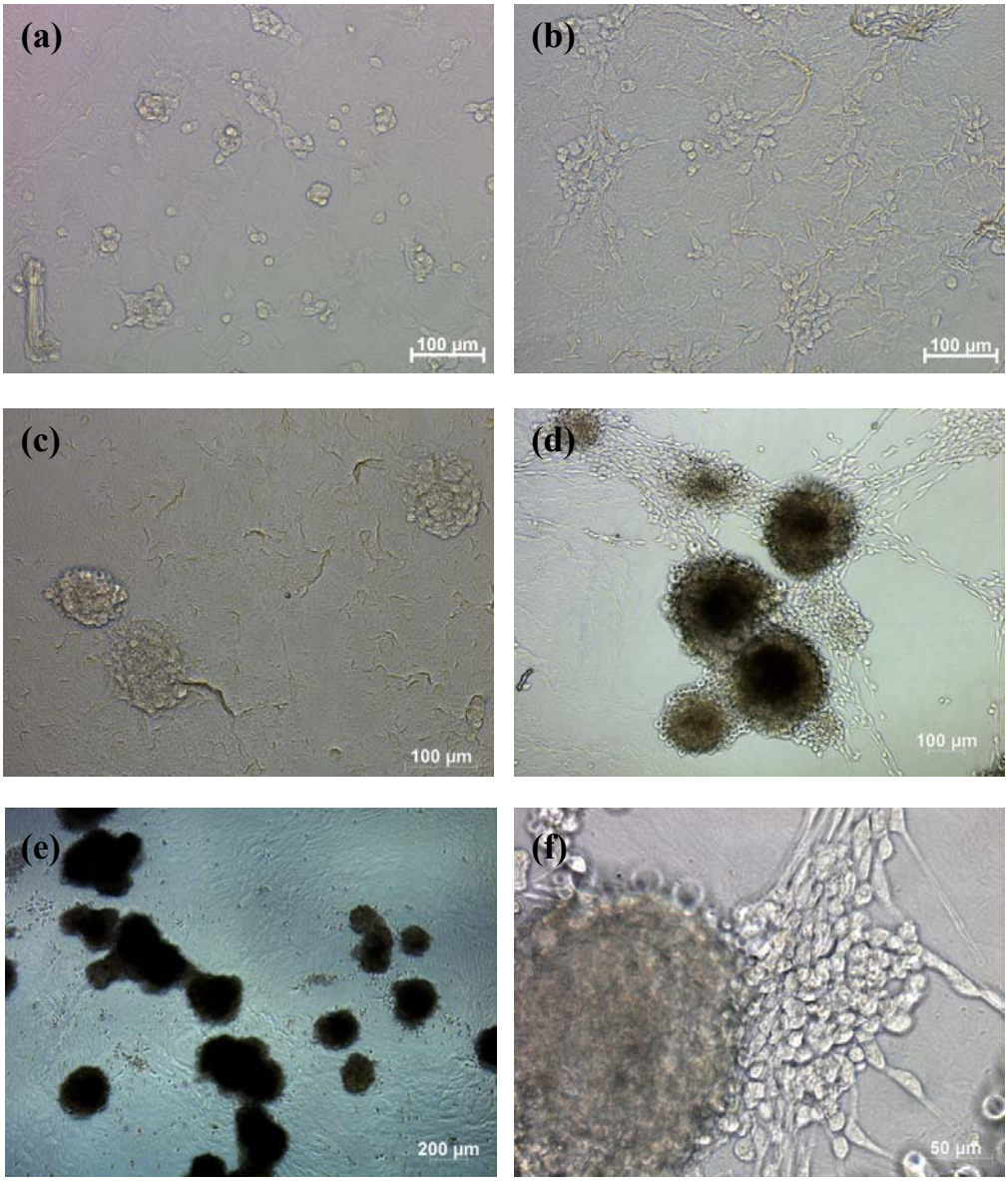


**Figure 19.** ATDC5 cells grown on Glu-PA/Lys-PA (a)1 day (b) 3 days (c) 7 days (d) 17 days (e), (f) 18 days

### 1.3.2.4 Quantitative analysis of aggregates on different peptide amphiphile scaffolds

Average areas of aggregates, total aggregate area and number of aggregates on different scaffolds were followed through 18 days. Effect of insulin was also investigated; two replicates of the experimental set up included media with insulin or media without insulin.

On three scaffolds, Glu-PA/Lys-PA (neutral), Glu-PA/Lys-PA (- charge), GAG-PA+Glu-PA/Lys-PA (- charge), average area of aggregates followed a similar trend during the 18 day-period. On these scaffolds, average area of aggregates increased slightly, through 5 to 11 days. Between days 11-14 and 14-18, average area increased more significantly. On both Glu-PA/Lys-PA scaffolds, the increase was very steep as opposed to GAG-PA+Glu-PA/Lys-PA (- charge). A sudden decrease in number of aggregates and significant increase in total area of aggregates, accompanied the sharp transition observed during 11-18 days. Unified aggregates started to appear from day 11, and unification increased through day 18 and as a result number of aggregates decreased and the average area increased. Increase in total area during this period (11-18 days) might be a result of coalescing of individual cells or very small clusters with aggregates.

For GAG-PA+Glu-PA/Lys-PA (- charge) scaffold, average aggregate areas on different days were smaller than other scaffolds. However, number of aggregates was much more than the others. Number of aggregates decreased below 100 at $18^{th}$ day in the absence of insulin, below 50 at $18^{th}$ day in the presence of insulin for scaffolds other than GAG-PA+Glu-PA/Lys-PA (- charge). For GAG-PA+Glu-PA/Lys-PA (- charge), number of aggregates remained 250-350 in the absence of insulin, about 100-150 in the presence of

insulin. From 9$^{th}$ day to 18$^{th}$ day the total area of aggregates in the absence of insulin was significantly larger for GAG-PA+Glu-PA/Lys-PA (- charge) scaffold when compared to total area for other scaffolds. In the presence of insulin, total area for this scaffold was larger than total area of other scaffolds through all days.

On 5$^{th}$ day, on GAG-PA/Lys-PA (neutral), aggregates were already had 2 times larger than the aggregates on other scaffolds. This shows that aggregation starts earlier on GAG-PA/Lys-PA (neutral) scaffold. The average area of aggregates on this scaffold, increased very slightly till 18$^{th}$ day. GAG-PA/Lys-PA (neutral) and GAG-PA+Glu-PA/Lys-PA (- charge) scaffolds had the same ratio of GAG-PA to total peptide amphiphiles. Different behavior of cells on GAG-PA/Lys-PA (neutral) scaffold might be relevant to differences in secondary structure and mechanical properties which were noted in Circular Dichroism and Rheology experiments.

When insulin was present in the media, progress of aggregation followed almost the same trend of increase in average area and decrease in number which was observed for cells cultured without insulin. Presence of insulin in the media, however, provided a rough doubling of the average aggregate areas and rough halving of the aggregate numbers for every combination. This is sound, since same numbers of cells were seeded initially. When total area of aggregates is considered, any profound effect triggered by insulin cannot be seen in general. Particularly, GAG-PA+Glu-PA/Lys-PA (- charge) as well as Glu-PA/Lys-PA (- charge) scaffolds initially had larger total area.

All together, these data may be suggesting that insulin did not pursue a proliferative role; it rather acted in aggregate formation and cell migration.

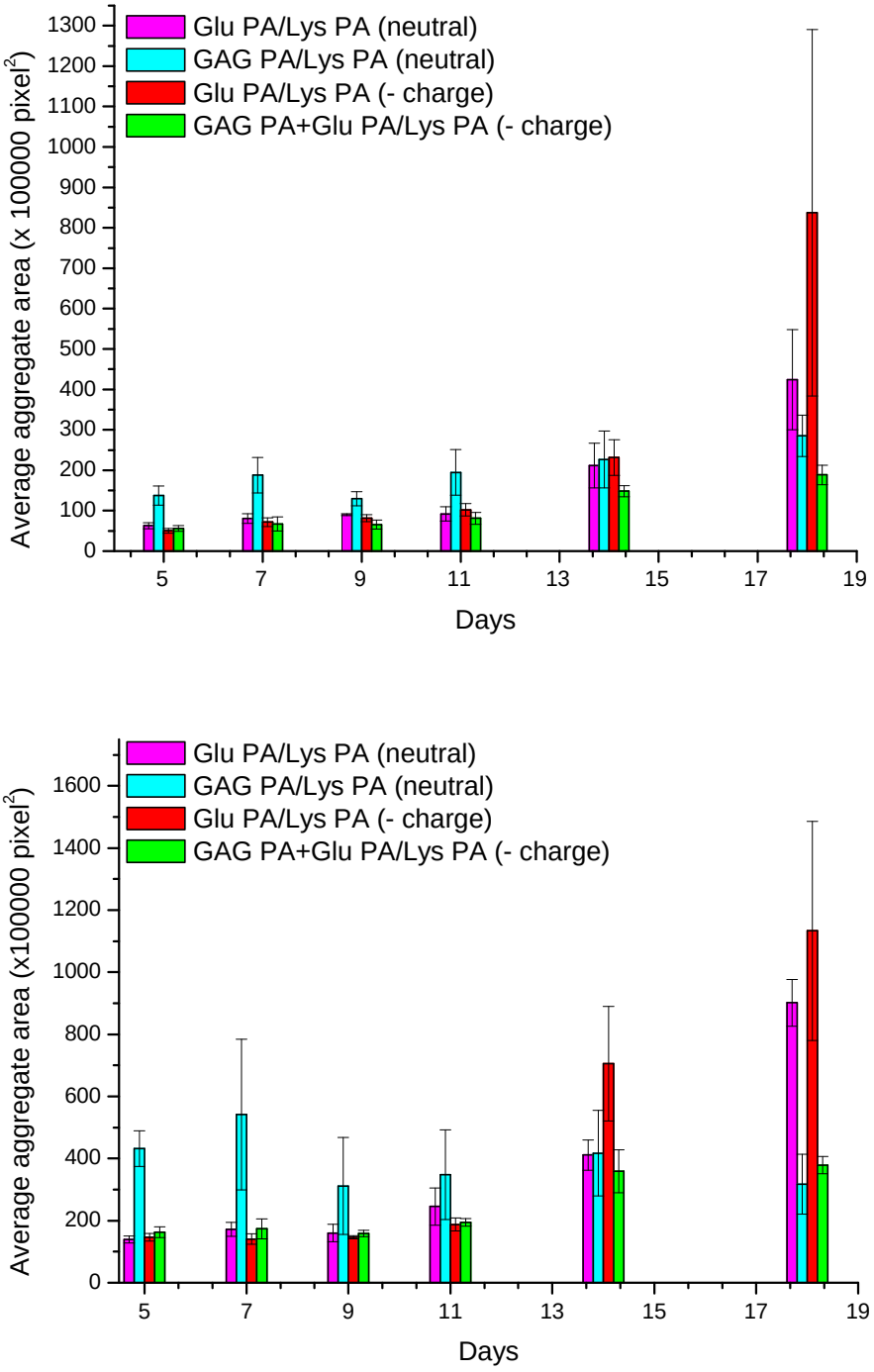


**Figure 20.** Average aggregate areas for ATDC5 cells grown on GAG-PA/Lys-PA (neutral), GAG-PA/Lys-PA (- charge), Lys-PA/Glu-PA (neutral) and Lys-PA/Glu-PA (- charge) for 18 days in media without insulin (at top), or with insulin (at bottom). Values represent mean ± S.D. (n=3)

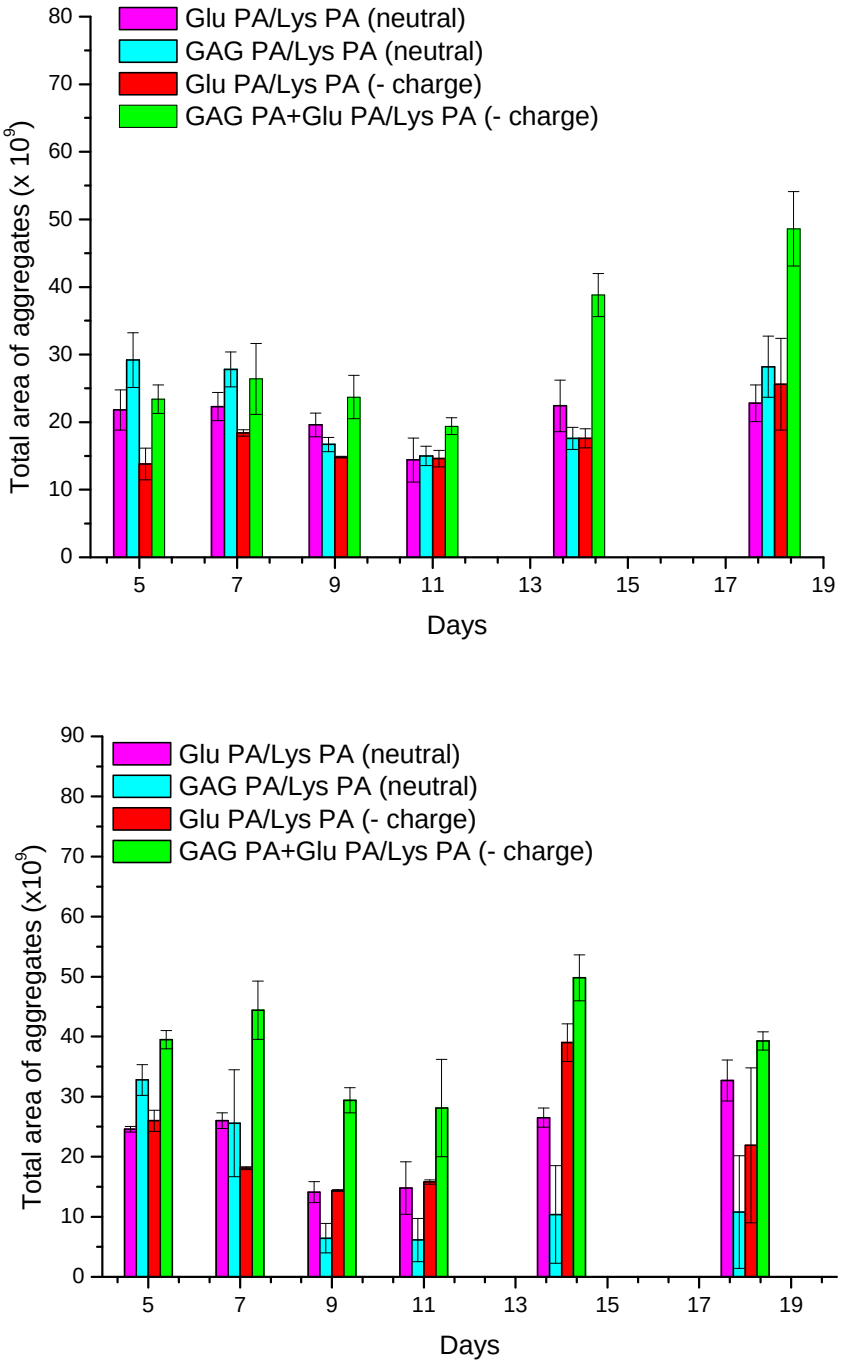


**Figure 21.** Total areas for ATDC5 cells grown on GAG-PA/Lys-PA (neutral), GAG-PA/Lys-PA (- charge), Lys-PA/Glu-PA (neutral) and Lys-PA/Glu-PA (- charge) for 18 days in media without insulin (at top), or with insulin (at bottom). Values represent mean ± S.D. (n=3)

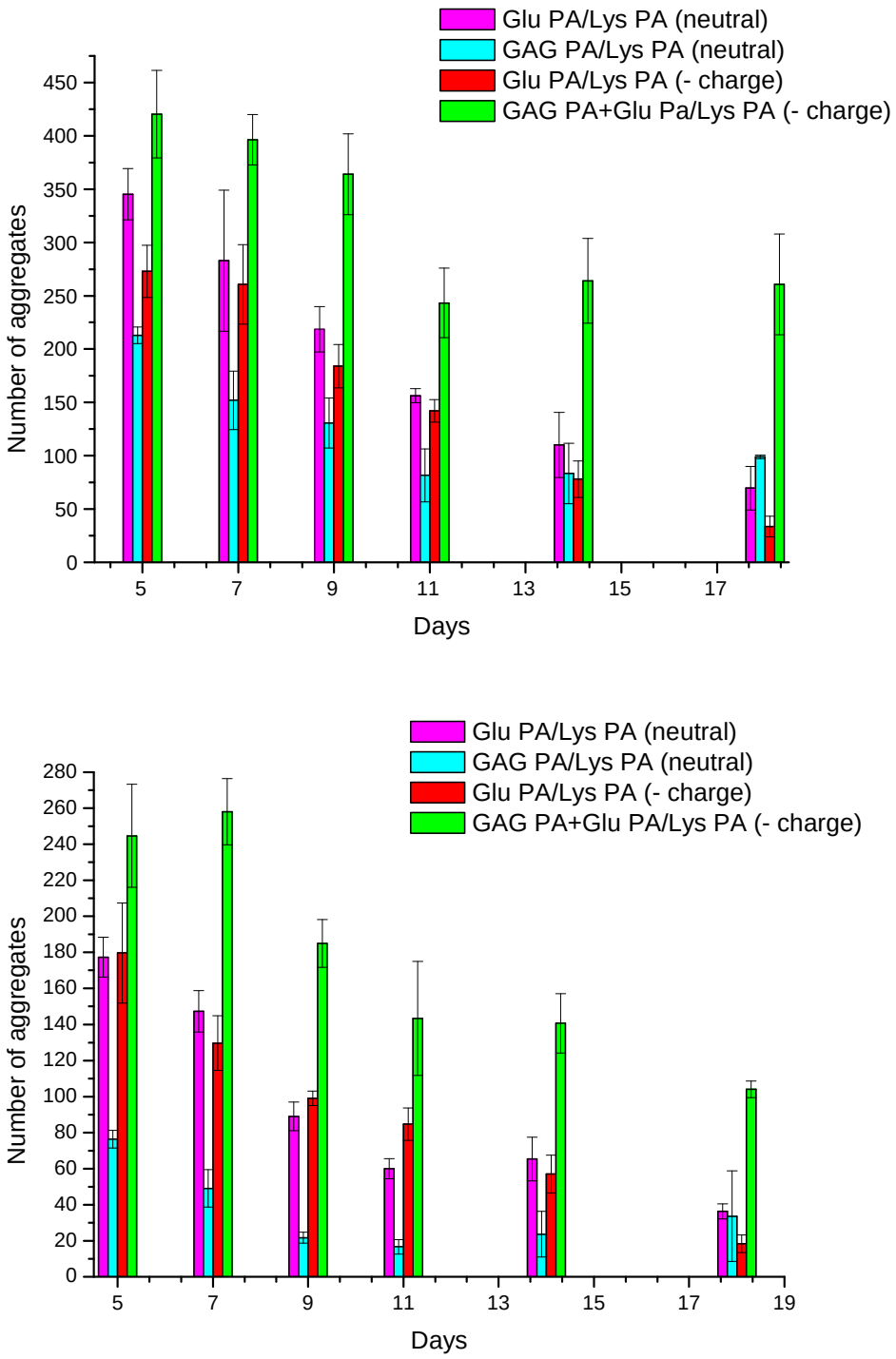


**Figure 22.** Number of aggregates for ATDC5 cells grown on GAG-PA/Lys-PA (neutral), GAG-PA/Lys-PA (- charge), Lys-PA/Glu-PA (neutral) and Lys-PA/Glu-PA (- charge) for 18 days in media without insulin (at top), or with insulin (at bottom). Values represent mean ± S.D. (n=3)

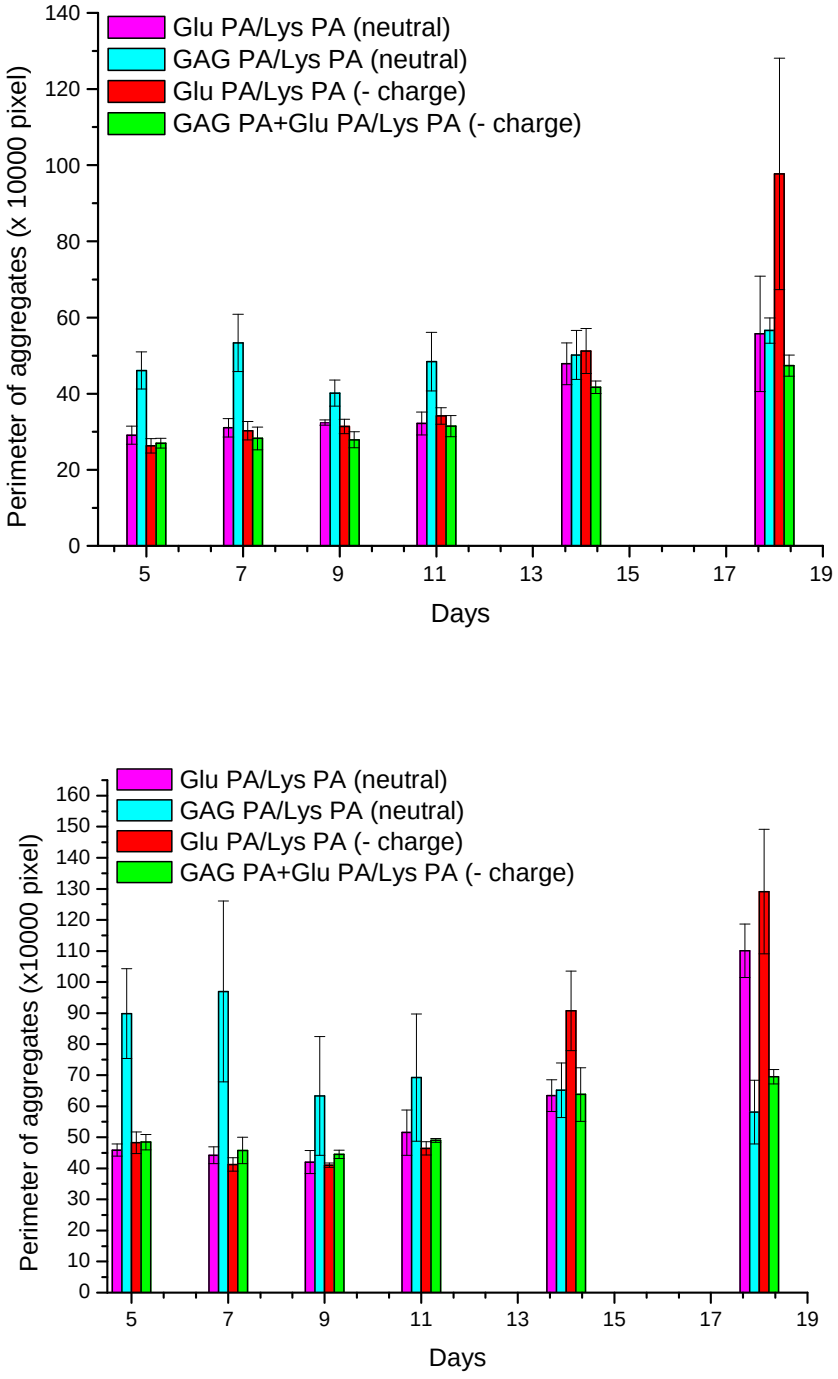


**Figure 23.** Average perimeters for ATDC5 cells grown on GAG-PA/Lys-PA (neutral), GAG-PA/Lys-PA (- charge), Lys-PA/Glu-PA (neutral) and Lys-PA/Glu-PA (- charge) for 18 days in media without insulin (at top), or with insulin (at bottom). Values represent mean ± S.D. (n=3)

### 1.3.2.5 Safranin-O Staining

Safranin-O is a cationic dye which binds to proteoglycans in cartilage in its orthochromatic form. Thus, it has been widely used for detecting changes in articular cartilage. Sarfanin-O is also used for detecting chondrogenesis as production of proteoglycans is accepted as a measure of chondrogenic differentiation.

Aggregates at various stages were stained with Safranin-O. ATDC5 cells that were grown on tissue culture plate, formed a confluent layer without any aggregates. These cells were faintly stained with Safranin-O (Figure 20-21 g, h). On the other hand, primary rabbit chondrocytes which are native of cartilage tissue had more lively stain (Figure 20-21 f).

On days 5, 9 and 14, aggregates formed on GAG-PA + Glu-PA/Lys-PA (- charge) and Glu-PA/Lys-PA (- charge) stained heavily with Safranin-O.

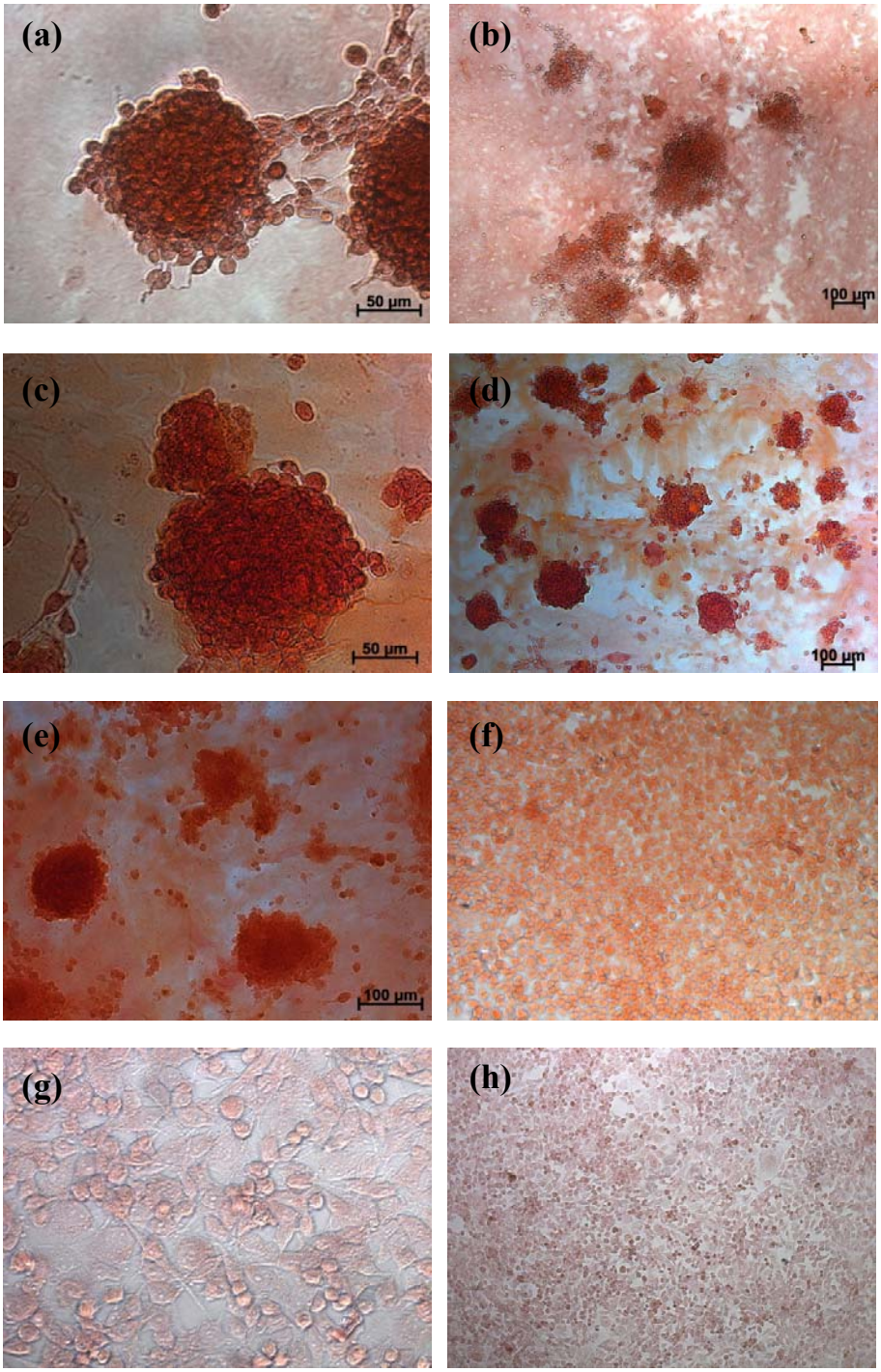


**Figure 24.** Safranin-O staining of ATDC5 cells and primary rabbit chondrocytes. Aggregates of ATDC5 cells seeded on Glu PA/Lys PA (- charge ) (a,b) for 5 days, (c,d) for 9 days, (e) for 14 days, (f) primary rabbit chondrocytes seeded on polystyrene culture plate, (g,h) ATDC5 cells seeded on polystyrene culture plate

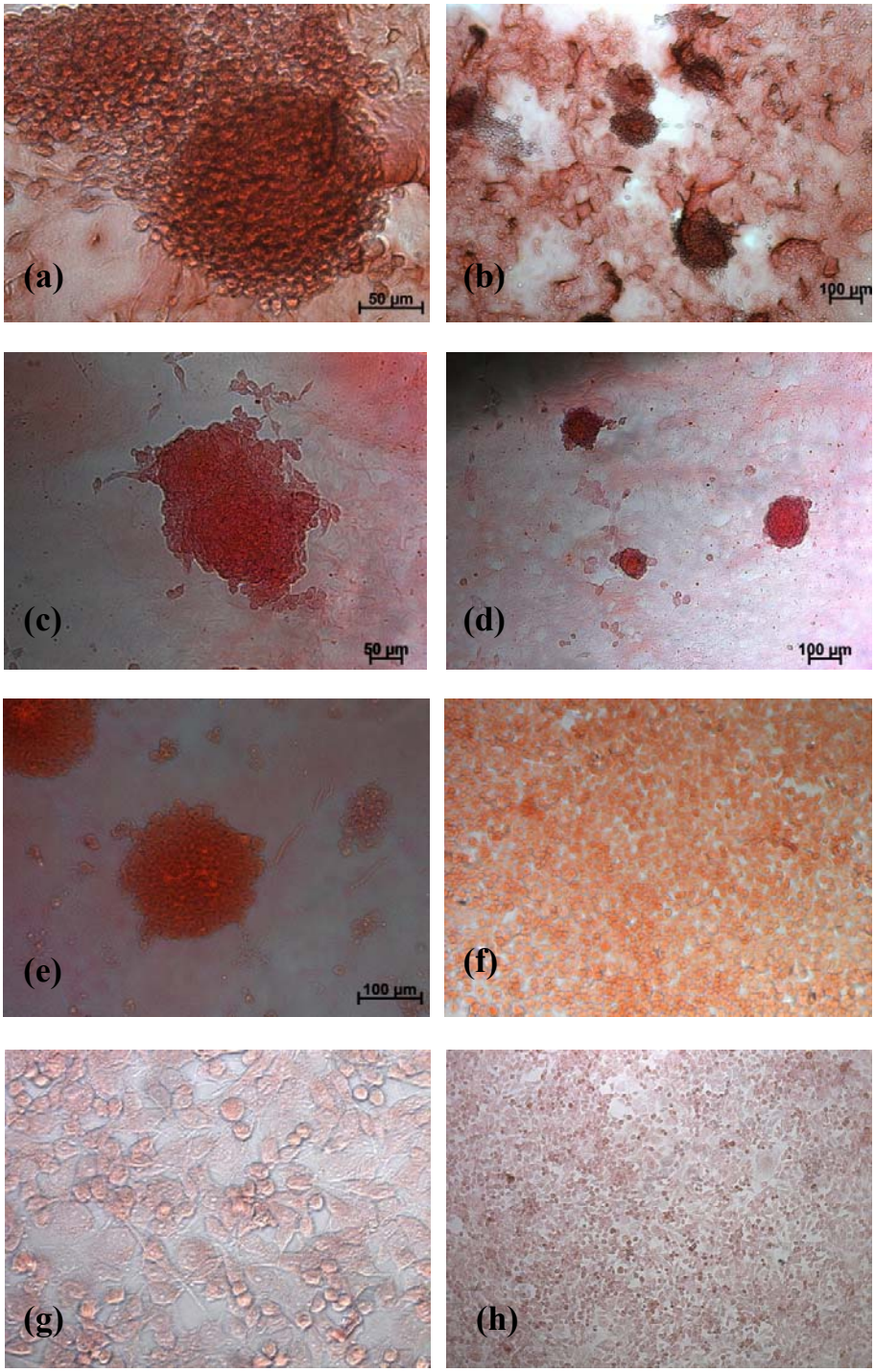


**Figure 25.** Safranin-O staining of ATDC5 cells and primary rabbit chondrocytes. Aggregates of ATDC5 cells seeded on GAG-PA+ Glu PA/Lys PA (- charge ) (a,b) for 5 days, (c,d) for 9 days, (e) for 14 days, (f) primary rabbitt chondrocytes seeded on polystyrene culture plate, (g,h) ATDC5 cells seeded on polystyrene culture plate

### 1.3.2.6 Scanning Electron Microscopy

Microphotographs of aggregates grown on Glu-PA/Lys-PA (- charge) of 5 days were obtained with scanning electron microscopy. Aggregates had approximately 100 μm diameter. Cells within aggregates gathered more round-like morphology like chondrocytes. Heavily produced extracellular matrix observed as dense fibrillar network filling around the cells is an indication of chondrogenic differentiation. Peptide amphiphile coating could also be distinguished and coating was well integrated with extracellular matrix produced by cells. These properties show biomimetic and biocompatible capabilities of peptide amphiphiles.

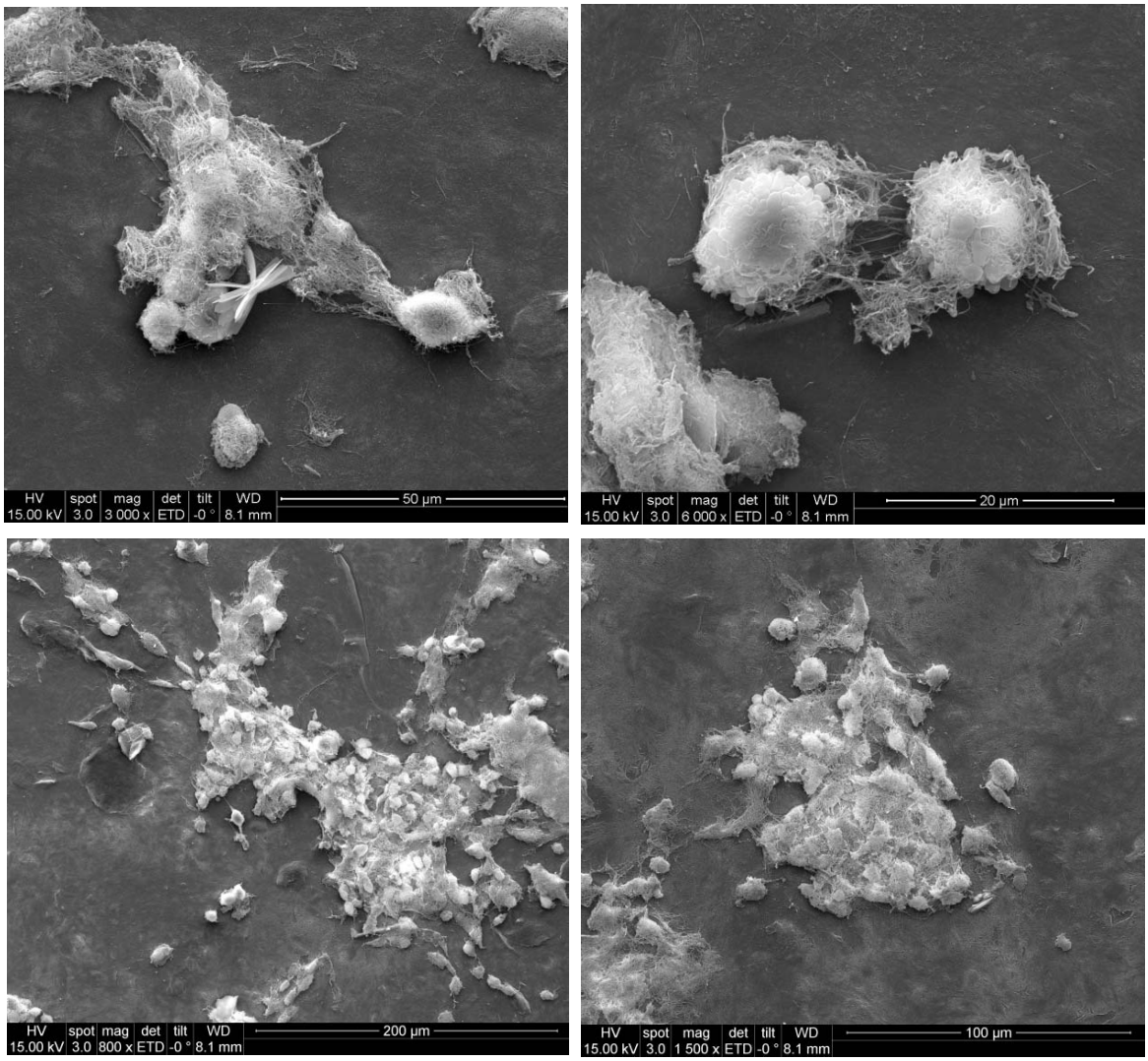


**Figure 26.** Aggregates observed with SEM at various scales

### 1.3.2.7 Immunocytochemistry

Expression of Collagen II which is a cartilage-specific marker was monitored with Collagen II antibody, in ATDC5 aggregates grown for 14 days. Aggregates at 14 days express Collagen II significantly whereas immunofluorescence relevant to Collagen II expression was not observed on ATDC5 cells grown on tissue culture plate for 14 days.

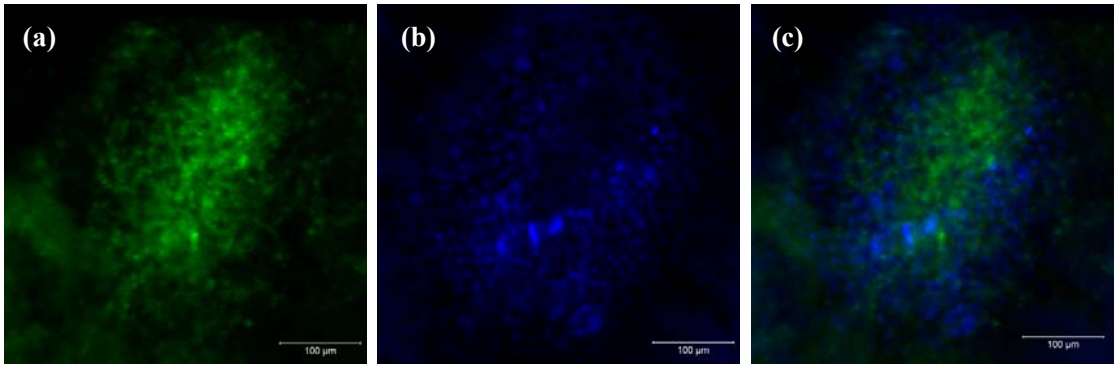


**Figure 27.** Collagen II expression within an aggregate grown on Glu PA/Lys PA (-charge) (a) Col II staining (b) Nuclei staining with TO-PRO (c) Merged image

## 1.4 Conclusion

Cartilage tissue is prone to damages via accidents and diseases like osteoarthritis and rheumatoid arthritis. Cartilage defects of critical size do not heal spontaneously. Extensive studies in various disciplines are carried on for regenerating cartilage. Models of chondrogenic differentiation are important for understanding development and regeneration of cartilage.

In this chapter, a model system for studying chondrogenic differentiation which does not require the use of any bioactive factors was developed. In this model, cartilage formation at developmental stage was mimicked with peptide amphiphiles as scaffolds and ATDC5 cells as chondrogenic progenitors.

When ATDC5 cells were seeded on four combinations of peptide amphiphiles, proliferation of cells diminished and the cells aggregated. These aggregates became compact and got larger in area with time. Aggregation did not require insulin, but addition of insulin to the culture medium resulted in two times larger aggregates. Aggregates contained dense extracellular matrix, expressed collagen II, and were stained with Safranin-O similar to native cartilage tissue. A significant difference of GAG-PA which is designed as a mimetic model for sulfate bearing glycosaminoglycans could not be inferred in two- dimensional culture. However, GAG-PA+Glu-PA (- charge) scaffold resulted in an additional increase of aggregate numbers which may suggest proliferative role. GAG-PA+Glu-PA (neutral) scaffold on the other hand, provided rapid aggregation but aggregate growth was not as extensive as other scaffolds.

From these results we can infer that peptide amphiphiles can mimic extracellular matrix and act as reservoir for growth factors which take role in differentiation. Moreover, peptide amphiphiles are biocompatible in integrating with the native matrix.

This model is convenient for studying several aspects of chondrogenic differentiation without supplementing any bioactive factors. Several stages of chondrogenic aggregation can be visualized within 18 days. Besides, this model can be employed before in vivo experiments to visualize the effects of drug and bioactive factor release.

# CHAPTER 2

# MORPHOLOGICAL ANALYSIS OF VARIOUS TISSUES FROM LYNX-3 LACKING BAC TRANSGENIC MICE IN COMPARISON WITH WILD TYPE MICE

## 2.1 Introduction

Cholinergic system has evolved through time beginning from early ages and it exists within a large spectrum of life forms including simple and complex organisms [169]. Components of cholinergic system include choline-acetyl transferases, acetylcholine, nicotinic acetylcholine receptors, muscarinic acetylcholine receptors, and choline esterases. In humans and other mammals, nicotinic and muscarinic acetylcholine receptors play a central role in neuronal and non-neuronal regulatory mechanisms [170]. Neuronal nAChRs are involved in many brain processes like learning and memory, reward, and mood [171]. In non-neuronal tissues, nicotinic and muscarinic acetylcholine receptors are involved in development [172], wound healing [173], immune regulation [174], and angiogenesis [175].

LY-6 superfamily is composed of cell surface proteins including lynx subfamily of proteins. Lynx1, a neuropeptide, is the first revealed member of lynx subfamily. Lynx2 is expressed within central nervous system similar to Lynx1 [176, 177].

Lynx3 is a recently discovered member of LY6SF, and expressed in central nervous system as well as lungs, trachea, esophagus, forestomach, thymus, female reproductive organ [178].

### 2.1.1 LY6 superfamily of genes/proteins

Ly6 superfamily is composed of protein members with three finger domains containing 4-5 S-S bonds. Some of the well-known members of the Ly6SF are ly6 genes, CD59, SLURP-1 and SLURP-2, E48 antigen, lynx1, and alpha neurotoxins such as alpha-bungarotoxin which is an antagonist of nAChRs [179]. Protein members are expressed in a wide variety of mammalian cells, being involved in diverse tasks.

Human CD59 gene is localized at chromosome region 11p13. It encodes 77 amino acid GPI anchored cell surface antigen detected by MEM43 and other antibodies. CD59 prevents formation of membrane attack complex (MAC) assembly on the host cells by binding to C5b-8 and C5b-9, thus prohibiting the host cells from being lysed [180].

E48 (LY6-D) is a specific marker for normal, malign, and transient squamous cells [181]. It serves as a molecular marker for the detection of squamous cells within blood and bone marrow [182]. E48 was shown to be involved in the association of head and neck squamous cells with endothelial cells [183].

SLURP-1 is a member of LY6SF without a GPI anchorage signal, in contrast to the most other members. It is an allosteric modulator of the keratinocytic α7 nicotinic acetylcholine receptors [184] which play role in the differentiation of the stratified squamous epithelium [185]. SLURP-1 was shown to have a proliferation suppressing effect at the same time promoting the expression of apoptotic enzymes and terminal differentiating markers

[186]. Mal de Meleda is an autosomal recessive disorder, characterized by mutations in the gene encoding SLURP-1 localized at 8q24.3 [187].

SLURP-2 is another secreted cholinergic signaling protein mainly expressed in epithelial tissues. It is overexpressed in psoriasis vulgaris, a hyperproliferative skin disorder [188]. Unlike, SLURP-1 which prefers α7 nAChRs, SLURP-2 acts on α3 nAChR subtypes. Contrasting with the roles of SLURP-1, SLURP-2 was assigned roles of supporting proliferation, slowing down the differentiation and hindering apoptosis [189]. These two secreted proteins have recently been shown to function in protection of the cells from the cancer inducing activity of tobacco derived nitrosamines [190, 191].

Many of the Ly-6 genes are located in the telomeric region of chromosome 8 (i.e. 8q24) of human genome which is syntenic to a locus at chromosome 15 of mice genome. 19q13.3 and 6p21.3 are two other regions at which the Ly-6 genes are likely to be found in human genome [192-194]. An SNP at the Ly-6 cluster locus at chromosome 8 was recently found to be associated with HIV susceptibility suggesting a role for Ly-6 genes in this region [195].

### 2.1.2 Lynx homologous genes

Lynx1, the first unraveled member of lynx gene family is highly expressed in central nervous system and lungs. Forming stable complexes with nicotinic acetylcholine receptors (nAChR), Lynx1 alters the sensitivity of these receptors which contributes to an overall inhibitory effect. Sequence homology between snake venom neurotoxin and Ly6 family of proteins as well as tertiary structural similarity had been elucidated without any common function between two relative protein subtypes being revealed except for lynx1.

Lynx1 shares primary and tertiary structure homology with snake venom neurotoxins which act as nAChR antagonists. Snake venom neurotoxins and lynx1, all have the ability to interact with nAChRs and modulate sensitivity of the receptors and the kinetics of ion channel gating. Unlike, neurotoxins which are soluble proteins, lynx1 is a GPI-anchored protein, and show its effect in membrane bound form. Chimerical constructs with GPI-anchorage sequence of lynx1 and the soluble neurotoxin sequence were designed and these were used for obtaining membrane bound form of several neurotoxins. In membrane bound form, similar to lynx1, recombinant neurotoxins could still interact with the receptors and modulate their activity [196].

Immunohistochemistry experiments showed colocalization of Lynx1 expression with α4 nAChRs within cortex, amygdala, habenula and substantia nigra in adult mice. Within cortex, amygdala, hippocampus and thalamic reticular nuclei, lynx1 colocalized with a7 nAChRs [197].

Lynx2, similar to Lynx1 is a neuromodulatory protein expressed in neuronal cell population. Lynx2 was specifically localized to anxiety-related brain areas. Since, higher levels of anxiety were observed for lynx2-KO mice, lynx2 was proposed to be a key element in anxiety-related behavioral mechanisms [176].

Lynx1 and Lynx2 proteins are involved in the modulation of brain plasticity within critical period during adulthood. Lynx1 mRNA levels in adult visual cortex elevated after the critical period, while lynx2 levels decreased. Lynx1, also called as cholinergic brake, is considered to be limiting the brain plasticity [198].

Lynx3 is also a modulator of nAChRs and is expressed in neurons and epithelia of a vast diversity of tissues. The tissues in which lynx3 is expressed include lungs, stomach, thymus, reproductive organs, spleen, and nasal cavity. Lynx1, lynx2 co-precipitated with α4β2, α4β4, α1β1γ and α7 nAChRs. Lynx3 co-precipitated α4β2, α4β4. All three homologues can modulate desensitization kinetics of α4β2 nAChRs (unpublished data).

Lynx subfamily of genes also occurs in other species such as *C. elegans*, *D. melanogester* and non-venomous snakes.

### 2.1.3 Acetylcholine receptors

Acetylcholine is a simple molecule playing a central role in cell function (Figure 1). It was firstly recognized as a molecule involved in transmitting signals among nerves. Besides neurotransmission, acetylcholine functions widely among non-neuronal tissues as will be explained later.

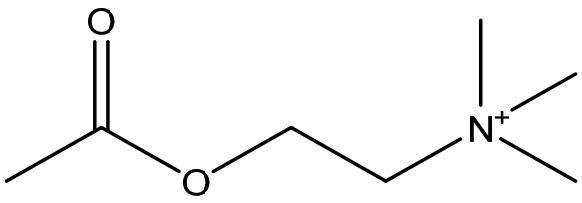


**Figure 28.** Chemical structure of acetylcholine, acetylcholine is an ester of acetic acid and N,N,N-trimethylethanolammonium cation

Acetylcholine is composed of AcetylCoA, a basic metabolite in Krebs cycle, and choline which is a quaternary amine which can be obtained from degradation of phospholipids of the cell membrane. Choline acetyl transferase enzyme is responsible for synthesizing

acetylcholine from two precursors. For humans, this enzyme is encoded by ChAT gene which was mapped to human chromosome 10. Expression of this enzyme is universal for every human tissue, while isoforms of the enzyme are observed for different tissues [170].

Acetylcholine acts through binding acetylcholine receptors anchored within cellular membrane. This system is thought to have emerged early in the history of life as its components are present in bacteria, fungi, protozoa, sponge, and simple plants. An organism with evolutionary significance is *Torpedo* genus producing electricity through cholinergic activity [169, 170].

Mammalian acetylcholine receptors are expressed by a wide diversity of cells within body. Two major types of acetylcholine receptors are mecanotrophic muscarinic acetylcholine receptors (mAChRs) and ionotrophic nicotinic acetylcholine receptors (nAChRs). Muscarinic acetylcholine receptors are G protein coupled receptors and intercellular pathways are induced as a result of interaction with G protein. Nicotinic acetylcholine receptors lead to cation ($Na^+$, $K^+$, $Ca^{++}$) inflow through the membrane [199].

While both receptors are activated by acetylcholine, these receptors may be activated by chemicals specific to each type of acetylcholine receptor. In the case of mAChRs, a toxin from mushroom *Amanita muscaria* called muscarine is an activator and a toxin from *Atropa belladona* called atropine is an inhibitor. Muscarinic acetylcholine receptors have slower activation kinetics than nicotinic acetylcholine receptors with a response time of milliseconds to seconds [200].

Nicotinic acetylcholine receptors are cationic receptor channels which can be activated in the presence of nicotine. Much of our knowledge about nAChRs was brought about with

studies on alpha-bungarotoxin, which is a snake venom that inhibit muscle type nAChRs. Alpha-bungarotoxin binds to nAChRs with an affinity which is about covalent bond strength. Making use of this high affinity, alpha-bungarotoxin conjugated columns were designed for isolation and purification of nAChRs [200-202]. The amino acid sequence of –NH2 terminal protein was identified after purification which enabled deciphering and cloning genes encoding nAChRs with reverse genetics methodologies. In a variety of mammalian cells, including muscle, skin, pancreas, lungs and neurons, nAChRs were reported to exist, having essential roles [200, 203].

Much of the knowledge for nAChR structure was gained from the studies with *Torpedo* nAChR [204, 205]. Low abundance of the receptor within whole protein soup lead to difficulties in isolating and revealing the structure. Herein, the electric organ of *Torpedo* ray in which nAChRs are massively produced, served as a source for nAChRs, partly solving this problem [200].

Nicotinic acetylcholine receptors are ligand gated channels belonging to Cys-loop receptor family. A pair of Cys-Cys bonds separated by 13 amino acids exists for this family of proteins at the extracellular portion of the protein. Other members of the family are 5-hydroxytryptamine type 3 (5-HT3) receptors, γ-aminobutyric acid type A (GABAA) and GABAC receptors, glycine receptors, and invertebrate glutamate and histidine receptors [200].

Nicotinic acetylcholine receptors are composed of five membrane spanning protein subunits arranged in a barrel like structure. Five subunits designated as 2 α subunits, β, δ and γ or ε, are made up of helices M1, M2, M3, and M4. M2 helices lie at the inner side

of the channel providing hydrophobic intercore for dehydration of the ions and passage of the ions through the pore. Acetylcholine interaction site is included within extracellular portion of acetylcholine α subunits [200, 206].

Binding of acetylcholine leads to opening of the channel, whereas continuous induction with acetylcholine causes channel closure, which is called desensitization. Upon binding, conformational changes in acetylcholine binding site and M2 helices were reported [207]. As the channel opens, the diameter of the pore becomes 0.65 nm and allows the passage of positively charged ions, $Na^+$ and $K^+$. Some subunit compositions, may allow passage of $Ca^{2+}$ ions through the membrane, in this way release of other neurotransmitters may be triggered [206, 208].

In vertebrates, according to the site of nAChR expression, subunit composition and ratio may differ. At neuromuscular junctions, α1, β1, δ, and γ or ε subunits unite to form the receptors in 2:1:1:1 ratio. Nicotinic acetylcholine receptors expressed in neurons are also composed of five subunits involving nine subtypes of α known as α2, α3, α4, α5, α6, α7, α8, α9, α10 and six subtypes of β known as β2, β3, β4, β5, β6, β7 [209, 210].

Acetylcholine activity was formerly known to be specific for nervous system. It has become evident, however, that acetylcholine receptors and ChAT (Choline-acetyl transferase) exist throughout the body within a diversity of cells indicating synthesis, storage, release of acetylcholine and reception of acetylcholine through receptors. The cholinergic system certainly has a particular importance for many important aspects of life at cellular level. Through acetylcholine receptors, cell cycle, differentiation, cell to cell

contact, migration and apoptosis are regulated within epithelial cells, endothelial cells, immune cells, mesothelial cells and mesenchymal cells [170].

Acetylcholine is released with the help of organic cation transporters and acts in autocrine or paracrine manner [211, 212]. Acetylcholine transport through the bloodstream is strictly prevented via rapid degradation by esterases.

One interesting example of how acetylcholine exerts its effects was demonstrated with keratinocytes which altered their morphology and lost cohesive properties when n-AChRs and m-AChRs were blocked with antagonists [213]. Similarly, bronchial epithelial cells became smaller, and each cell lost contact with neighbors when treated with antagonist [170, 214]

During developmental stages, keratinocytes express specific combination of muscarinic acetylcholine receptor subtypes. In this way, control of biological outputs during stages of keratinocyte maturation as a result of acetylcholine reception can be managed [215].

Acetylcholine was found to be expressed throughout the epithelium that lines the inner and outer surfaces of rat airway, gastrointestinal, reproductive and urinary tracts (bronchi, mouth, small and large intestine, gall bladder, vagina, skin and pulmonary pleura) [216].

Keratinocyte muscarinic and nicotinic acetylcholine receptors, act oppositely for $Ca^{2+}$ intake from extracellular fluid. Simulation of the muscarinic and nicotinic receptors concurrently, maintains balanced $Ca^{2+}$ concentration and metabolism [217].

Simulation with acetylcholine is also key in mediating keratinocyte migration. M4 mAChR -/- murine keratinocytes showed impaired migration, and inhibition of

keratinocytes with atropine had a similar effect. Besides, activation of M4 with muscarine resulted in increased migration of M3 mAChR -/- keratinocytes, which exhibited increased migration distance, showing adverse effect to M4 type receptors. Wound healing response, in parallel to migration of keratinocytes, was improved in M3−/− but weakened in M4−/− knockout mice [217, 218]. Moreover, hair follicle cycle was disturbed in M4−/− knockout mice [219].

Human and rat airway cells, likewise, express mAChRs. nAChRs and mAChRs are effected by ACh [216, 220]. Nicotinic acetylcholine receptors were shown to be involved in migration of bronchial epithelium cells and wound healing of lung epithelium [221].

In intestine epithelial cells, cholinergic system is involved in directional fluid movement within intestinal tract by regulating chlorine secretion [222]. Similarly, ion and fluid movements are modulated by acetylcholine in mucosal and glandular epithelial cells [223, 224].

Acetylcholine receptors also have role in attracting immune cells towards airway epithelial barrier and stimulating mucus activity. Acetylcholine may also alter immune responses. Activation of α7 with acetylcholine inhibits the release of pro-inflammatory factors such as tumor necrosis factor or IL1-β from immune cells. The process was named as cholinergic anti-inflammatory pathway [224, 225].

## 2.2 Experimental Section

Morphologies of different tissues for Lynx3 KO mice and WT mice were investigated. Cloning of KO constructs was performed by Dr. Ayşe Begüm Tekinay with C57B16 genomic DNA containing bacterial artificial chromosomes from Research Genetics, and

10 kb genomic DNA containing clones from Open BioSystems as template. Histological sectioning and Hematoxylene Eosin staining were also done by Dr. Ayşe Begüm Tekinay. Briefly, mice were perfused with PBS, then perfusion solution containing 1.4% Na-cacodylate, paraformaldehyde, 4% sucrose followed by perfusion wash solution containing 0.034% Na-cacodylate, 0.023% $CaCl_2$, 0.8% sucrose, 0.8% NaCl and 0.4% dextrose. Tissues were sectioned with a microtome. Tissue sections were analyzed with light field microscopy at 10x and 40x magnifications.

## 2.3 Results and Discussion

### 2.3.1 Trachea

It was shown that lynx3 is heavily expressed within the pseudostratified ciliated columnar epithelium lining of upper and lower respiratory tract. Covering the inner surfaces of nasal cavities and trachea, this type of epithelium is basically composed of ciliated cells and goblet cells which together act to protect lungs from foreign materials brought by air. Goblet cells secrete mucus, a sticky material rich in glycoproteins, which traps airborne particles and microorganisms. Ciliated cells, repel the trapped particles outwards, by coordinated movements of cilia on their apical surfaces. Structurally resistant to wear and abrasion, the epithelial layer also provides mechanical protection from airflow [226, 227]. A third type of cell, representing 3% of the epithelial layer exist and is called “brush cell”, a name coming from brushy appearance of blunt and short extensions present at the apical membranes of the cells. Function of brush cells has been uncertain for a long time, but these cells have been considered to be chemosensors [228].

It is almost impossible to distinguish between epithelial cell phenotypes mentioned above from trachea section images of wild type mice and lynx3 BAC transgenic mice displayed at Figure 1. Cilia structures however can be seen and these are present for both wild type and lynx3 deficient mice. Wild type mice and lynx3 deficient mice are similar in morphologies of tracheal epithelium as well as surrounding cartilage and smooth muscle layers and overall trachea. Retention of morphologies other than epithelium is an expected result since lynx3 expression is limited to the epithelium. Also, lynx3 is related with the cholinergic system which acts mostly atocrine/paracrine.

Acetylcholine is important in epithelial proliferation, wound healing mechanisms [170, 214]. Within trachea, acetylcholine is also involved in regulation of cilia movement, recruitment of immune cells for protection from infection. Recently, brush cells were reported to express ChAT enzyme and vesicular acetylcholine transporters and some of these cells are in direct contact with vagal nerve fibers and their role for regulation of respiratory rate was discovered [228].

Any significant difference in epithelial proliferation is not observed between wild type and lynx3 deficient BAC transgenic mice. Moreover, any inflammatory conditions or abnormalities cannot be seen in KO and WT mice.

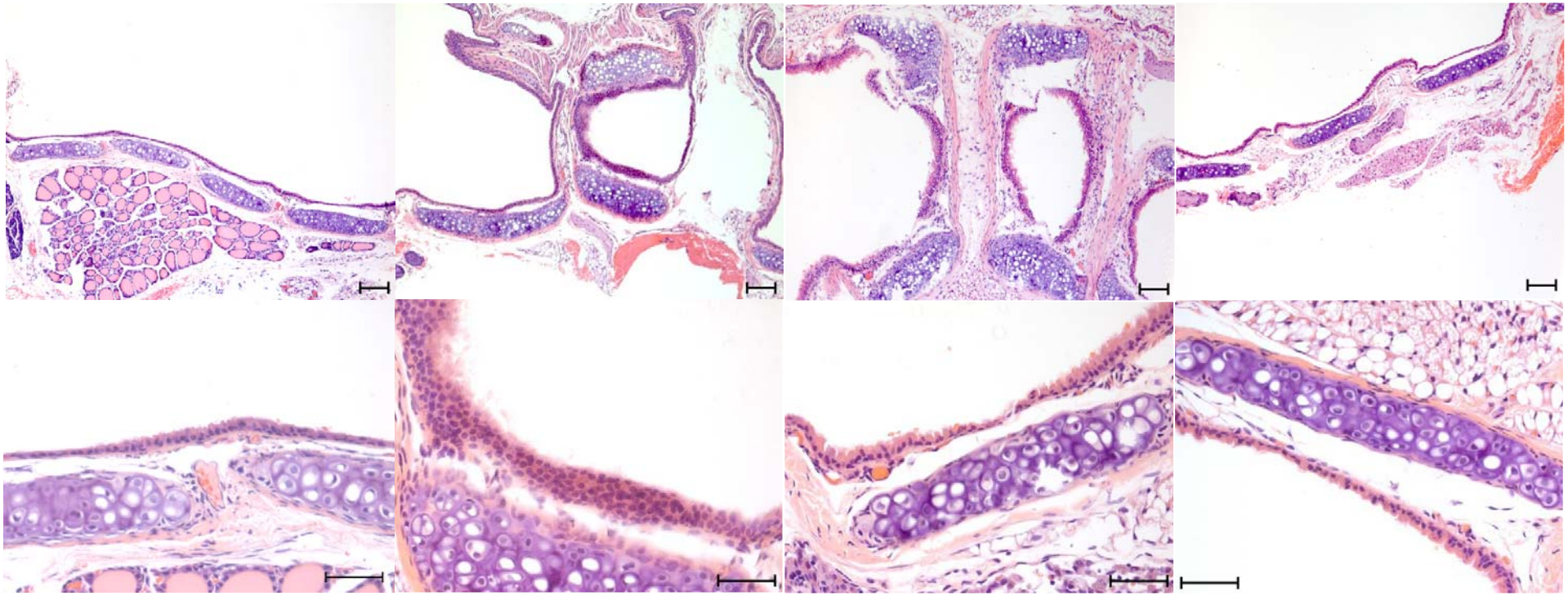

**Figure 29.** Hematoxyline & Eosin stained sections of cartilaginous airways of various phenotypes. From left to right: WT female, lynx3 KO female, WT male, KO male. Top: 10x objective scale bar: 100 µm, Bottom: 40x objective scale bar: 50um

### 2.3.2 Lungs

Tracheal expression of lynx3 is followed by lynx3 expression within bronchi and bronchioli. In bronchi, ciliated simple columnar epithelium cells and in bronchioli cuboidal epithelium cells express lynx3. As in tracheal epithelium, any significant difference in morphology between wild type and lynx3-/- BAC transgenic mice was not observed. Any inflammatory condition or physiological abnormality was not observed.

Cholinergic stimulation is mostly associated with cell-cell adhesion, proliferation, migration and wound healing for epithelial cells within lungs. Treatment of bronchial cells with ACh receptor antagonists of strong affinity resulted in cell shrinkage and loss of contact between neighbor cells. Absence of lynx3 inhibition of ACh receptors does not have an apparent impact on these mentioned properties, at least during early developmental stages [170, 214, 229].

Functional redundancy may have served as a means to maintain wild type morphology in lynx3-/- BAC transgenic mice. Expression of lynx1 which is a homologue with similar function in bronchial epithelium has been revealed [230]. Functionally similar proteins like lynx1, might be regulated in a way to compensate for the insufficiency caused by lynx3 deficiency.

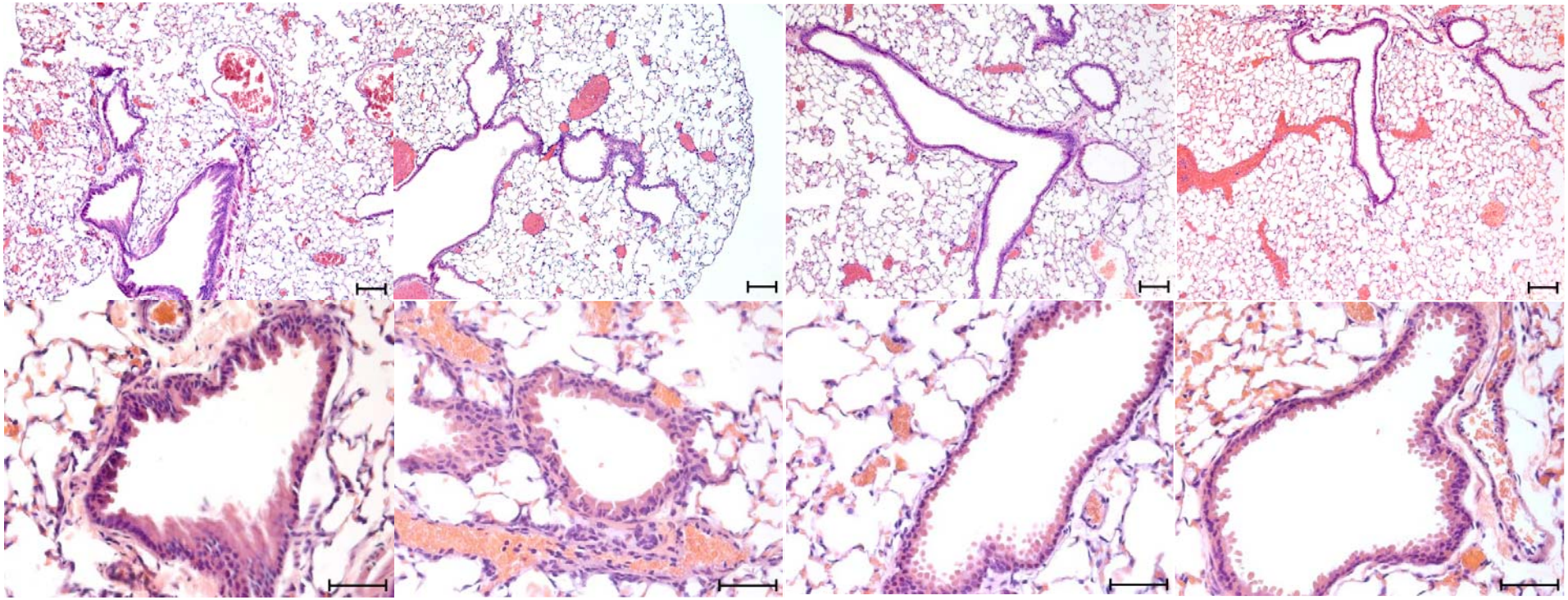

**Figure 30.** Hematoxyline & Eosin stained sections of lungs for lynx3 expressing and lynx3 deficient mice. From left to right: WT female, lynx3 KO female, WT male, KO male. Top: 10x objective scale bar:100 µm, Bottom: 40x objective scale bar: 50 µm

### 2.3.3 Esophagus

In esophagus, lynx3 is expressed in stratified squamous epithelium lining the inner cavity. Esophageal mucosa of lynx3 BAC transgenic male mouse (Figure 32., top right), was disrupted at some regions and is thinner than others. Larger esophageal diameters for lynx3 BAC transgenic mice than for wild type mice might be due to different sectioning positions or dilation. In BAC transgenic mice esophagus posed asymmetrically. There might be possible differences in smooth mucle contractile properties. Mucosal breaks and circumferential asymmetry might also be associated with esophagitis and GERD (Gastroesophageal reflux disease) [231].

In oral keratinocytes blocking of nicotinic acetylcholine receptors resulted in loss of cell-cell contact and cell motility. Furthermore, stimulation of nAChRs by tobacco derived nitrosamines lead to changes in patways which contribute to cancer. Tobacco smoking is an important factor in development of oral and esophageal cancer. Nicotinic acetylcholine receptor subtypes present in esophageal mucosa are α3, α5, α7 and β2 similar to oral keratinocytes [232].

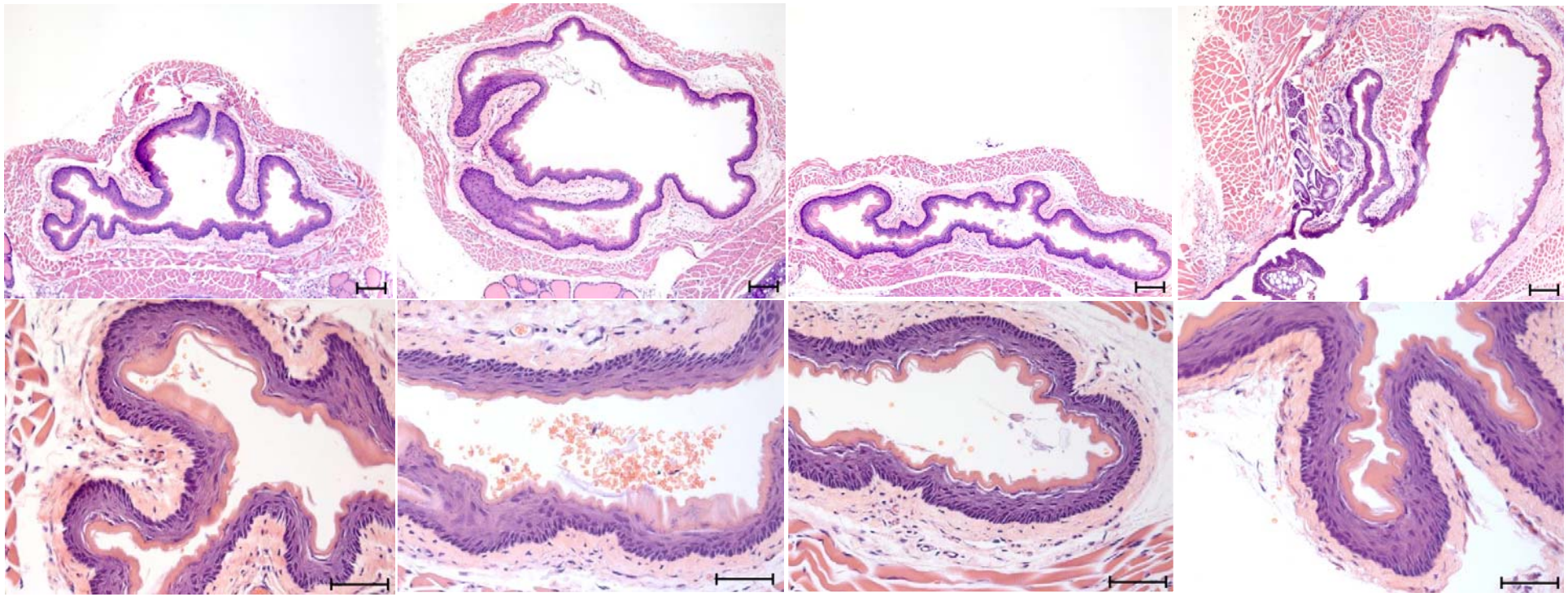

**Figure 31.** Hematoxyline & Eosin stained sections of esophagus for lynx3 expressing and lynx3 deficient mice. From left to right: WT female, lynx3 KO female, WT male, KO male. Top: 10x objective scale bar:100 µm, Bottom: 40x objective scale bar: 50 µm

### 2.3.4 Stomach

Lynx3 expression was observed within non glandular part of stomach called forestomach. Forestomach is adjacent to esophagus and stratified squamous epithelium lines inside. Mucosal ridge which separates forestomach from glandular stomach can be seen in micrographs given in Figure 5. Epithelium, connective tissue, circular and longitudinal smooth muscles are well arranged in all mice. Moreover any severe morphological abnormality was not conspicuous. Within the forestomaches of lynx3-/- BAC transgenic mice, however, the average lengths of the mucosal folds were apparently reduced with respect to forestomaches of wild type mice.

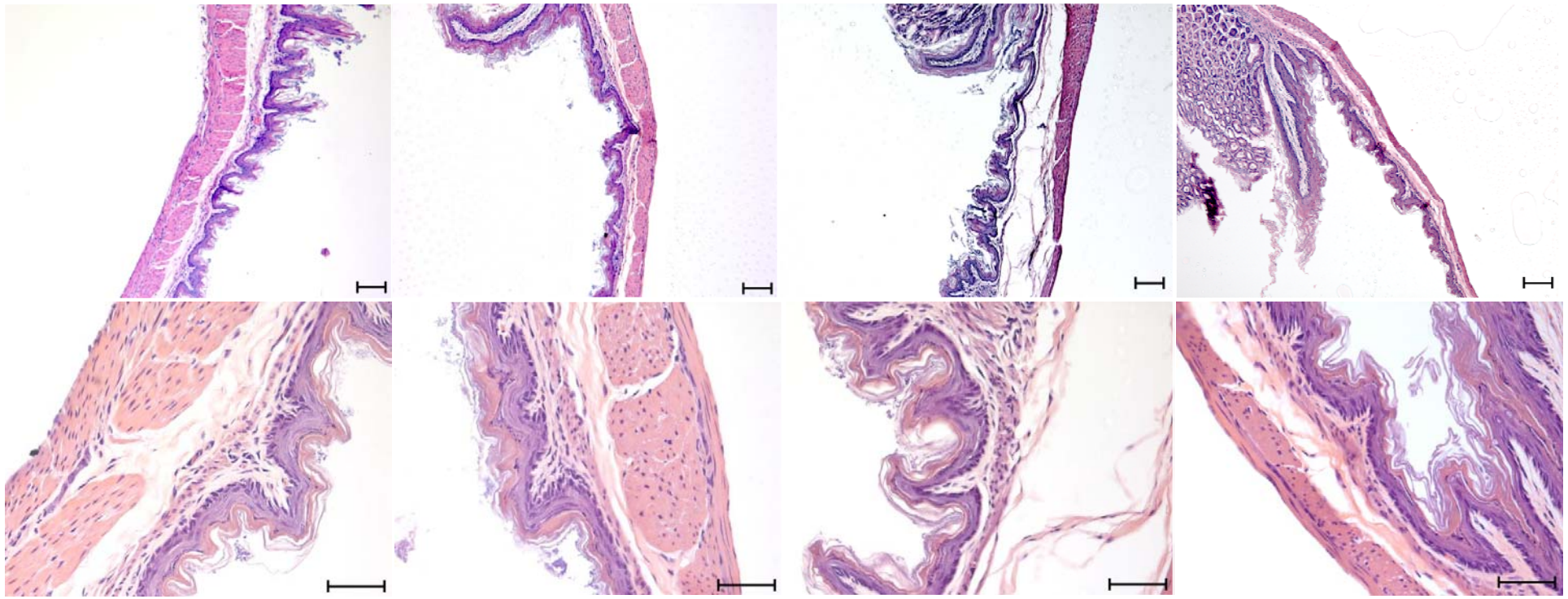

**Figure 32.** Hematoxyline & Eosin stained sections of esophagus for lynx3 expressing and lynx3 deficient mice. From left to right: WT female, lynx3 KO female, WT male, KO male. Top: 10x objective scale bar:100 µm, Bottom: 40x objective scale bar: 50 µm

### 2.3.5 Thymus

In thymus, lynx3 is expressed within scattered epithelial cells and lymphocytes. Any significant difference between thymic morphologies of lynx3 BAC transgenic mice and wild type mice cannot be observed (Figure 6).

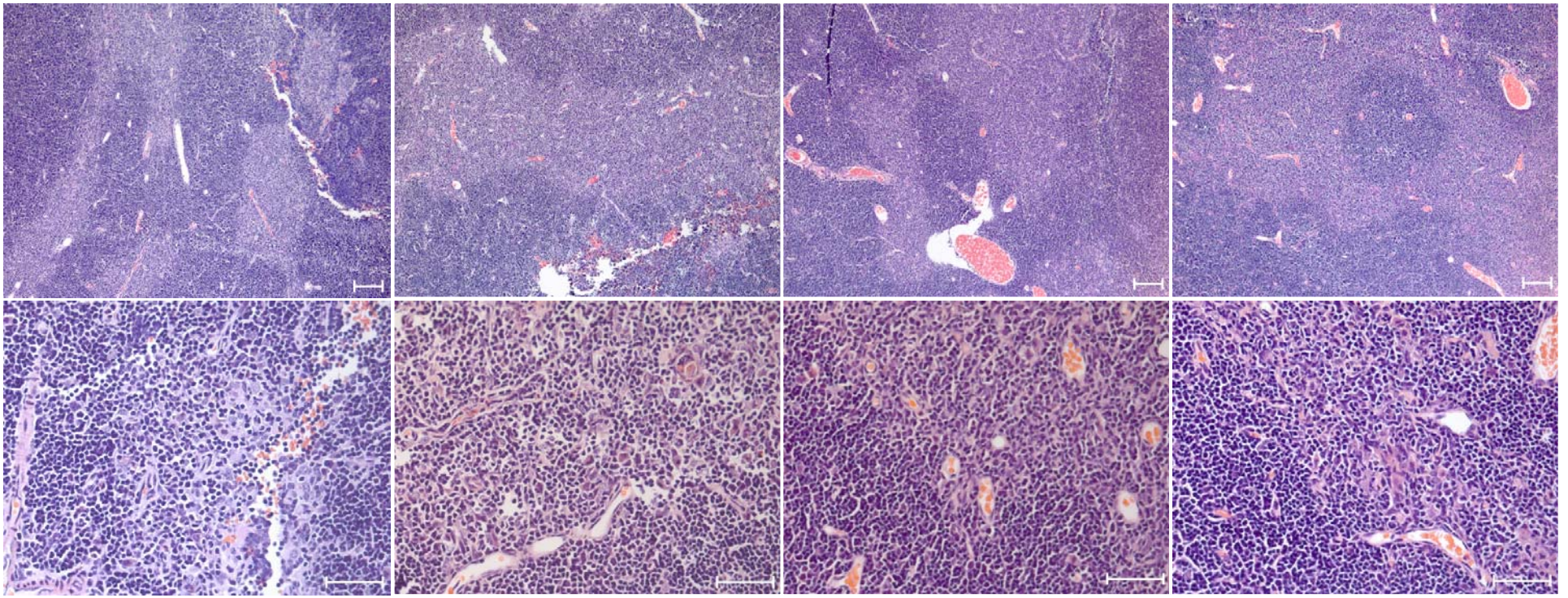

**Figure 33.** Hematoxyline & Eosin stained sections of thymus for lynx3 expressing and lynx3 deficient mice. From left to right: WT female, lynx3 KO female, WT male, KO male. Top: 10x objective scale bar:100 µm, Bottom: 40x objective scale bar: 50 µm

### 2.3.6 Female reproductive organ

Lynx3 expression in female reproductive organ is localized to squamous stratified epithelium. In wild type female mouse, reproductive tract with two different morphologies were observed. One of them has within bulky mucosa and the other has thinner mucosa. In lynx3-/- BAC transgenic mice the reproductive organ with the bulky epithelial layer could not be observed.

In lynx3 BAC transgenic mice, foreign bodies were present inside the epithelial layer, which are likely to be immune cells. This is a possible indication of activated immunity around epithelial cells of the female reproductive organ in lynx3 deficient mice.

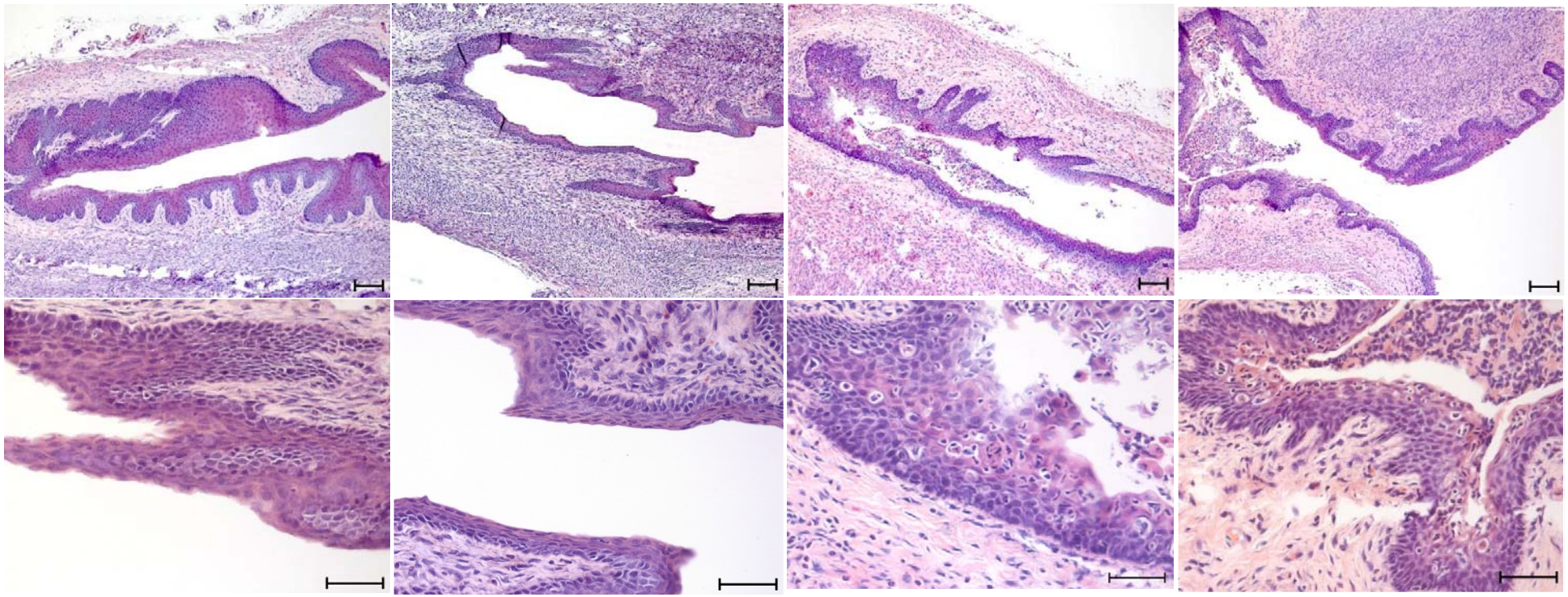

**Figure 34.** Hematoxyline & Eosin stained sections of female reproductive organ for lynx3 expressing and lynx3 deficient mice. From left to right: WT female, WT female, KO female, KO female. Top: 10x objective scale bar:100 µm, Bottom: 40x objective scale bar: 50 µm

## 2.4 Conclusion

In this study, various tissues of wild type and lynx3 deficient mice were histologically compared with a focus on epithelial tissue.

In respiratory tract, pseudostratified columnar epithelium of trachea, ciliated columnar epithelia of lungs were investigated. Any distinctive features between wild type mice and lynx 3 deficient mice could not be observed.

In alimentary tract, stratified squamous epithelium of esophagus and forestomach was investigated. Esophageal epithelia were similar for both WT and transgenic mice. Esophagi of transgenic mice were more asymmetric than esophagi of WT mice. Moreover, non-glandular stomachs of lynx3 BAC transgenic mice had smaller mucosal curvature.

Scattered epithelium cells and lymphocytes within thymuses of all mice had similar morphology.

Non-keratinizing stratified epithelia of female reproductive organs of lynx3 deficient mice contained foreign bodies which are possibly immune cells. In wild type mouse, these bodies were not observed.

Moving from these results more detailed investigation of these should be done in order to better understand the function of lynx3.

# CHAPTER 3

# CHARACTERIZATION OF PEPTIDE AMPHIPHILES AS DNA DELIVERY AGENTS

## 3.1 Introduction

Effective transportation of DNA into the cells is an important step towards accomplishing gene therapy. Naked DNA is prone to degradation by intracellular or extracellular enzymes and it can barely pass the plasma membrane [233].

Viruses are natural cargo delivery systems which have been specialized in loading their genetic material within a variety of cells in a highly efficient way. Viral components may be effective as DNA delivery agents, however these are asscoiated with certain health risks such as toxicity, and inflammation [234]. Non-viral delivery systems have also been promising in gene delivery, and some of them became commonly used in transfection protocols. Cationic lipids and polymers are two main groups of non-viral-delivery agents.

### 3.1.1 Cell Penetrating Peptides

Basic proteins like histones have been known for a long time for crossing over membranes with relative ease. These proteins also enhance the passage of other molecules to which they are associated [235].

Knowledge about ability of proteins with high basic amino acid content to easily translocate into cytoplasm inspired scientists to study protein chemistry to develop novel non-viral vectors [236-238]. As a result of these studies, small protein-like molecules

commonly known as cell penetrating peptides have emerged. These molecules can spontaneously bind DNA to form compact complexes and they have been drawing a lot of attention.

Cell penetrating peptides can cross the plasma membrane and transfer genetic material into the cell which is attached to them via covalent or physical bonds [239]. Peptides can be designed and functionalized further to be involved in multiple roles like stabilizing DNA in body fluids, targeting cell types and receptors, and facilitating escape from lysosomal degradation [240]. Cationic peptides are composed largely of basic amino acids including lysine, arginine and histidine.

Poly-L-Lysine is a well studied DNA carrier. This polypeptide enhances internalization of DNA to some extent but it exerts toxic properties which increases with growing chain length and requires additional agents for providing endosomal escape and release within the cytoplasm [241-243]. Moreover, high polydispersity of poly-L-Lysine products decreases control over further chemical processes. Small peptides with repeated lysine residues can be synthesized at precise molecular weights. Peptides are also advantageous as they are less toxic than high molecular weight polypeptides [244]. Cys-Trp-Lys(n) peptides with at least 13 lysine residues can form stable and compact peptide-DNA complexes whereas peptides having less than 8 lysine residues form unstable large condensates of micron size [245].

Cationic peptides with sequence YKAK(n)WK varying in the number of Lys residues were tested for efficiency in forming stable DNA complexes and in gene transfection. $YKAK_8WK$ molecules made stable complexes with DNA, however, supplementing with

GLFRALLRLLRSWRLLLRA peptide, which was designed for facilitating endosomal escape, was required to achieve efficient transfer and expression of genes [246].

Polylysine peptides are capable of entering into the cell however these are not very good at penetrating endosomal membranes, which they become encapsulated within. Inclusion of histidine residues were shown to be useful in mediating endosomal escape of peptide-DNA complexes. This effect is probably caused by buffering capacity of histidine imidazole rings in slightly acidic interior environment of endosomes [247]. A histidine rich peptide $H_5$WYG was reported to cross cellular membranes after an incubation for 15 minutes and remained intact within serum without losing activity [248].

Homomeric peptides composed of nine basic amino acid residues were evaluated for their ability to enter cytosol. Peptides were covalently attached to fluorescent dyes for tracking. Nona-arginine peptides were found to be better at passing membrane than nonapeptides composed of lysine, histidine and ornithine [249].

Epitopes derived from proteins of viral coats can promote endosomal escape or nuclear transportation. An amphipatic part within TAT protein of human immunodeficiency virus 1, HIV-1, which is 9 amino acids long can bind DNA stably and help its internalization. Using TAT peptides, transfection efficiency reached to 6-8 times higher levels with respect to control peptides [250].

Penetratine derived from the transcription factor Antennapedia of Drosophila melanogaester is another well known peptide able to translocate plasma membrane. Penetratine has been succesful in various studies in delivering nucleic acids [251].

Beside high basic content, high hydrophobic moment with alpha helix forming propensity is also seen among peptides with cell penetrating ability. An example to such peptides might be transportan, composed of 26 amino acids in which active part of a ligand called galanin and a 14 amino acids long wasp venom toxin are combined with a lysine residue. Transportan molecules could rapidly internalize within a variety of cell types and accumulated in nucleoli [252].

In a study, four different cell penetrating peptides were compared in delivering peptide cargo and in disrupting cellular membrane. Peptides with high hydrophobic moments and low basic content, namely transportan and MAP were found to be more efficient cargo deliverers and effective at lower doses in disrupting the cellular membrane compared to peptides with high basic content which are TAT and penetratin [253]. A directly proportional relation between amount of membrane leakage and hydrophobicity moment is apparent [253]. Proteasomes are intercellular entities which are considered to be possibly degradating peptide-DNA complexes which might decrease efficiency. In the sequence of Epstein Barr virus nuclear antigen I protein, a block of 238 amino acids composed purely of reoccuring Gly-Ala subsequences can prevent the protein from being lysed by proteasomes. In this regard, peptides with Gly-Ala dipeptide repeats were designed to block proteasomes. Elevated gene expression observed as a result of incorporation of Gly-Ala repeats within cell penetrating peptide designs proves usefulness of this particular motif [254].

Peptides may also be designed to include signals to import DNA within the nucleus to allow for transcription to proceed. Signals for nuclear localization can be extracted from viruses and nuclear proteins. Seven aminoacid-peptide PKKKRKV, derived from large

tumor antigen of simian virus 40 accelerated the transport of DNA to the nucleus so that DNA accumulated in 100 times shorter period [255]. Pentapeptide KRPRP is another minimal nuclear localization signal derived from adenovirus E1a protein [256]. Peptides PAAKRVKLD, RQRRNELKRSP are derived from human c-myc protein nuclear localization signal [257].

### 3.1.2 Peptide amphiphiles in gene delivery

Amphiphilicity is considered to be important in interaction of peptides with cell membranes. Many peptides of viral origin that lead to fusion of lipid bilayers are amphiphilic, such as influenza hemaglutinin derived GLFEAIAEFIEGGWEGLIEG and GLFKAIAKFIKGGWKGLIKG [258]. In de novo design of peptides for cellular internalization of nucleic acid loads, some researchers focused on micelle forming or self assembling amphiphilic peptide molecules.

RV peptides assemble into micellar structures due to hydrophilic arginine residues and hydrophobic valine residues in their chemical structure. Four different RV peptides were synthesized varying in number of arginine residues, $R_1V_6$, $R_2V_6$, $R_3V_6$ and $R_4V_6$. Packing DNA to compose micellar DNA-peptide condensates, peptides could efficiently deliver plasmid DNA into HEK293 cells. $R_3V_6$ and $R_4V_6$ formed more stable complexes and could deliver DNA at lower quantities than $R_2V_6$ and $R_1V_6$. In contrast to polyethyleneimine and poly-L-lysine, RV peptides did not show cytotoxicity, which is thought to be due to low charge density per molecule [259].

Molecules that contain hydrophobic alkyl chain conjugated to N terminal of water soluble peptides are frequently called as peptide amphiphiles. Peptide amphiphiles can assemble into various micellar structures like vesicles and nanofibers. Fibrillar scaffolds assembled

from peptide amphiphiles have been frequently used in studies of regenerative medicine for culturing cells. Peptide amphiphiles also hold potential for nucleic acid internalization applications, since the presence of hydrophobic core may improve interaction with plasma membrane [260, 261].

DNA-binding peptide amhiphile, bZIP, bearing the sequence from yeast transcription factor GCN4 as DNA binding fragment was synthesized with solid phase peptide synthesis. The sequence taken from GCN4 is 30 amino acids long and in the nucleus this block folds into alpha helices to further form coiled coils of leucine zipper motifs. Attaching an alkyl tail to GCN4 was reported to enhance formation of alpha helices and improved the orientation of peptides to better resemble its original conformation. These peptide amphiphiles formed lamellar assemblies with DNA. The assemblies, however, need further stabilization like polymerization of hydrophobic alkyl chains. [262].

Peptide nucleic acid-peptide amphiphile molecules can constitute nanofibers and can strongly bind oligonucleotides in a sequence specific manner with oligonucleotides combined within peptide amphiphile structure. These molecules might be useful in RNA interference applications, which need further investigation [263].

In another study, fatty acids were conjugated to cell penetrating peptides in order to investigate the influence of hydrophobic moiety to transfection efficiency. Transfection efficiency, improved significantly, reaching almost the same levels with lipofectamine when stearic acid was attached to N termini of TAT, FHV and octaarginine peptides [261]. Incorporation of lauryl and cholesteryl moieties to octaarginine also improved transfection efficiency [261].

In this study, peptide amphiphiles with cationic amino acid groups were synthesized. Ability of peptide amphiphiles and their combinations to stabilize DNA was investigated. Primary studies for evaluating transfection efficiency of molecules were performed.

## 3.2 Materials and Methods

### 3.2.1 Materials

Materials used for peptide amphiphile synthesis were the same as described in the first chapter. Plasmid-DNA used in this study is pEGFP-N2.

### 3.2.2 Design and Synthesis of Peptide Amphiphiles

Three peptide amphiphile molecules were designed and synthesized for this study. Each peptide amphiphile had an alkyl tail with 12 carbons, followed by a beta sheet forming sequence 'VVAG', similar with the peptide amphiphiles described in Chapter 1. Peptide ampiphiles used in the study, are named according to the positively charged amino acid residues at C termini. Lysine, lysine-arginine and histidine are charged amino acids found at the C termini of Lys-PA, LysArg-PA and His-PA respectively. Based on the ability of peptide amphiphiles to form nanofibers, we thought that peptide amphiphiles can condense DNA and form large arrays of positively charged residues which were shown to be effective in gene delivery. In this way, peptide amphiphile nanofibers can serve as convenient platforms for gene delivery with relatively high efficiency and low toxicity. Chemical structures of peptide amphiphiles used in this study are shown in Figure 36.

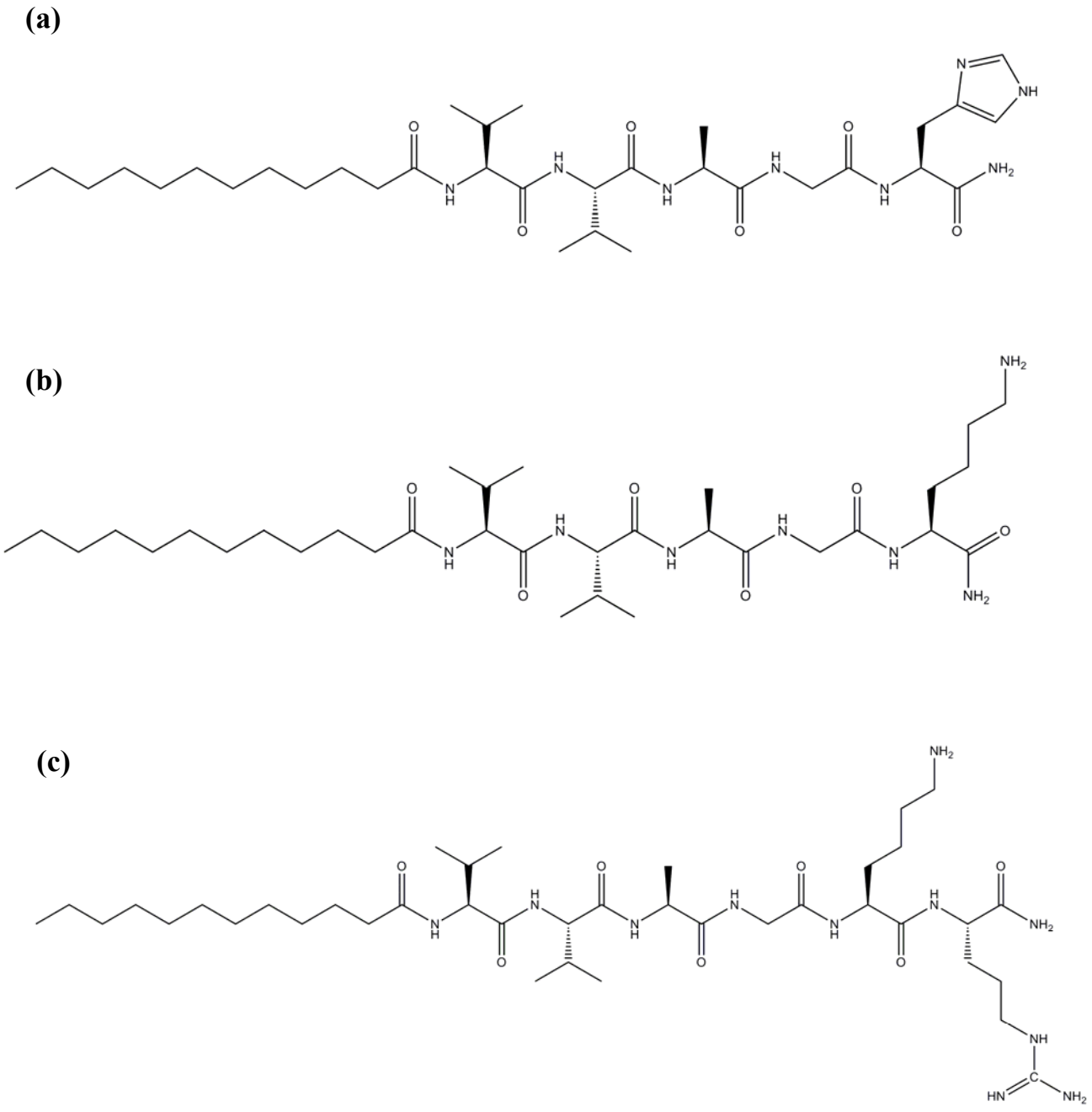


**Figure 35.** Chemical structures of peptide amphiphiles (a) His-PA, (b) Lys-PA, (c) LysArg-PA

Peptide amphiphiles were synthesized on 0.25 or 0.5 mmole scale with standard solid phase Fmoc chemistry on automated peptide synthesizer. Rink Amide MBHA resin was used as solid support. Fmoc groups were cleaved by treating the solid phase with 20% piperidine in DMF for a period of 20 minutes. Fmoc protected amino acids were dissolved in 10 ml DMF and activated with O-Benzotriazole-N,N,N',N'-tetramethyluronium-hexafluoro-phosphate (HBTU), and of N-ethyl-diisopropylamine (DIEA) in an For the purpose of blocking unreacted ends, resin was treated with 10% acetic anhydride for 30 minutes after each coupling. After coupling all Fmoc protected amino acids by applying the steps mentioned above, alkyl tail was attached following the same protocol, but using lauric acid instead of Fmoc protected amino acid.

Fully grown peptide amphiphiles were cleaved from resin, and side chain protective groups of functional groups were removed in a cleavage step for 2 hours with trifluoroacetic acid (TFA): triisopropylsilane (TIS): water at the ratio 95:2.5:2.5. Solution containing the cleavage products was collected at a round bottom flask and resin was washed several times with DCM. DCM was removed, and TFA was removed to a large extent with rotary-evaporation. Cleavage solution containing peptide amphiphile was triturated by adding ice-cold diethylether into the solution which was left overnight at -20 °C. Diethylether was decanted after centrifugation at 8000 rpm for 15 minutes. Product was dissolved in dd$H_2O$, frozen at -80 °C and freeze-dried at -50 °C for two days. Peptide amphiphiles were obtained in the form of powder.

### 3.2.3 LC-MS

Molecular mass and purity of peptide amphiphiles were confirmed with Agilent 6530-1200 Q-TOF LC-MS equipped with ESI-MS. Purity by peptide content was monitored at 220 nm. Zorbax Extend-C18 21.2 x 150 mm column was used. A: 0.1 % trifluoroacetic acid in water and B: 0.1% trifluoroacetic acid in acetonitrile gradient was used.

### 3.2.4 Biuret test

A standard curve is obtained from serial dilution of BSA solutions in the concentration range of 1 mg/ml-10 mg/ml. For obtaining measurements, 150 µl Biuret reagent was added on 50 µl of peptide amphiphile or BSA and incubated for ten minutes at room temperature. Absorbance at 545 nm was recorded for each measurement. Concentrations of peptide amphiphile solutions were estimated with respect to standard curve.

### 3.2.5 Gel retardation assay

Gel retardation assay was performed by running an agarose gel loaded with PA-DNA complexes and naked DNA and visualizing the extent of retardation caused by peptide amphiphiles. In the first experiment, fixed amount of DNA was mixed with peptide amphiphiles in a way that positive to negative (Z+/Z-) charge ratio for each peptide amphiphile-DNA mixture varied between 0.25:1 and 2:1. Mixtures were incubated at room temperature for 45 minutes. Incubated samples and plasmid DNA with loading dye were loaded to wells of a 1% agarose gel with EtBr. 80 mV was applied for an hour. Bands were visualized by UV illumination with a gel imaging system.

In a second experiment peptide amphiphile-DNA mixtures obtained at 2:1 (+/-) charge ratios were prepared for following formulations: His-PA/DNA, LysArg-PA/DNA, Lys-PA/DNA, Lys-PA+His-PA/DNA, LysArg-PA+His-PA/DNA. Mixtures were incubate for

30 minutes at room temperature. Incubated samples and plasmid DNA with loading dye were loaded to wells of a 1.5% agarose gel . 100 mV was applied for an hour. Bands were visualized by UV illumination with a gel imaging system.

### 3.2.6 Circular Dichroism

Circular Dichroism study was performed with J-815 JASCO spectrophotometer. All spectra were obtained at a wavelength interval of 190-300 nm. Spectra were obtained at a digital integration time of 4 s, bandwidth of 1 nm, and data pitch of 0.1 nm. Three subsequent spectra were averaged for each sample. Quartz cuvettes with 2 mm pathlengths were used for measurements. According to the following formula, ellipticity was converted to molar ellipticity with the unit degree $cm^2$ $mol^{-1}$.

$$[\theta] = \frac{100x\theta}{(Cxl)}$$

**[θ]**:Molar ellipticity, **θ:Ellipticity in degrees C:Concentration in M l:length in cm**

### 3.2.7 In vitro transfection

PA-DNA complexes were tested in vitro for their EGFP gene transfection efficiency. Peptide amphiphile-DNA mixtures were incubated for 30 minutes at room temperature and then added dropwise on MCF7 cells seeded on 24-well plates at a cell density of 15000 cells/well. Cultured cells were monitored every 24 hours. Fluorescence emmission of cells indicated EGFP protein expression as a result of transfected DNA. *In vitro* studies were carried by Murat Kılınç.

## 3.3 Results and Discussion

### 3.3.1 Characterization of peptide amphiphile-DNA complexes

Agarose gel electrophoresis was performed to evaluate stability of peptide amphiphile-DNA complexes prepared at different positive to negative charge ratios. The results clearly showed that DNA was retarded in the presence of peptide amphiphiles, with more prominent retardation at higher positive to negative charge ratio (Z+/Z-). For Lys-PA and LysArg-PA, DNA partially migrated when the Z+/Z- ratios are 0.5:1 and 0.25:1 (i.e. when there is excess negative charge). When this ratio is equal to or greater than 1:1 DNA is fully retarded.

In general, data obtained from gel retardation assays are assessed in two different aspects. First, DNA which is well stabilized by complexing agent, deprives of its motility and don't migrate when an electric field is applied. Unstable DNA which can escape positively charged molecules can migrate without hindrance causing occurrence of a band in the proximity of naked DNA. Stability of any complex of DNA can be assessed by the amount of DNA stayed in well and amount of migrated DNA; less migration of DNA accounting to more stable DNA complexes [264, 265].

In another aspect, in some studies DNA-peptide complexes tend to fluoresce less with Ethidium Bromide leading to fader bands on the gel. This might be through quenching of EtBr [266]. Failure of EtBr to diffuse effectively within large aggregates might also be a possible reason. Partially diminished bands observed for PA-DNA samples may also be showing formation of stable complexes.

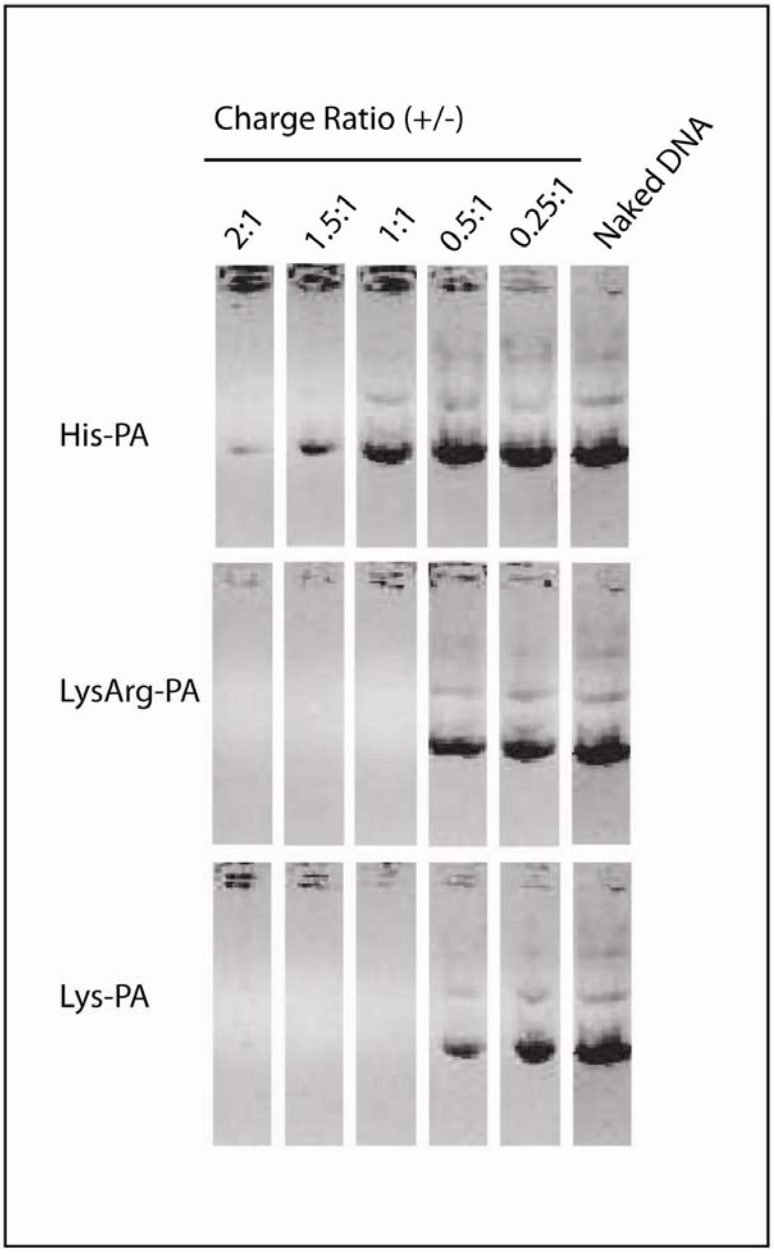


**Figure 36.** Agarose gel electrophoresis of peptide amphiphile-DNA complexes at various charge ratios and naked DNA

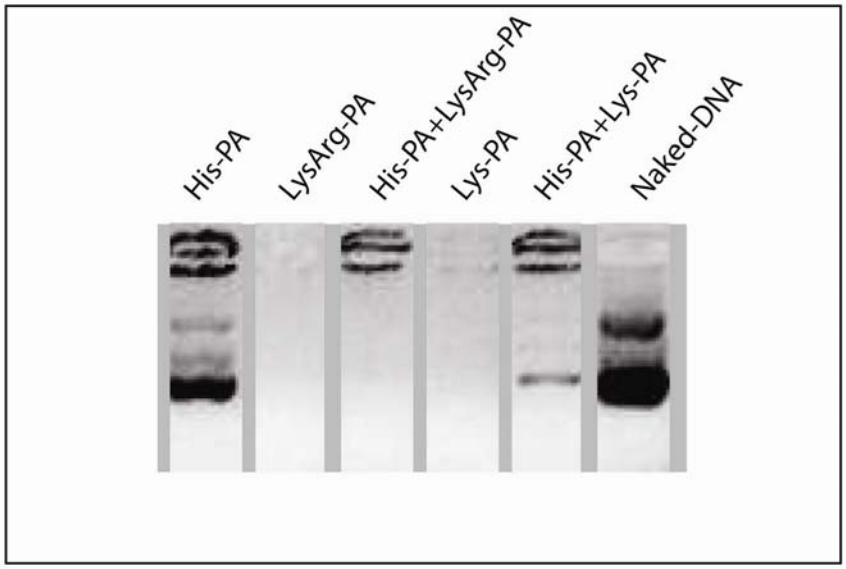


**Figure 37.** Agarose gel electrophoresis of several peptide amphiphile-DNA complexes at 2:1 positive to negative charge ratio

Circular dichroism spectra of peptide amphiphile-DNA complexes were recorded in far UV region in order to assess the chiral morphology of PA-DNA complexes, as well as effect of time and Z+/Z- charge ratio on the structure.

For investigating the effect of charge ratio, varying concentrations of positively charged peptide amphiphiles were used in forming complexes without changing the concentration of DNA. In order to know whether the concentration of the peptide amphiphiles used in this study influences circular dichroic features, spectra obtained for different concentrations of each peptide amphiphile were compared. As a result, CD spectra normalized to peptide amphiphile did not change or changed slightly between used concentrations.

Mixing of plasmid DNA with one of positively charged peptide amphiphiles at 2:1 Z+/Z- charge ratio resulted in intensified positive signal which is near 200 nm. This change in signal is more significant when plasmid-DNA mixture was incubated for one hour.

Intensification of 200 nm signal was also observed at the charge ratio 4:1 (Z+/Z-) after one hour incubation, however, difference was less pronounced when compared to 2:1 (Z+/Z-) samples.

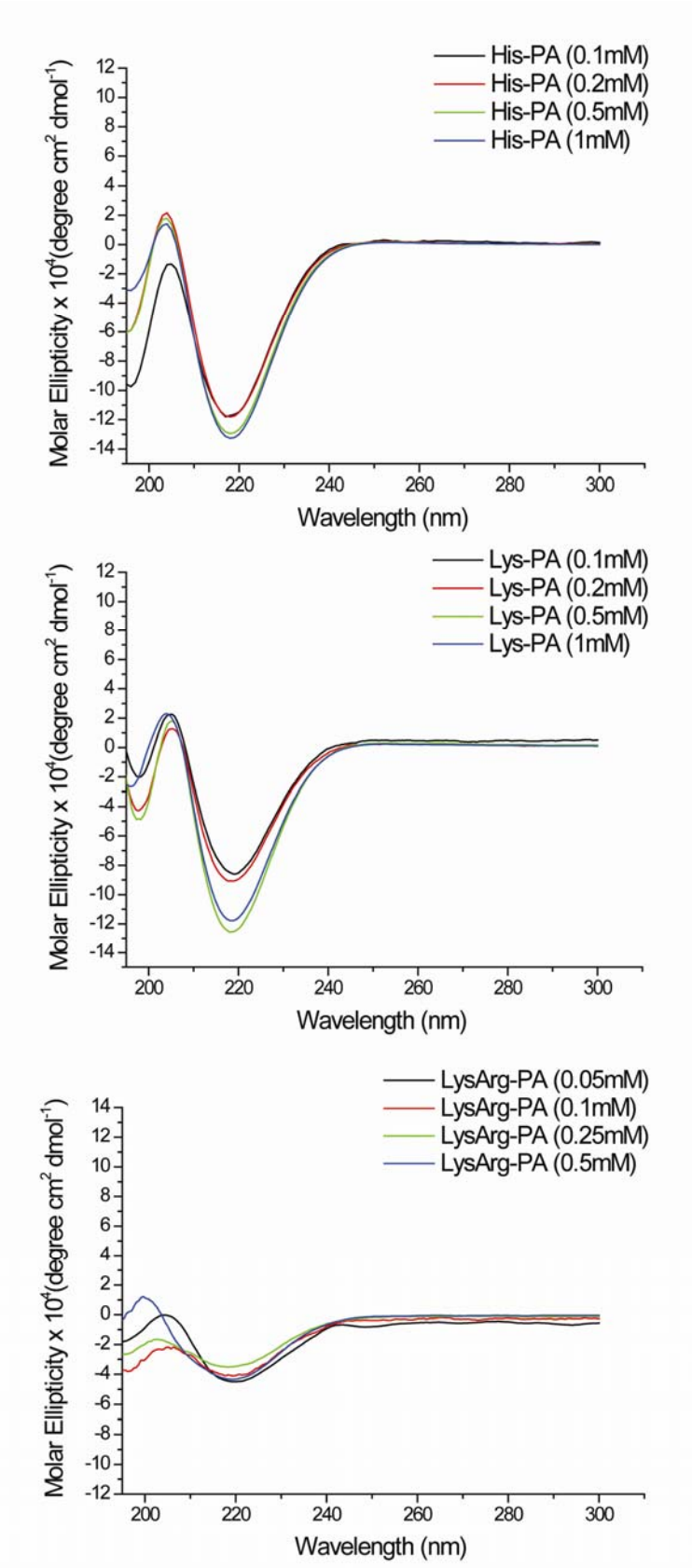


**Figure 38.** Circular Dichroism spectra of peptide amphiphiles at changing molar concentrations

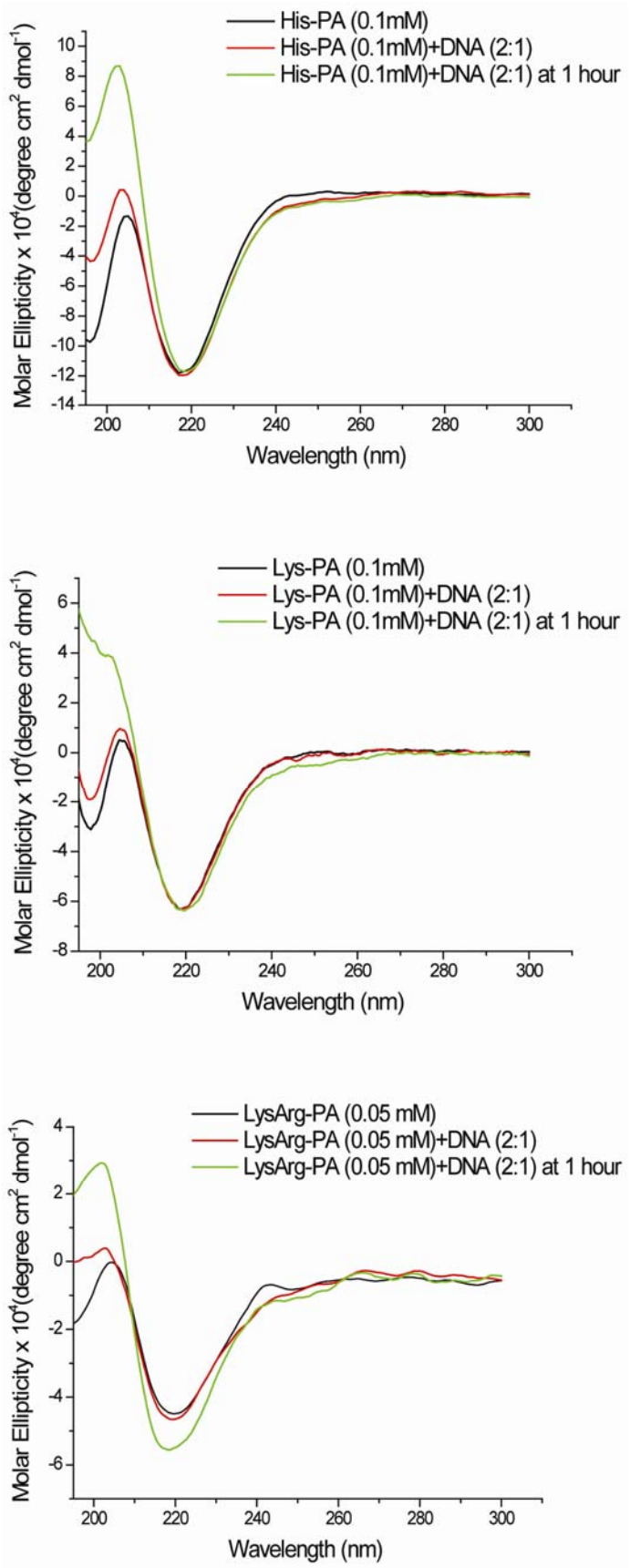


**Figure 39.** Circular Dichroism of peptide amphiphile-DNA complexes at 2:1 positive to negative charge ratio (Z+/Z-)

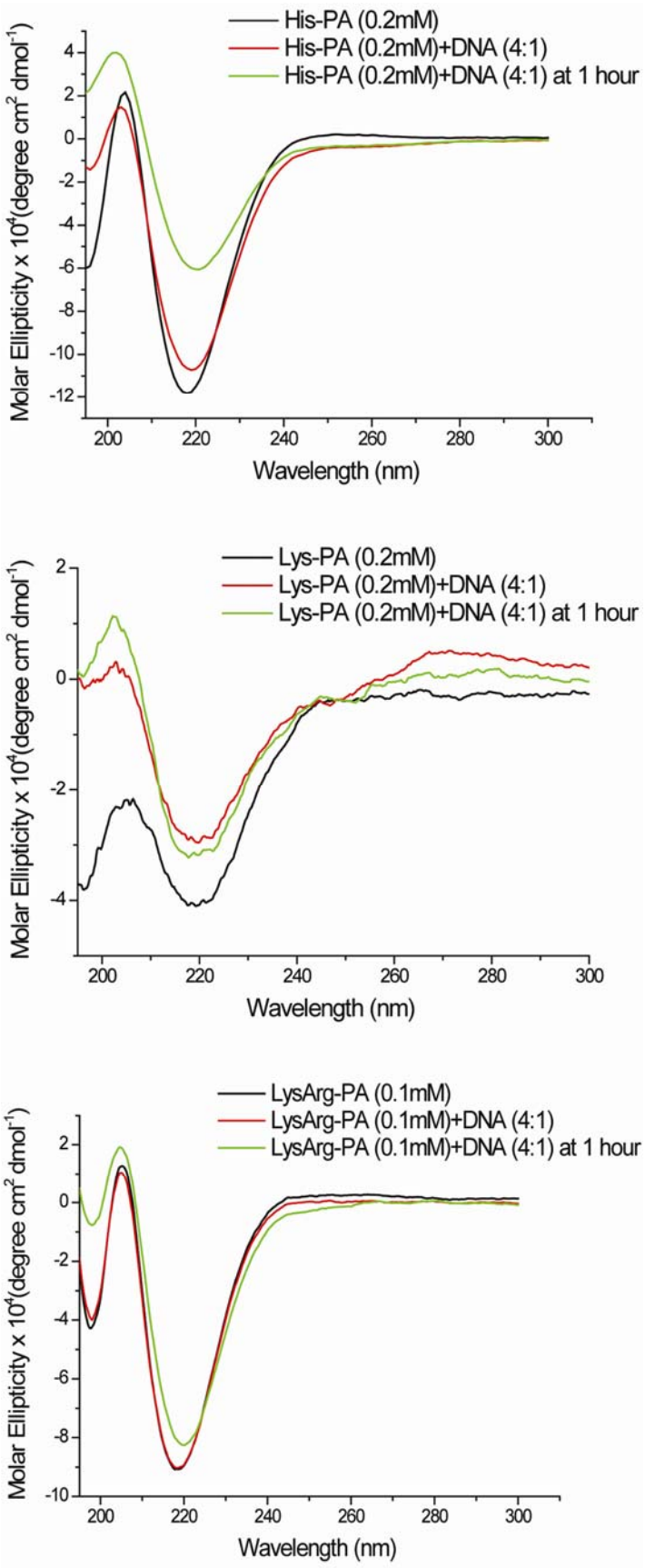


**Figure 40.** Circular Dichroism of peptide amphiphile-DNA complexes at 4:1 positive to negative charge ratio (Z+/Z-)

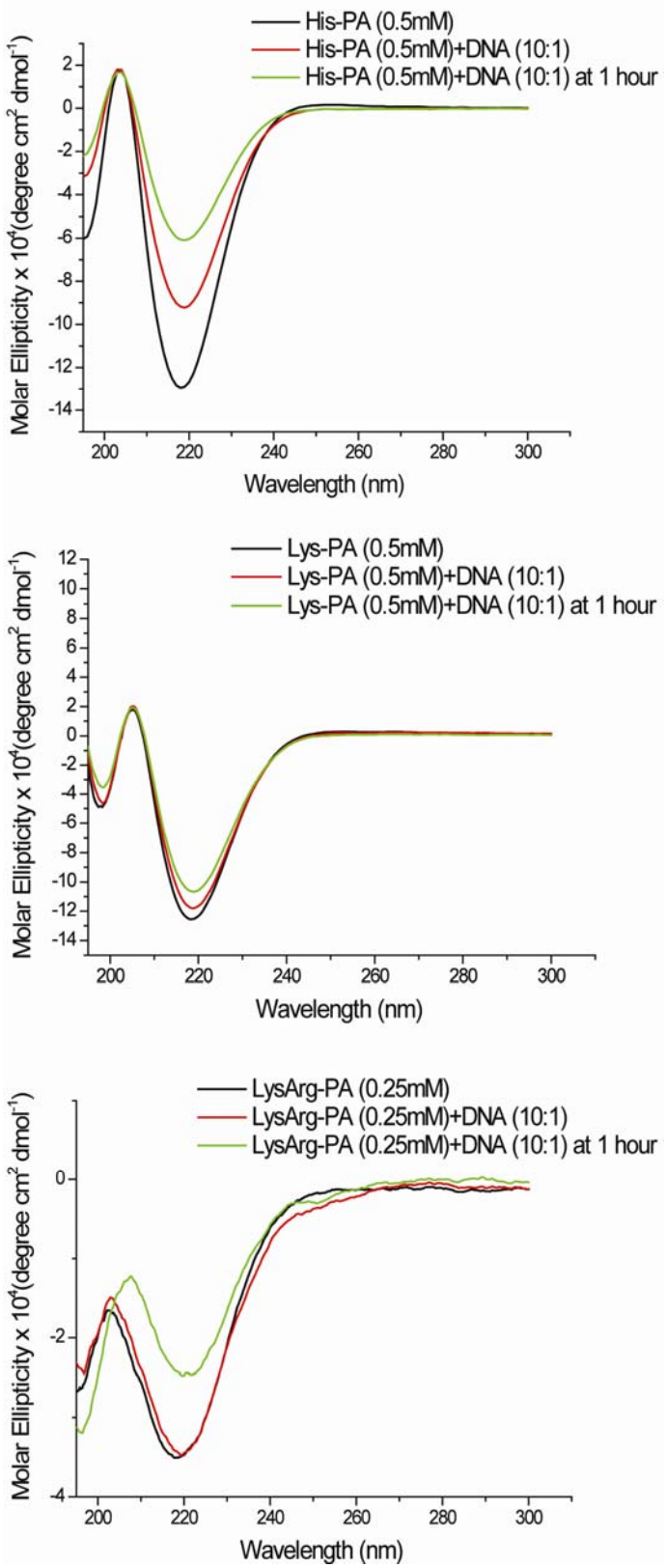


**Figure 39.** Circular Dichroism of peptide amphiphile-DNA complexes at 10:1 positive to negative charge ratio (Z+/Z-)

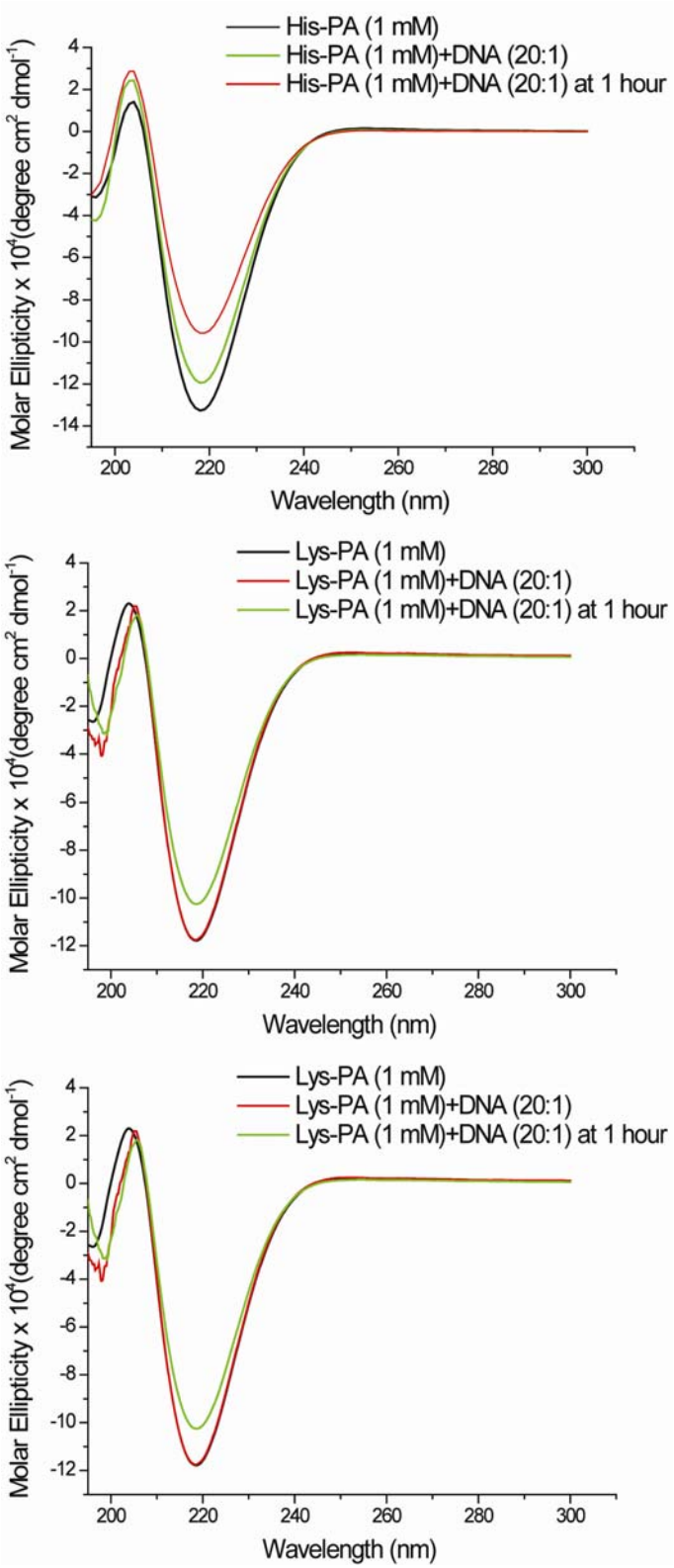


**Figure 40.** Circular Dichroism of peptide amphiphile-DNA complexes at 20:1 positive to negative charge ratio (Z+/Z-)

### 3.3.2 In vitro transfection

Transfection efficiencies of PA complexes were investigated by monitoring fluorescence led by EGFP gene expressed as a result of successful gene delivery. After two days, cells incubated with His-PA/DNA and His-PA+Lys-PA/DNA complexes emitted green fluorescence wherease cells incubated with Lys-PA/DNA, LysArg-PA/DNA complexes lacked fluorescence. Little fluorescence was observed in the case of LysArg-PA+His-PA/DNA complex. On the other hand, incubation of cells with only naked DNA was sufficient for successful transfection.

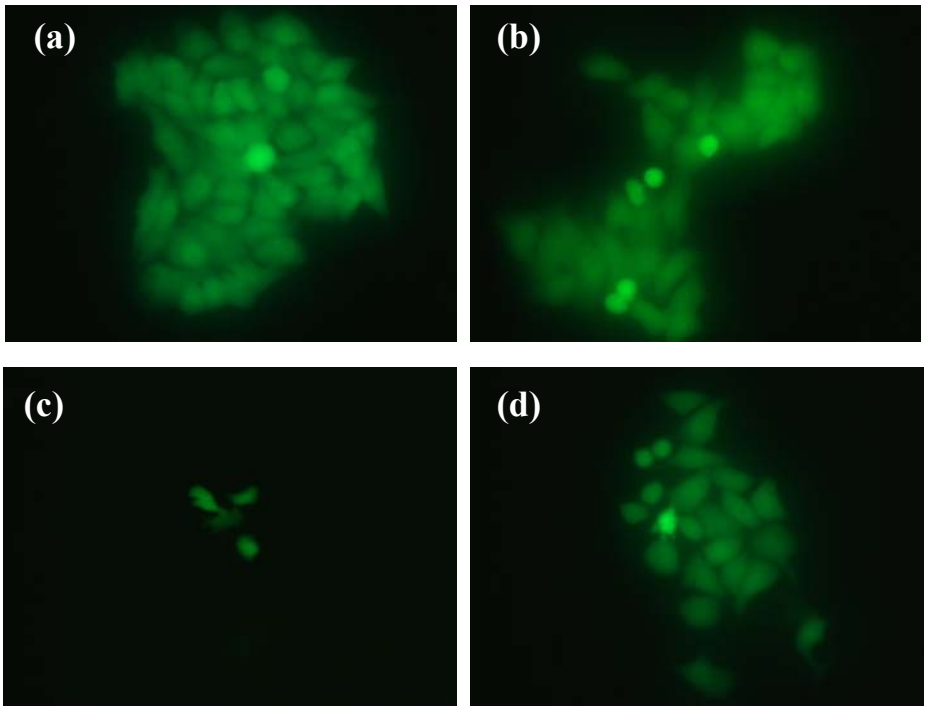


**Figure 41.** Transfected MCF7 cells with plasmid DNA-peptide amphiphile complexes and naked DNA on day 2. Cells were exposed to (a) His-PA/DNA, (b) Lys-PA+His-PA/DNA, (c) LysArg-PA+His-PA/DNA, (d) DNA .

Interestingly, complexes which were inferred to be more stable according to gel retardation assay seem to fail delivery of the gene, besides leading to inferior results compared to naked DNA. Less stable complexes formed by His-PA and mixture of His-PA with Lys-PA, LysArg/PA were able to transfect the cells but at similar efficiencies with naked DNA. An interpretation of this might have been facilitation of gene expression in the presence of His-PA due to endosomal escape provided by His-PA. However, a comparable amount of transfected cells in the presence of uncomplexed DNA refer to lack of any contribution of His-PA in increasing transfection efficiency. Apparently, there is an inverse relation between stable complex forming and transfection efficiency among tested peptide amphiphiles. This is contrary with results of several studies in which more stable complexes provide better transfection. The interactions with negatively charged polyphosphate backbone of DNA form the basis of stable complex formation and the same interactions formed with medium contents like phosphate molecules might be leading to neutralization and consequent lose of activity for peptide amphiphiles. Formation of local gels was observed for Lys-PA/DNA and LysArg-PA/DNA complexes when these were mixed with DMEM. This might be causing DNA to become entrapped and not delivered within the cell resulting in absence of transfection.

### 3.3.3 Conclusion

Cell penetrating peptides are molecular tools capable of packing DNA in compact packages and delivering DNA within the cell and increasing the possibility of gene expression to a great extent. Amphiphilic properties are gaining more attention in peptides' ability to deliver negatively charged molecules inside the cells. In this chapter, we devised anmphiphilic peptide systems which could condense DNA and make it more

stable and help its pass the cell membrane in order to be expressed inside the cell. Three different peptide amphiphiles were produced for evaluating particular merits of different cationic aminoacids. Peptide amphiphiles successfully stabilized DNA which is possibly due to neutralization and beta sheet formation. However, peptide amphiphiles were not efficient in transfecting DNA as tested in vitro and the cause of low efficiency is not very clear.

In the future, it is essential to investigate why peptide amphiphiles were not efficient DNA transporters although they stabilized DNA effectively. Different in vitro transfection protocols might be tried in order to see whether interaction of peptide amphiphiles with the medium components create disturbance in complex arriving the cell. Peptide amphiphile oligonucleotide complexes may be assembled and may be tracked via a fluorescent reporter directly attached on oligonucleotide. Moreover, different peptide amphiphiles can be designed and synthesized which are better at buffering the ionic constituents of the media which would avoid formation of unwanted aggregates and also help endosomal escape.

# 4 References


1. Gold, G.E., et al., *MRI of articular cartilage in OA: novel pulse sequences and compositional/functional markers.* Osteoarthritis Cartilage, 2006. **14 Suppl A**: p. A76-86.
2. Heinegard, D. and A. Oldberg, *Structure and biology of cartilage and bone matrix noncollagenous macromolecules.* FASEB J, 1989. **3**(9): p. 2042-51.
3. Taipale, J. and J. Keski-Oja, *Growth factors in the extracellular matrix.* FASEB J, 1997. **11**(1): p. 51-9.
4. Li, S.W., et al., *Transgenic mice with targeted inactivation of the Col2 alpha 1 gene for collagen II develop a skeleton with membranous and periosteal bone but no endochondral bone.* Genes Dev, 1995. **9**(22): p. 2821-30.
5. Jakob, M., et al., *Specific growth factors during the expansion and redifferentiation of adult human articular chondrocytes enhance chondrogenesis and cartilaginous tissue formation in vitro.* J Cell Biochem, 2001. **81**(2): p. 368-77.
6. Eyre, D., *Collagen of articular cartilage.* Arthritis Res, 2002. **4**(1): p. 30-5.
7. O'Driscoll, S.W., *The healing and regeneration of articular cartilage.* J Bone Joint Surg Am, 1998. **80**(12): p. 1795-812.
8. Arden, N. and M.C. Nevitt, *Osteoarthritis: epidemiology.* Best Pract Res Clin Rheumatol, 2006. **20**(1): p. 3-25.
9. Clouet, J., et al., *From osteoarthritis treatments to future regenerative therapies for cartilage.* Drug Discov Today, 2009. **14**(19-20): p. 913-25.
10. Min, B.H., S.R. Park, and S.H. Park, *Method for differenciating mesenchymal stem cell and culturing chondrocytes using alginate coated fibrin/ha composite scaffold*. 2009, WO2009017267.
11. Dadsetan, M., M. Yaszemski, and L. Lu, *Photocrosslinkable oligo (poly (ethylene glycol) fumarate) hydrogels for cell and drug delivery*. 2006, EP1877000.
12. Jaworowicz, W., *Sustained-release formulations comprising crystals, macromolecular gels, and particulate suspensions of biologic agents*. 2008, WO2008082563.
13. Geistlich, P. and L. Schloesser, *Collagen matrix for tissue regeneration containing therapeutic genetic material*. 2003, EP1283063.
14. Guilak, F., B.T. Estes, and A. Wu, *Tissue Engineering Methods and Compositions*. 2009, US20090196901.
15. Shah, R.N., N.A. Shah, and S.I. Stupp, *Novel peptide-based scaffolds for cartilage regeneration and methods for their use*. 2010, WO2010120830.
16. Bujia, J., et al., *Engineering of cartilage tissue using bioresorbable polymer fleeces and perfusion culture.* Acta Otolaryngol, 1995. **115**(2): p. 307-10.
17. Hench, L.L. and J.M. Polak, *Third-generation biomedical materials.* Science, 2002. **295**(5557): p. 1014-7.
18. Sharim, H. and S. Beck, *Intra-articular implant for treating irregularities in cartilage surfaces*. 2008, WO2008120215.
19. Vange, J., et al., *Degradable Hydrophilic Block Copolymers with Improved Biocompatibility for Soft Tissue Regeneration*. 2007, WO2007101443.
20. Kirkpatrick, S.R. and R.C. Svrluga, *Method and system for modifying the wettability characteristics of a surface of a medical device by the application of gas cluster ion beam technology and medical devices made thereby*. 2008, WO2009036373.
21. Chang, K.Y. and L.W. Cheng, *Porous composite biomaterials and production method of the same*. 2012, US2012122219.

22. Jayasuriya, A.C. and N.A. Ebraheim, *Hybrid Biomimetic Particles, Methods of Making Same and Uses Therefor*. 2008, WO2008130529.
23. Tanaka, J., et al., *Glycosaminoglycan-polycation complex crosslinked by polyfunctional crosslinking agent and process for producing the same*. 2008, EP1419792.
24. Yudoh, K., *Biomaterials for regenerative medicine*. 2008, EP1935438.
25. Stone, K.R., *Galactosidase-treated prosthetic devices*. 2009, US7594934.
26. Ayares, D. and P. Rohricht, *Tissue products derived from animals lacking any expression of functional alpha 1, 3 galactosyltransferase*. 2005, EP2433492.
27. Luck, E.E. and J.R. Daniels, *Non-antigenic collagen and articles of manufacture*. 1984, US4488911.
28. Iwasaki, N., et al., *Composition for treatment of cartilage disease*. 2008, EP2127687.
29. Sivananthan, S. and P. Warnke, *Tissue regeneration by endocultivation*. 2006, WO2006109137.
30. Hutmacher, D.W., *Scaffolds in tissue engineering bone and cartilage.* Biomaterials, 2000. **21**(24): p. 2529-43.
31. Walter, M.A., N.C. Leatherbury, and M.O. Niederauer, *Moldable, hand-shapable biodegradable implant material*. 2003, EP0880368.
32. Alsberg, E. and O. Jeon, *Photocrosslinked biodegradable hydrogel*. 2009, US2011008443.
33. Yang, J. and J. Dey, *Bio-polymer and scaffold-sheet method for tissue engineering*. 2011, US7923486.
34. Shastri, V.R., et al., *Three-dimensional polymer matrices*. 2002, US6471993.
35. Johnstone, B. and C. Bahney, *Bioresponsive hydrogel*. 2010, WO2010123938.
36. Hubbell, J.A., et al., *Biomaterials formed by nucleophilic addition reaction to conjugated unsaturated groups*. 2010, US7744912.
37. Rueger, D. and R. Kildey, *Methods of treating cartilage defects*. 2007, WO2007061924.
38. *Compositions and methods for repair of tissues*. 2007, WO2007146232.
39. Zhang, R., D. Peluso, and E. Morris, *Methods and compositions for healing and repair of articular cartilage*. 2004, US7842669.
40. Harrison, A.J., et al., *Bmp binding proteins for use in bone or cartilage regeneration*. 2004, US20040176287.
41. Van, A.H.M.S.M., J.S. Pieper, and H.T.B. Van Moerkerk, *Type II collagen matrices for use in cartilage engineering*. 2004, US200421385.
42. Billinghurst, R.C., et al., *Enhanced cleavage of type II collagen by collagenases in osteoarthritic articular cartilage.* J Clin Invest, 1997. **99**(7): p. 1534-45.
43. Hollander, A.P., et al., *Increased damage to type II collagen in osteoarthritic articular cartilage detected by a new immunoassay.* J Clin Invest, 1994. **93**(4): p. 1722-32.
44. Parma, B. and A. Gigante, *Multimicrolamellar Collagen Membranes*. 2009, US20090269586.
45. Geistlich, P. and L. Schloesser, *Resorbable extracellular matrix containing collagen I and collagen II for reconstruction of cartilage*. 2003, EP1312383.
46. *Injectable collagen-based delivery system for bone morphogenic proteins*. 2000, WO2000047114.
47. Devore, D.P. and R.A. Eiferman, *Collagen modulators for use in photoablation eximer laser keratectomy*. 2001, US6204365 2001.
48. Liu, L. and R.C. Spiro, *Collagen-polysaccharide matrix for bone and cartilage repair*. 2004, EP1374857.
49. Hermida, E.H.O., *Use of a mixture of sodium hyaluronate and chondroitin sulfate for the treatment of osteoarthritis*. 2005, US6949525.
50. Wang, C.T., et al., *Therapeutic effects of hyaluronic acid on osteoarthritis of the knee. A meta-analysis of randomized controlled trials.* J Bone Joint Surg Am, 2004. **86-A**(3): p. 538-45.
51. Serban, M.A., G. Yang, and G.D. Prestwich, *Synthesis, characterization and chondroprotective properties of a hyaluronan thioethyl ether derivative.* Biomaterials, 2008. **29**(10): p. 1388-99.

52. Della Valle, F. and A. Romeo, *Esters of hyaluronic acid*. 1989, US4851521.
53. Campoccia, D., et al., *Semisynthetic resorbable materials from hyaluronan esterification.* Biomaterials, 1998. **19**(23): p. 2101-27.
54. Radice, M., et al., *Injectable hyaluronic acid derivative with pharmaceuticals/cells*. 2007, US7157080.
55. Moeller, M., B. Kaufmann, and R. Gurny, *Process for the esterification of hyaluronic acid with hydrophobic organic compounds*. 2012, WO2012013670.
56. Pietrangelo, A. and V. Travagli, *Esters of hyaluronic acid with rhein, process for their preparation and compositions comprising the same*. 2010, US7834173.
57. Aeschlimann, D. and P. Bulpitt, *Functionalized derivatives of hyaluronic acid, formation of hydrogels in situ using same, and methods for making and using same*. 2003, US20070149441.
58. Balazs, E.A. and A. Leshchiner, *Cross-linked gels of hyaluronic acid and products containing such gels*. 1986, US4582865.
59. Bellini, D. and A.M. Zanellato, *Ester derivatives of hyaluronic acid for the preparation of hydrogel materials by photocuring*. 2008, US7462606.
60. Lindblad, G.T., *Hyaluronic acid preparation to be used for treating inflammations of skeletal joints*. 1989, US4801619.
61. Ferry, J.D., *Polymerization of fibrinogen.* Physiol Rev, 1954. **34**(4): p. 753-60.
62. Meinhart, J., M. Fussenegger, and W. Hobling, *Stabilization of fibrin-chondrocyte constructs for cartilage reconstruction.* Ann Plast Surg, 1999. **42**(6): p. 673-8.
63. Ting, V., et al., *In vitro prefabrication of human cartilage shapes using fibrin glue and human chondrocytes.* Ann Plast Surg, 1998. **40**(4): p. 413-20; discussion 420-1.
64. Atlas, R. and I. Nur, *Fibrin based scaffold, preparation and use thereof*. 2012, WO2012020412.
65. Eyrich, D., et al., *Long-term stable fibrin gels for cartilage engineering.* Biomaterials, 2007. **28**(1): p. 55-65.
66. Yayon, A., M. Azachi, and M. Gladnikoff, *Freeze-dried fibrin matrices and methods for preparation thereof*. 2010, US7714107.
67. Nettles, D.L., S.H. Elder, and J.A. Gilbert, *Potential use of chitosan as a cell scaffold material for cartilage tissue engineering.* Tissue Eng, 2002. **8**(6): p. 1009-16.
68. Chenite, A. and A. Selmani, *Highly biocompatible dual thermogelling chitosan/glucosamine salt compositions*. 2012, US20120052012.
69. Lu, J.X., et al., *Effects of chitosan on rat knee cartilages.* Biomaterials, 1999. **20**(20): p. 1937-44.
70. Lahiji, A., et al., *Chitosan supports the expression of extracellular matrix proteins in human osteoblasts and chondrocytes.* J Biomed Mater Res, 2000. **51**(4): p. 586-95.
71. Tokura, S., et al. *Molecular weight dependent antimicrobial activity by chitosan*: Hüthig & Wepf.
72. Singla, A.K. and M. Chawla, *Chitosan: some pharmaceutical and biological aspects--an update.* J Pharm Pharmacol, 2001. **53**(8): p. 1047-67.
73. Khor, E. and L.Y. Lim, *Implantable applications of chitin and chitosan.* Biomaterials, 2003. **24**(13): p. 2339-49.
74. Kumar, M.N., et al., *Chitosan chemistry and pharmaceutical perspectives.* Chem Rev, 2004. **104**(12): p. 6017-84.
75. Koshugi, J., *Chitin derivative, material comprising said derivative and process for the preparation thereof*. 1982, EP0013181.
76. Hirano, S., H. Tsuchida, and N. Nagao, *N-acetylation in chitosan and the rate of its enzymic hydrolysis.* Biomaterials, 1989. **10**(8): p. 574-6.
77. Suh, J.K. and H.W. Matthew, *Application of chitosan-based polysaccharide biomaterials in cartilage tissue engineering: a review.* Biomaterials, 2000. **21**(24): p. 2589-98.

78. Chenite, A., et al., *Temperature-controlled pH-dependent formation of ionic polysaccharide gels*. 2002, US6344488.
79. Hoemann, C. and J. Sun, *Formulation and method for rapid preparation of isotonic and cytocompatible chitosan solutions without inducing chitosan precipitation*. 2011, WO2011060553.
80. Stanford, E., *On algin: a new substance obtained from some of the commoner species of marine algae.* Chem. News, 1883. **96**: p. 254-257.
81. Smidsrod, O. and G. Skjak-Braek, *Alginate as immobilization matrix for cells.* Trends Biotechnol, 1990. **8**(3): p. 71-8.
82. Becker, T.A. and D.R. Kipke, *Flow properties of liquid calcium alginate polymer injected through medical microcatheters for endovascular embolization.* J Biomed Mater Res, 2002. **61**(4): p. 533-40.
83. Kong, H., K. Lee, and D. Mooney, *Decoupling the dependence of rheological/mechanical properties of hydrogels from solids concentration.* Polymer, 2002. **43**(23): p. 6239-6246.
84. Lee, K., et al., *Controlling mechanical and swelling properties of alginate hydrogels independently by cross-linker type and cross-linking density.* Macromolecules, 2000. **33**: p. 4291-4294.
85. Griffith-Cima, L., et al., *Tissue formation by injecting a cell-polymeric solution that gels in vivo*. 2004, US6730298.
86. Kavalkovich, K., et al., *Alginate layer system for chondrogenic differentiation of human mesenchymal stem cells*. 2004, US6761887.
87. Kaplan, D.L., et al., *Electrospun pharmaceutical compositions*. 2004, Google Patents.
88. Kaplan, D.L., et al., *Silk biomaterials and methods of use thereof*. 2011, US8071722.
89. Lu, S., et al., *Modified silk films containing glycerol*. 2010, WO2010042798.
90. Munirah, S., et al., *The use of fibrin and poly(lactic-co-glycolic acid) hybrid scaffold for articular cartilage tissue engineering: an in vivo analysis.* Eur Cell Mater, 2008. **15**: p. 41-52.
91. Zhang, X., et al., *Synthesis and characterization of the paclitaxel/MPEG-PLA block copolymer conjugate.* Biomaterials, 2005. **26**(14): p. 2121-8.
92. Kulkarni, R., *Assimilable hydrophilic prosthesis*. 1980, US4181983.
93. Kulkarni, R.K., et al., *Biodegradable poly(lactic acid) polymers.* J Biomed Mater Res, 1971. **5**(3): p. 169-81.
94. Lu, L., et al., *In vitro and in vivo degradation of porous poly(DL-lactic-co-glycolic acid) foams.* Biomaterials, 2000. **21**(18): p. 1837-45.
95. Li, S., *Hydrolytic degradation characteristics of aliphatic polyesters derived from lactic and glycolic acids.* J Biomed Mater Res, 1999. **48**(3): p. 342-53.
96. Kaplan, D.L., et al., *Silk fibroin materials and use thereof*. 2010, US20100279112.
97. Elisseeff, J., et al., *Photoencapsulation of chondrocytes in poly(ethylene oxide)-based semi-interpenetrating networks.* J Biomed Mater Res, 2000. **51**(2): p. 164-71.
98. Grad, S., et al., *The use of biodegradable polyurethane scaffolds for cartilage tissue engineering: potential and limitations.* Biomaterials, 2003. **24**(28): p. 5163-71.
99. Chia, S.L., et al., *Biodegradable elastomeric polyurethane membranes as chondrocyte carriers for cartilage repair.* Tissue Eng, 2006. **12**(7): p. 1945-53.
100. Healy, K.E., A. Rezania, and R.A. Stile, *Designing biomaterials to direct biological responses.* Ann N Y Acad Sci, 1999. **875**: p. 24-35.
101. Muratoglu, O.K., et al., *PVA hydrogel*. 2007, US7985781.
102. Kus, W.M., et al., *Carbon fiber scaffolds in the surgical treatment of cartilage lesions.* Ann Transplant, 1999. **4**(3-4): p. 101-2.
103. He, X., et al., *A Novel Cylinder-Type PLLA-Collagen Hybrid Sponge for Cartilage Tissue Engineering.* Tissue Eng Part C Methods, 2009.

104. Yoo, H.S., et al., *Hyaluronic acid modified biodegradable scaffolds for cartilage tissue engineering.* Biomaterials, 2005. **26**(14): p. 1925-33.
105. Chang, K.Y., et al., *The application of type II collagen and chondroitin sulfate grafted PCL porous scaffold in cartilage tissue engineering.* J Biomed Mater Res A, 2009.
106. Wayne, J.S., et al., *In vivo response of polylactic acid-alginate scaffolds and bone marrow-derived cells for cartilage tissue engineering.* Tissue Eng, 2005. **11**(5-6): p. 953-63.
107. Villanueva, I., C.A. Weigel, and S.J. Bryant, *Cell-matrix interactions and dynamic mechanical loading influence chondrocyte gene expression and bioactivity in PEG-RGD hydrogels.* Acta Biomater, 2009. **5**(8): p. 2832-46.
108. Tan, H., et al., *RGD modified PLGA/gelatin microspheres as microcarriers for chondrocyte delivery.* J Biomed Mater Res B Appl Biomater, 2009. **91**(1): p. 228-38.
109. Todd, S.J., et al., *Enzyme-activated RGD ligands on functionalized poly(ethylene glycol) monolayers: surface analysis and cellular response.* Langmuir, 2009. **25**(13): p. 7533-9.
110. Guler, M.O., et al., *Presentation of RGDS epitopes on self-assembled nanofibers of branched peptide amphiphiles.* Biomacromolecules, 2006. **7**(6): p. 1855-63.
111. Storrie, H., et al., *Supramolecular crafting of cell adhesion.* Biomaterials, 2007. **28**(31): p. 4608-18.
112. Hubbell, J.A. and D.A. Rothenfluh, *Polypeptide ligands for targeting cartilage and methods of use thereof*. 2010, US20100080850.
113. Brack, A. and L.E. Orgel, *Beta structures of alternating polypeptides and their possible prebiotic significance.* Nature, 1975. **256**(5516): p. 383-7.
114. Rippon, W.B., H.H. Chen, and A.G. Walton, *Spectroscopic characterization of poly(Glu-Ala).* J Mol Biol, 1973. **75**(2): p. 369-75.
115. Pierre, S., et al., *Conformational studies of sequential polypeptides containing lysine and tyrosine.* Peptide Science. **17**(8): p. 1837-1848.
116. Seipke, G., H.A. Arfmann, and K.G. Wagner, *Synthesis and properties of alternating poly(Lys-Phe) and comparison with the random copolymer poly(Lys 51, Phe 49).* Biopolymers, 1974. **13**(8): p. 1621-33.
117. Osterman, D.G. and E.T. Kaiser, *Design and characterization of peptides with amphiphilic beta-strand structures.* J Cell Biochem, 1985. **29**(2): p. 57-72.
118. Kisiday, J., et al., *Self-assembling peptide hydrogel fosters chondrocyte extracellular matrix production and cell division: implications for cartilage tissue repair.* Proc Natl Acad Sci U S A, 2002. **99**(15): p. 9996-10001.
119. Ozbas, B., et al., *Hydrogels and uses thereof*. 2010, US7884185.
120. Hosseinkhani, H., et al., *Osteogenic differentiation of mesenchymal stem cells in self-assembled peptide-amphiphile nanofibers.* Biomaterials, 2006. **27**(22): p. 4079-86.
121. Galler, K.M., et al., *Self-assembling peptide amphiphile nanofibers as a scaffold for dental stem cells.* Tissue Eng Part A, 2008. **14**(12): p. 2051-8.
122. Shah, R.N., et al., *Supramolecular design of self-assembling nanofibers for cartilage regeneration.* Proc Natl Acad Sci U S A, 2010. **107**(8): p. 3293-8.
123. Zamora, P.O., et al., *Positive modulator of bone morphogenic protein-2*. 2010, EP1725576.
124. Kinney, W.A., et al., *Collagen-related peptides*. 2009, WO2009017482.
125. Chmielewski, J., M. Pires, and D. Przybyla, *Collagen peptide conjugates and uses therefor*. 2009, WO2009140573.
126. Yu, M., et al., *Compositions Comprising Modified Collagen and Uses Therefor*. 2005, US2008287342.
127. Engler, A.J., et al., *Matrix elasticity directs stem cell lineage specification.* Cell, 2006. **126**(4): p. 677-689.

128. Bjerre, L., et al., *Three-dimensional nanostructured hybrid scaffold and manufacture thereof*. 2010, EP2266635.
129. Elisseeff, J.H., C.G. Williams, and B. Sharma, *Multi-layered polymerizing hydrogels for tissue regeneration*. 2006, EP1673440.
130. Roy, K. and L. Nguyen, *Multi-layered hydrogel constructs and associated methods*. 2011, US20110262493.
131. Li, W.J., *Tissue Engineered Cartilage, Method of Making Same, Therapeutic and Cosmetic Surgical Applications Using Same*. 2012, US8202551.
132. Fukutomi, C., et al., *Scaffold material*. 2007, WO2007102606.
133. Luginbuehl, R., G. Richards, and L.A. Gwynn, *Prosthetic Device For Cartilage Repair*. 2004, US20070282455.
134. Mansmann, K.A., *Resorbable scaffolds to promote cartilage regeneration*. 2003, US6530956.
135. Bentz, H., A.M. Garcia, and J.A. Hubbell, *Gel-infused sponges for tissue repair and augmentation*. 2002, US20030095993.
136. Madihally, S.V. and H.W. Matthew, *Porous chitosan scaffolds for tissue engineering.* Biomaterials, 1999. **20**(12): p. 1133-42.
137. Niwa, H., et al., *Support for tissue regeneration and process for producing the same*. 2008, US7445793.
138. Shimoboji, T., *Hyaluronic acid modification product*. 2008, US7456275.
139. Chung, H. and T. Park, *Self-assembled and nanostructured hydrogels for drug delivery and tissue engineering.* Nano Today, 2009. **4**(5): p. 429-437.
140. Langer, R.S., et al., *Semi-interpenetrating or interpenetrating polymer networks for drug delivery and tissue engineering*. 2009, US7625580.
141. Seliktar, D. and M. Gonen-Wadmany, *Compositions and methods for scaffold formation*. 2008, US20100137510.
142. Jeong, B., et al., *Thermogelling biodegradable copolymer aqueous solutions for injectable protein delivery and tissue engineering.* Biomacromolecules, 2002. **3**(4): p. 865-8.
143. Geistlich, P. and L. Schloesser, *Resorbable extracellular matrix containing collagen I and collagen II for reconstruction of cartilage*. 2002, Google Patents.
144. Hartgerink, J.D., E. Beniash, and S.I. Stupp, *Peptide-amphiphile nanofibers: a versatile scaffold for the preparation of self-assembling materials.* Proc Natl Acad Sci U S A, 2002. **99**(8): p. 5133-8.
145. Kafienah, W., et al., *Three-dimensional tissue engineering of hyaline cartilage: comparison of adult nasal and articular chondrocytes.* Tissue Eng, 2002. **8**(5): p. 817-26.
146. Mandl, E.W., et al., *Fibroblast growth factor-2 in serum-free medium is a potent mitogen and reduces dedifferentiation of human ear chondrocytes in monolayer culture.* Matrix Biol, 2004. **23**(4): p. 231-41.
147. Brittberg, M., et al., *Treatment of deep cartilage defects in the knee with autologous chondrocyte transplantation.* N Engl J Med, 1994. **331**(14): p. 889-95.
148. Bhatia, R. and J.M. Hare, *Mesenchymal stem cells: future source for reparative medicine.* Congest Heart Fail, 2005. **11**(2): p. 87-91; quiz 92-3.
149. Noel, D., et al., *Multipotent mesenchymal stromal cells and immune tolerance.* Leuk Lymphoma, 2007. **48**(7): p. 1283-9.
150. Decker, J.D., J.J. Marshall, and S.W. Herring, *Differential cell replication within the periosteum of the pig mandibular ramus.* Acta Anat (Basel), 1996. **157**(2): p. 144-50.
151. Nelson, C.E., et al., *Analysis of Hox gene expression in the chick limb bud.* Development, 1996. **122**(5): p. 1449-1466.
152. Searls, R.L. and M.Y. Janners, *The initiation of limb bud outgrowth in the embryonic chick.* Developmental Biology, 1971. **24**(2): p. 198-213.

153. Saunders, J.W., Jr., *The proximo-distal sequence of origin of the parts of the chick wing and the role of the ectoderm.* J Exp Zool, 1948. **108**(3): p. 363-403.
154. Todt, W.L. and J.F. Fallon, *Development of the apical ectodermal ridge in the chick wing bud.* J Embryol Exp Morphol, 1984. **80**: p. 21-41.
155. Ord, M.G. and L.A. Stocken, *Cell and tissue regeneration: a biochemical approach*. 1984: Wiley.
156. Khan, I.M., et al., *The Development of Synovial Joints.* Current Topics in Developmental Biology, Vol 79, 2007. **79**: p. 1-36.
157. Pitsillides, A.A. and D.E. Ashhurst, *A critical evaluation of specific aspects of joint development.* Dev Dyn, 2008. **237**(9): p. 2284-94.
158. Hall, B.K. and T. Miyake, *Divide, accumulate, differentiate: Cell condensation in skeletal development revisited.* International Journal of Developmental Biology, 1995. **39**(6): p. 881-893.
159. Atsumi, T., et al., *A chondrogenic cell line derived from a differentiating culture of AT805 teratocarcinoma cells.* Cell Differ Dev, 1990. **30**(2): p. 109-16.
160. Shukunami, C., et al., *Chondrogenic differentiation of clonal mouse embryonic cell line ATDC5 in vitro: differentiation-dependent gene expression of parathyroid hormone (PTH)/PTH-related peptide receptor.* J Cell Biol, 1996. **133**(2): p. 457-68.
161. Oldershaw, R.A., et al., *Directed differentiation of human embryonic stem cells toward chondrocytes.* Nat Biotechnol, 2010. **28**(11): p. 1187-94.
162. Hamilton, D.W., et al., *Chondrocyte aggregation on micrometric surface topography: a time-lapse study.* Tissue Eng, 2006. **12**(1): p. 189-99.
163. Barna, M. and L. Niswander, *Visualization of cartilage formation: insight into cellular properties of skeletal progenitors and chondrodysplasia syndromes.* Dev Cell, 2007. **12**(6): p. 931-41.
164. Dana, A., et al., *Interfiber interactions alter the stiffness of gels formed by supramolecular self-assembled nanofibers.* Soft Matter, 2011. **7**(7): p. 3524-3532.
165. Bulut, S., et al., *Slow Release and Delivery of Antisense Oligonucleotide Drug by Self-Assembled Peptide Amphiphile Nanofibers.* Biomacromolecules, 2011.
166. Toksoz, S., et al., *Electrostatic effects on nanofiber formation of self-assembling peptide amphiphiles.* J Colloid Interface Sci, 2011. **356**(1): p. 131-7.
167. Manning, M.C., M. Illangasekare, and R.W. Woody, *Circular dichroism studies of distorted alpha-helices, twisted beta-sheets, and beta turns.* Biophys Chem, 1988. **31**(1-2): p. 77-86.
168. Chen, T., et al., *Enzyme-catalyzed gel formation of gelatin and chitosan: potential for in situ applications.* Biomaterials, 2003. **24**(17): p. 2831-41.
169. Wessler, I., et al., *The non-neuronal cholinergic system in humans: expression, function and pathophysiology.* Life Sci, 2003. **72**(18-19): p. 2055-61.
170. Wessler, I. and C.J. Kirkpatrick, *Acetylcholine beyond neurons: the non-neuronal cholinergic system in humans.* Br J Pharmacol, 2008. **154**(8): p. 1558-71.
171. Miwa, J.M., R. Freedman, and H.A. Lester, *Neural systems governed by nicotinic acetylcholine receptors: emerging hypotheses.* Neuron, 2011. **70**(1): p. 20-33.
172. Khaldoyanidi, S., et al., *The cholinergic system is involved in regulation of the development of the hematopoietic system.* Life Sciences, 2007. **80**(24-25): p. 2352-2360.
173. Grando, S.A., M.R. Pittelkow, and K.U. Schallreuter, *Adrenergic and cholinergic control in the biology of epidermis: physiological and clinical significance.* J Invest Dermatol, 2006. **126**(9): p. 1948-65.
174. Razani-Boroujerdi, S., et al., *Role of muscarinic receptors in the regulation of immune and inflammatory responses.* J Neuroimmunol, 2008. **194**(1-2): p. 83-8.
175. Cooke, J.P., *Angiogenesis and the role of the endothelial nicotinic acetylcholine receptor.* Life Sci, 2007. **80**(24-25): p. 2347-51.

176. Greengard, P., et al., *A role for LYNX2 in anxiety-related behavior.* Proceedings of the National Academy of Sciences of the United States of America, 2009. **106**(11): p. 4477-4482.
177. Bamezai, A., *Mouse Ly-6 proteins and their extended family: markers of cell differentiation and regulators of cell signaling.* Archivum Immunologiae Et Therapiae Experimentalis, 2004. **52**(4): p. 255-266.
178. Tekinay, A.B., *Targeted Disruption of Lynx2 Reveals Distinct Functions for Lynx Homologues in Learning and Behavior*. 2007, The Rockefeller University.
179. Tsetlin, V., *Snake venom alpha-neurotoxins and other 'three-finger' proteins.* European Journal of Biochemistry, 1999. **264**(2): p. 281-286.
180. Bickmore, W.A., et al., *Colocalization of the Human Cd59 Gene to 11p13 with the Mic11 Cell-Surface Antigen.* Genomics, 1993. **17**(1): p. 129-135.
181. Quak, J.J., et al., *A 22-Kd Surface-Antigen Detected by Monoclonal Antibody-E-48 Is Exclusively Expressed in Stratified Squamous and Transitional Epithelia.* American Journal of Pathology, 1990. **136**(1): p. 191-197.
182. Brakenhoff, R.H., et al., *Sensitive detection of squamous cells in bone marrow and blood of head and neck cancer patients by E48 reverse transcriptase polymerase chain reaction.* Clinical Cancer Research, 1999. **5**(4): p. 725-732.
183. Witz, I.P., et al., *Human Ly-6 antigen E48 (Ly-6D) regulates important interaction parameters between endothelial cells and head-and-neck squamous carcinoma cells.* International Journal of Cancer, 2002. **98**(6): p. 803-810.
184. Hohl, D., et al., *Identification of SLURP-1 as an epidermal neuromodulator explains the clinical phenotype of Mal de Meleda.* Human Molecular Genetics, 2003. **12**(22): p. 3017-3024.
185. Grando, S.A., et al., *Central role of alpha 7 nicotinic receptor in differentiation of the stratified squamous epithelium.* Journal of Cell Biology, 2002. **159**(2): p. 325-336.
186. Arredondo, J., et al., *Biological effects of SLURP-1 on human keratinocytes.* J Invest Dermatol, 2005. **125**(6): p. 1236-41.
187. Fischer, J., et al., *Mutations in the gene encoding SLURP-1 in Mal de Meleda.* Human Molecular Genetics, 2001. **10**(8): p. 875-80.
188. Tsuji, H., et al., *SLURP-2, a novel member of the human Ly-6 superfamily that is up-regulated in psoriasis vulgaris.* Genomics, 2003. **81**(1): p. 26-33.
189. Arredondo, J., et al., *SLURP-2: A novel cholinergic signaling peptide in human mucocutaneous epithelium.* J Cell Physiol, 2006. **208**(1): p. 238-45.
190. Arredondo, J., A.I. Chernyavsky, and S.A. Grando, *Overexpression of SLURP-1 and -2 alleviates the tumorigenic action of tobacco-derived nitrosamine on immortalized oral epithelial cells.* Biochem Pharmacol, 2007. **74**(8): p. 1315-9.
191. Grando, S.A., *Basic and clinical aspects of non-neuronal acetylcholine: biological and clinical significance of non-canonical ligands of epithelial nicotinic acetylcholine receptors.* J Pharmacol Sci, 2008. **106**(2): p. 174-9.
192. LeClair, K.P., et al., *Murine Ly-6 multigene family is located on chromosome 15.* Proc Natl Acad Sci U S A, 1987. **84**(6): p. 1638-42.
193. Huppi, K., R. Duncan, and M. Potter, *Myc-1 is centromeric to the linkage group Ly-6--Sis--Gdc-1 on mouse chromosome 15.* Immunogenetics, 1988. **27**(3): p. 215-9.
194. Stroncek, D.F., L. Caruccio, and M. Bettinotti, *CD177: A member of the Ly-6 gene superfamily involved with neutrophil proliferation and polycythemia vera.* J Transl Med, 2004. **2**(1): p. 8.
195. Loeuillet, C., et al., *In vitro whole-genome analysis identifies a susceptibility locus for HIV-1.* PLoS Biol, 2008. **6**(2): p. e32.
196. Heintz, N., et al., *Tethering naturally occurring peptide toxins for cell-autonomous modulation of ion channels and receptors in vivo.* Neuron, 2004. **43**(3): p. 305-311.

197. Heintz, N., et al., *Novel modulation of neuronal nicotinic acetylcholine receptors by association with the endogenous prototoxin lynx1.* Neuron, 2002. **33**(6): p. 893-903.
198. Hensch, T.K., et al., *Lynx1, a Cholinergic Brake, Limits Plasticity in Adult Visual Cortex.* Science, 2010. **330**(6008): p. 1238-1240.
199. Wessler, I., C.J. Kirkpatrick, and K. Racke, *The cholinergic 'pitfall': acetylcholine, a universal cell molecule in biological systems, including humans.* Clin Exp Pharmacol Physiol, 1999. **26**(3): p. 198-205.
200. Albuquerque, E.X., et al., *Mammalian nicotinic acetylcholine receptors: from structure to function.* Physiol Rev, 2009. **89**(1): p. 73-120.
201. Chen, D. and J.W. Patrick, *The alpha-bungarotoxin-binding nicotinic acetylcholine receptor from rat brain contains only the alpha7 subunit.* J Biol Chem, 1997. **272**(38): p. 24024-9.
202. Whiting, P. and J. Lindstrom, *Purification and characterization of a nicotinic acetylcholine receptor from rat brain.* Proc Natl Acad Sci U S A, 1987. **84**(2): p. 595-9.
203. Karlin, A. and M.H. Akabas, *Toward a structural basis for the function of nicotinic acetylcholine receptors and their cousins.* Neuron, 1995. **15**(6): p. 1231-44.
204. Unwin, N., *Acetylcholine receptor channel imaged in the open state.* Nature, 1995. **373**(6509): p. 37-43.
205. Miyazawa, A., Y. Fujiyoshi, and N. Unwin, *Structure and gating mechanism of the acetylcholine receptor pore.* Nature, 2003. **423**(6943): p. 949-55.
206. Akabas, M.H., et al., *Acetylcholine receptor channel structure probed in cysteine-substitution mutants.* Science, 1992. **258**(5080): p. 307-10.
207. Doyle, D.A., *Structural changes during ion channel gating.* Trends Neurosci, 2004. **27**(6): p. 298-302.
208. Dwyer, T.M., D.J. Adams, and B. Hille, *The permeability of the endplate channel to organic cations in frog muscle.* J Gen Physiol, 1980. **75**(5): p. 469-92.
209. McGehee, D.S., *Molecular diversity of neuronal nicotinic acetylcholine receptors.* Ann N Y Acad Sci, 1999. **868**: p. 565-77.
210. Millar, N.S., *Assembly and subunit diversity of nicotinic acetylcholine receptors.* Biochem Soc Trans, 2003. **31**(Pt 4): p. 869-74.
211. Wessler, I., et al., *Release of non-neuronal acetylcholine from the isolated human placenta is mediated by organic cation transporters.* Br J Pharmacol, 2001. **134**(5): p. 951-6.
212. Schlereth, T., et al., *In vivo release of non-neuronal acetylcholine from the human skin as measured by dermal microdialysis: effect of botulinum toxin.* Br J Pharmacol, 2006. **147**(2): p. 183-7.
213. Grando, S.A., *Biological functions of keratinocyte cholinergic receptors.* J Investig Dermatol Symp Proc, 1997. **2**(1): p. 41-8.
214. Klapproth, H., K. Racke, and I. Wessler, *Modulation of the airway smooth muscle tone by mediators released from cultured epithelial cells of rat trachea.* Naunyn Schmiedebergs Arch Pharmacol (Suppl), 1994. **349**: p. R72.
215. Ndoye, A., et al., *Identification and mapping of keratinocyte muscarinic acetylcholine receptor subtypes in human epidermis.* J Invest Dermatol, 1998. **111**(3): p. 410-6.
216. Klapproth, H., et al., *Non-neuronal acetylcholine, a signalling molecule synthesized by surface cells of rat and man.* Naunyn-Schmiedebergs Archives of Pharmacology, 1997. **355**(4): p. 515-523.
217. Grando, S.A., M.R. Pittelkow, and K.U. Schallreuter, *Adrenergic and cholinergic control in the biology of epidermis: Physiological and clinical significance.* Journal of Investigative Dermatology, 2006. **126**(9): p. 1948-1965.

218. Chernyavsky, A.I., et al., *The M4 muscarinic receptor-selective effects on keratinocyte crawling locomotion.* Life Sci, 2003. **72**(18-19): p. 2069-73.
219. Hasse, S., et al., *The M4 muscarinic acetylcholine receptor plays a key role in the control of murine hair follicle cycling and pigmentation.* Life Sci, 2007. **80**(24-25): p. 2248-52.
220. Metzen, J., et al., *Proliferative effect of acetylcholine on rat trachea epithelial cells is mediated by nicotinic receptors and muscarinic receptors of the M1-subtype.* Life Sci, 2003. **72**(18-19): p. 2075-80.
221. Tournier, J.M., et al., *alpha3alpha5beta2-Nicotinic acetylcholine receptor contributes to the wound repair of the respiratory epithelium by modulating intracellular calcium in migrating cells.* American Journal of Pathology, 2006. **168**(1): p. 55-68.
222. Hardcastle, J., P.T. Hardcastle, and J.M. Noble, *The involvement of calcium in the intestinal response to secretagogues in the rat.* J Physiol, 1984. **355**: p. 465-78.
223. Acevedo, M., *Effect of acetyl choline on ion transport in sheep tracheal epithelium.* Pflugers Arch, 1994. **427**(5-6): p. 543-6.
224. Borovikova, L.V., et al., *Vagus nerve stimulation attenuates the systemic inflammatory response to endotoxin.* Nature, 2000. **405**(6785): p. 458-62.
225. Pavlov, V.A. and K.J. Tracey, *The cholinergic anti-inflammatory pathway.* Brain Behav Immun, 2005. **19**(6): p. 493-9.
226. Alexander, I., et al., *Epithelial surfaces of the trachea and principal bronchi in the rat.* Thorax, 1975. **30**(2): p. 171-7.
227. Knowles, M.R. and R.C. Boucher, *Mucus clearance as a primary innate defense mechanism for mammalian airways.* Journal of Clinical Investigation, 2002. **109**(5): p. 571-577.
228. Krasteva, G., et al., *Cholinergic chemosensory cells in the trachea regulate breathing.* Proceedings of the National Academy of Sciences of the United States of America, 2011. **108**(23): p. 9478-9483.
229. Zia, S., et al., *Nicotine enhances expression of the alpha 3, alpha 4, alpha 5, and alpha 7 nicotinic receptors modulating calcium metabolism and regulating adhesion and motility of respiratory epithelial cells.* Res Commun Mol Pathol Pharmacol, 1997. **97**(3): p. 243-62.
230. Sekhon, H.S., et al., *Expression of lynx1 in developing lung and its modulation by prenatal nicotine exposure.* Cell Tissue Res, 2005. **320**(2): p. 287-97.
231. Yamagishi, H., et al., *Tongue-like Barrett's esophagus is associated with gastroesophageal reflux disease.* World J Gastroenterol, 2008. **14**(26): p. 4196-203.
232. Grando, S.A., et al., *Choline acetyltransferase, acetylcholinesterase, and nicotinic acetylcholine receptors of human gingival and esophageal epithelia.* Journal of Dental Research, 2000. **79**(4): p. 939-949.
233. Mintzer, M.A. and E.E. Simanek, *Nonviral vectors for gene delivery.* Chem Rev, 2009. **109**(2): p. 259-302.
234. Thomas, C.E., A. Ehrhardt, and M.A. Kay, *Progress and problems with the use of viral vectors for gene therapy.* Nat Rev Genet, 2003. **4**(5): p. 346-58.
235. Ryser, H.J. and R. Hancock, *Histones and basic polyamino acids stimulate the uptake of albumin by tumor cells in culture.* Science, 1965. **150**(3695): p. 501-3.
236. Kawashima, S., S. Inoue, and T. Ando, *Interaction of basic oligo-L-amino acids with deoxyribonucleic acid. Oligo-L-ornithines of various chain lengths and herring sperm DNA.* Biochim Biophys Acta, 1969. **186**(1): p. 145-57.
237. Futaki, S., et al., *Arginine-rich peptides. An abundant source of membrane-permeable peptides having potential as carriers for intracellular protein delivery.* J Biol Chem, 2001. **276**(8): p. 5836-40.

238. Burckhardt, G., C. Zimmer, and G. Luck, *Conformation and reactivity of DNA in the complex with proteins. III. Helix-coil transition and conformational studies of model complexes of DNA's with poly-L-histidine.* Nucleic Acids Research, 1976. **3**(3): p. 537-59.
239. Zorko, M. and U. Langel, *Cell-penetrating peptides: mechanism and kinetics of cargo delivery.* Adv Drug Deliv Rev, 2005. **57**(4): p. 529-45.
240. Mahato, R.I., *Non-viral peptide-based approaches to gene delivery.* Journal of Drug Targeting, 1999. **7**(4): p. 249-268.
241. McKenzie, D.L., K.Y. Kwok, and K.G. Rice, *A potent new class of reductively activated peptide gene delivery agents.* Journal of Biological Chemistry, 2000. **275**(14): p. 9970-9977.
242. Wadhwa, M.S., et al., *Peptide-mediated gene delivery: Influence of peptide structure on gene expression.* Bioconjugate Chemistry, 1997. **8**(1): p. 81-88.
243. Gottschalk, S., et al., *A novel DNA-peptide complex for efficient gene transfer and expression in mammalian cells.* Gene Therapy, 1996. **3**(5): p. 448-457.
244. Martin, M.E. and K.G. Rice, *Peptide-guided gene delivery.* Aaps Journal, 2007. **9**(1): p. E18-E29.
245. McKenzie, D.L., W.T. Collard, and K.G. Rice, *Comparative gene transfer efficiency of low molecular weight polylysine DNA-condensing peptides.* Journal of Peptide Research, 1999. **54**(4): p. 311-318.
246. Gottschalk, S., et al., *A novel DNA-peptide complex for efficient gene transfer and expression in mammalian cells.* Gene Ther, 1996. **3**(5): p. 448-57.
247. Midoux, P. and M. Monsigny, *Efficient gene transfer by histidylated polylysine/pDNA complexes.* Bioconjug Chem, 1999. **10**(3): p. 406-11.
248. Midoux, P., et al., *Membrane permeabilization and efficient gene transfer by a peptide containing several histidines.* Bioconjug Chem, 1998. **9**(2): p. 260-7.
249. Plank, C., et al., *Branched cationic peptides for gene delivery: Role of type and number of cationic residues in formation and in vitro activity of DNA polyplexes (vol 10, pg 322, 1999).* Human Gene Therapy, 1999. **10**(13): p. 2272-2272.
250. Rudolph, C., et al., *Oligomers of the arginine-rich motif of the HIV-1 TAT protein are capable of transferring plasmid DNA into cells.* Journal of Biological Chemistry, 2003. **278**(13): p. 11411-11418.
251. Derossi, D., G. Chassaing, and A. Prochiantz, *Trojan peptides: the penetratin system for intracellular delivery.* Trends in Cell Biology, 1998. **8**(2): p. 84-87.
252. Pooga, M., et al., *Cell penetration by transportan.* Faseb Journal, 1998. **12**(1): p. 67-77.
253. Hallbrink, M., et al., *Cargo delivery kinetics of cell-penetrating peptides.* Biochim Biophys Acta, 2001. **1515**(2): p. 101-9.
254. Kim, J., C.P. Chen, and K.G. Rice, *The proteasome metabolizes peptide-mediated nonviral gene delivery systems.* Gene Therapy, 2005. **12**(21): p. 1581-1590.
255. Lanford, R.E., P. Kanda, and R.C. Kennedy, *Induction of Nuclear Transport with a Synthetic Peptide Homologous to the Sv40 T-Antigen Transport Signal.* Cell, 1986. **46**(4): p. 575-582.
256. Lyons, R.H., B.Q. Ferguson, and M. Rosenberg, *Pentapeptide Nuclear-Localization Signal in Adenovirus E1a.* Molecular and Cellular Biology, 1987. **7**(7): p. 2451-2456.
257. Dang, C.V. and W.M.F. Lee, *Identification of the Human C-Myc Protein Nuclear Translocation Signal.* Molecular and Cellular Biology, 1988. **8**(10): p. 4048-4054.
258. Kamata, H., et al., *Amphiphilic Peptides Enhance the Efficiency of Liposome-Mediated DNA Transfection.* Nucleic Acids Research, 1994. **22**(3): p. 536-537.
259. Ryu, D.W., et al., *Amphiphilic Peptides With Arginines and Valines for the Delivery of Plasmid DNA.* Journal of Cellular Biochemistry, 2011. **112**(5): p. 1458-1466.
260. Katayama, S., et al., *Acylation of octaarginine: Implication to the use of intracellular delivery vectors.* Journal of Controlled Release, 2011. **149**(1): p. 29-35.

261. Futaki, S., et al., *Stearylated arginine-rich peptides: A new class of transfection systems.* Bioconjugate Chemistry, 2001. **12**(6): p. 1005-1011.
262. Bitton, R., et al., *Self-assembly of model DNA-binding peptide amphiphiles.* Langmuir, 2005. **21**(25): p. 11888-11895.
263. Guler, M.O., et al., *Enhanced oligonucleotide binding to self-assembled nanofibers.* Bioconjugate Chemistry, 2005. **16**(3): p. 501-503.
264. Park, C.B., H.S. Kim, and S.C. Kim, *Mechanism of action of the antimicrobial peptide buforin II: buforin II kills microorganisms by penetrating the cell membrane and inhibiting cellular functions.* Biochem Biophys Res Commun, 1998. **244**(1): p. 253-7.
265. Jung, M.R., et al., *Controlled release of cell-permeable gene complex from poly(L-lactide) scaffold for enhanced stem cell tissue engineering.* Journal of Controlled Release, 2011. **152**(2): p. 294-302.
266. Chugh, A. and F. Eudes, *Study of uptake of cell penetrating peptides and their cargoes in permeabilized wheat immature embryos.* FEBS J, 2008. **275**(10): p. 2403-14.